JPL PUBLICATION 82-90

E83-10321
CR-170381

"Made available under NASA sponsorship in the interest of early and wide dissemination of Earth Resources Survey Program information and without liability for any use made thereof."

Seasat Synthetic-Aperture Radar Data User's Manual

Steven H. Pravdo
Bryan Huneycutt
Benjamin M. Holt
Daniel N. Held

(E83-10321) SEASAT SYNTHETIC-APERTURE RADAR DATA USER'S MANUAL (Jet Propulsion Lab.) 112 p HC A06/MF A01 CSCL 17I

N83-29746

Unclas
G3/43 00321

March 1, 1983

NASA
National Aeronautics and
Space Administration

Jet Propulsion Laboratory
California Institute of Technology
Pasadena, California

JPL PUBLICATION 82-90

Seasat Synthetic-Aperture Radar Data User's Manual

Steven H. Pravdo
Bryan Huneycutt
Benjamin M. Holt
Daniel N. Held

March 1, 1983

National Aeronautics and
Space Administration

Jet Propulsion Laboratory
California Institute of Technology
Pasadena, California

The research described in this publication was carried out by the Jet Propulsion Laboratory, California Institute of Technology, under contract with the National Aeronautics and Space Administration.

Acknowledgments

We thank T. Bicknell and C. Wu for helpful discussions. L. Fu gave useful comments on the text. R. Hall, J. Dugdale, and I. Steen are acknowledged for their help in the preparation of the manuscript.

Contents

Seasat SAR Areal Coverage

Tables

Abstract

This manual contains descriptions of the Seasat Synthetic-Aperture Radar (SAR) system, the data processors, the extent of the image data set, and the means by which a user obtains this data. An evaluation of the data quality is included. The manual alerts the user to some potential problems with the existing volume of Seasat SAR image data, and allows him to modify his use of that data accordingly.

Secondly, the manual focuses on the ultimate capabilities of the raw data set and evaluates the potential of this data for processing into accurately located, amplitude-calibrated imagery of high resolution. This allows the user to decide whether his needs will require special-purpose data processing of the SAR raw data.

Section I
Introduction

A. Seasat

The National Aeronautics and Space Administration's (NASA) Seasat was the first Earth-orbiting satellite designed for remote sensing of the Earth's oceans (e.g., Born, Dunne, and Lame, 1979). Five complementary experiments were onboard to measure surface wind speeds and directions, wave heights, sea-surface temperatures, wavelengths and wave directions, and to identify cloud, land, and water features. This manual will describe one of the instruments, the Seasat Synthetic-Aperture Radar (SAR), and include such topics as the basic principles behind the SAR technique, the operation of the Seasat SAR, and the capabilities and limitations of the data acquired with the Seasat SAR.

Seasat, managed by the Jet Propulsion Laboratory (JPL), was launched on June 28, 1978, into a nearly circular, 800-km-high orbit with an inclination angle of 108 deg. Approximately 14 Earth orbits were completed each day. Some 10 days after launch, data collection for the experiments began. The instruments consisted of a radar altimeter capable of measuring spacecraft height above the ocean surface with an accuracy of ±10 cm and significant wave height with an accuracy of ±0.5 m (Tapley et al., 1979; Townsend, 1980); a microwave scatterometer designed to measure wind speed to ±2 ms^{-1} and wind direction to ±20 deg (Jones et al., 1979; Johnson et al., 1980); a scanning multichannel microwave radiometer (SMMR) capable of measuring sea-surface temperature with an error of less than 1 deg (SMMR Mini Workshop III, 1980; Njoku, Stacéy, and Barath, 1980); a visible and infrared radiometer (VIRR) designed to identify cloud, land, and water features (McClain and Marks, 1979; McClain et al., 1980); and the SAR. Figure 1-1 illustrates the in-orbit satellite configuration.

The Seasat SAR operated for approximately 100 days until October 10, 1979, when a massive short circuit in the satellite electrical system ended the mission. The following paragraphs will describe the basics of the SAR technique and the characteristics of the Seasat SAR.

B. Synthetic-Aperture Radar

Radar is a remote sensing device that transmits a pulsed electromagnetic wave and receives reflections of the wave from the target. An image, which is the two-dimensional projection of a three-dimensional scene, is constructed from analysis of the returned signals. The theoretical resolution of this image, r_R or r_{AZ}, has the following forms for each of the two dimensions, where R refers to the range direction (i.e., along the path from the radar to the target), and AZ refers to the cross-range or azimuthal direction, which is perpendicular to the range (e.g., Tomiyasu, 1978):

$$r_R = c\tau/2 = c/2f \tag{1}$$

$$r_{AZ} = \frac{\lambda R}{2L} \tag{2}$$

In the above formula, c is the speed of light, τ is the effective radar pulse length, f the signal bandwidth, λ is the radar wavelength, R is the slant range, and L is the length of the synthesized aperture. With the SAR technique, the effective aperture length, L, is substantially larger than the physical length of the radar antenna, thus improving the azimuthal resolution (see Equation 2). This is accomplished by moving the radar antenna while illuminating the target and coherently processing the returned signals. A large radar aperture is

ORIGINAL PAGE IS
OF POOR QUALITY

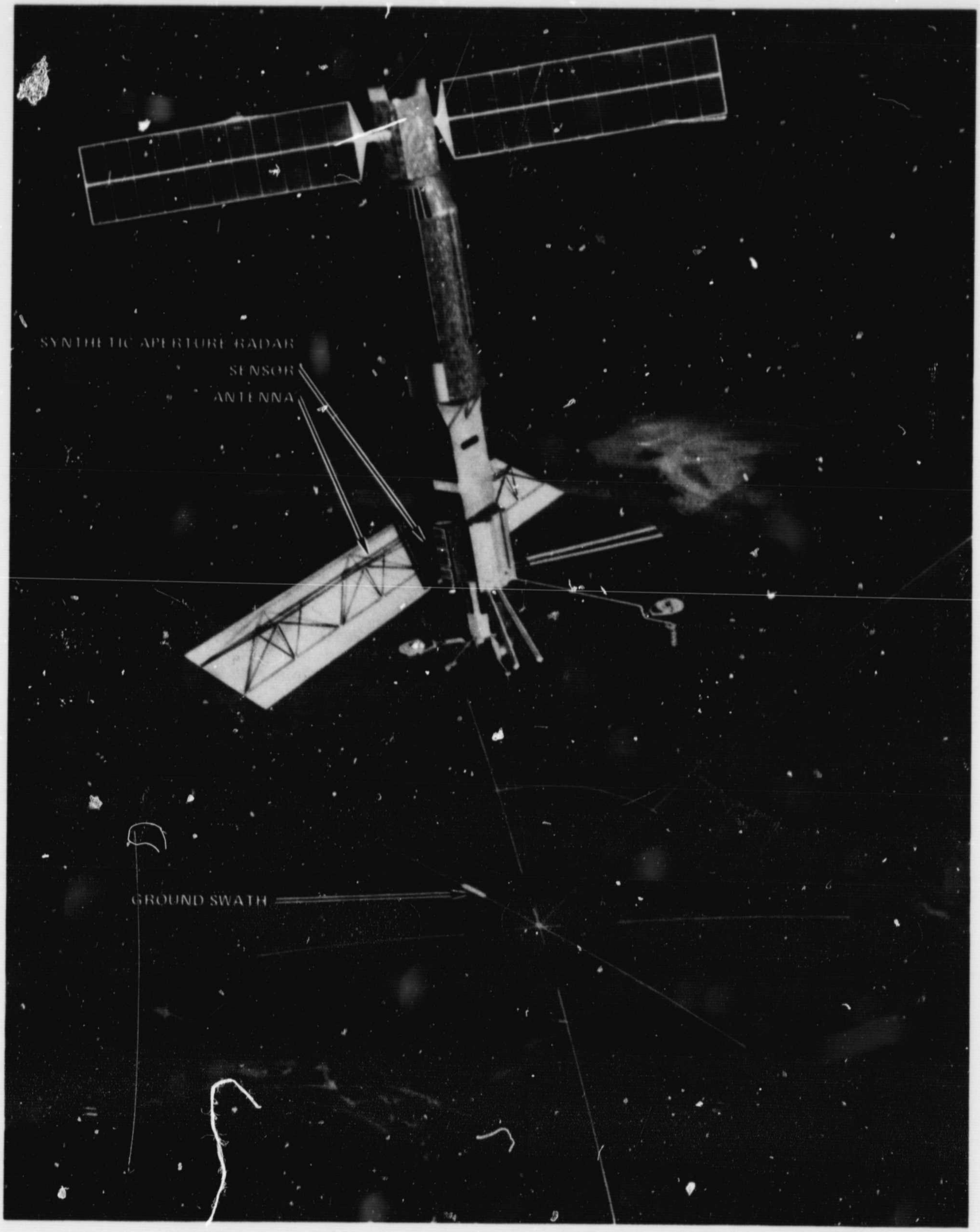

Figure 1-1. Seasat satellite

synthesized in this way. If v is the antenna velocity and t is the target illumination time, then Equation 2 can be rewritten as:

$$r_{AZ} = \frac{\lambda R}{2vt} \quad (3)$$

Figure 1-2 illustrates the SAR geometry. For the "broadside" SAR shown in the figure, the range direction is perpendicular to the antenna flight path. The slant range is measured from the SAR to the target while the ground range is measured along the surface. The hatched region is the area illuminated by the radar at any given time. Its dimensions are determined by the dimensions of the physical antenna (d_R by d_{AZ}), the radar wavelength, the slant range, and the incidence angle (i). They are approximately equal to:

$$\ell_{AZ} = \frac{\lambda R}{d_{AZ}} \equiv \theta_{AZ} R \quad (4)$$

$$\ell_R = \frac{\lambda R}{d_R \cos i} \equiv \theta_R R/\cos i \quad (5)$$

where θ is also known as the beamwidth.

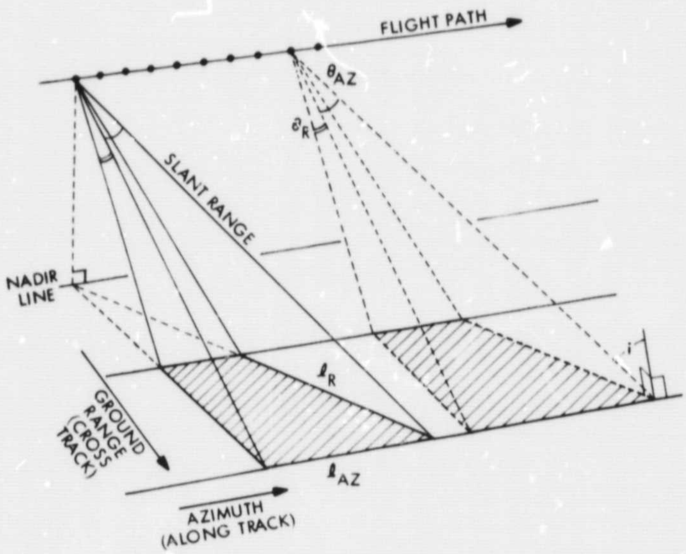

Figure 1-2. SAR ground illumination

Signals reflected from a ground swath must be coherently processed to create an image. The phases of the reflected waves are interpreted using a precise knowledge of the SAR position and motion. For a satellite-borne SAR, this requires accurate values for the orientation, altitude, velocity, and other orbital elements of the spacecraft. In addition, the rotational velocity of the Earth must be taken into account since the reflected signals will be Doppler shifted by varying amounts depending on the target latitude; the Doppler shift will be largest near the equator and smallest at the highest orbital latitudes. Imprecision in these values leads to phase errors and a consequent blurring of the image. Ionospheric irregularities may also result in phase errors by affecting the signal propagation velocity. In particular, magnetic storms can greatly increase the electron column density and the ionospheric inhomogeneity between the SAR and the target. (Burns and Fremouw, 1970). These and other sources of phase error (e.g., system noise) will cause image misregistration and shift, azimuth and range defocus and walk, main-lobe loss, and an increase in the sidelobes of the image (Tomiyasu, 1978).

The SAR image is a measure of the radar backscatter (reflectivity) of the target scene. The backscatter depends upon the composition, slope, and roughness-size scale of the surface material (Active Microwave Workshop Report, 1975; Ford et al., 1980). Bright regions (high reflectivity) can be due to roughness on a size scale comparable to the radar wavelength, target inclination toward the SAR, or a large dielectric constant, which may be present, for example, in soil with a high moisture content (see also Long, 1975).

Certain geometric effects related to variable elevation in the target scene result in nonrecoverable ambiguities or distortions of the image. These include shortening, layover, and shadowing. If a surface were perfectly flat, surface elements closer to the subnadir point of the SAR would be illuminated and reflect the radar signals before surface elements farther from the subnadir point. Thus, the signals would reflect from "near"- range to "far"-range elements progressively in time. However, if a surface element is elevated relative to its surroundings, it will intercept the radar signal sooner and appear in the radar image to be closer than it is. Figure 1-3(a) illustrates how this effect results in an apparent shortening of slopes inclined toward the radar; i.e., slope AB appears in the radar image as shortened slope $A'B'$. The "radar image plane" in the figure is a geometrical representation (a right-angle projection) of the conversion between target range and location on the resulting image. For extreme cases of shortening (Figure 1-3(b)), the ordering of surface elements on the radar image is the reverse of the ordering on the ground; i.e., B' appears at a nearer range than A', while actually A is at a nearer range than B. This is known as "layover." The elevated element can also stop the radar signal from illuminating elements in its shadow (Figure 1-3(c)).

SAR data can be optically and/or digitally processed. Optical processing is generally simpler and faster. For this method, the received signal is recorded on film (called "signal

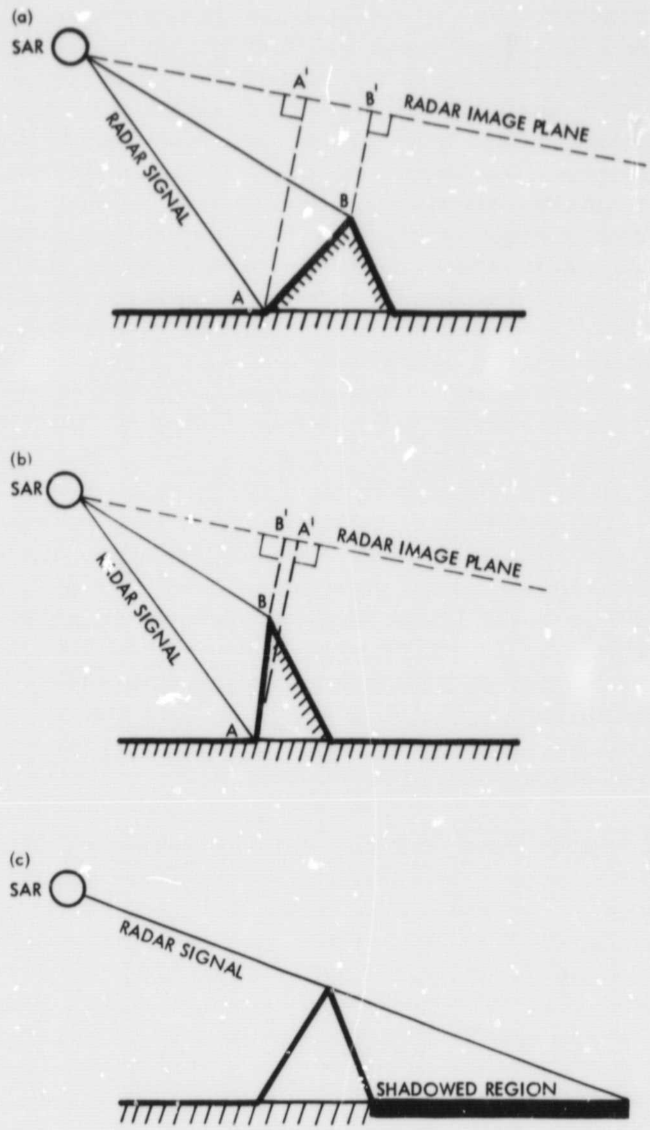

Figure 1-3. Effects of surface height variations on SAR: (a) shortening; (b) layover; (c) shadowing

film") for processing in an analog-optical computer referred to as a "correlator." Signals from target elements at different ranges within the ground swath are recorded along the width of the signal film, while along-track azimuth data are recorded along its length. This signal-film data is then transferred onto image film by passing a parallel beam of coherent light through the signal film and focusing the light through a series of lenses onto the image film (e.g., Tomiyasu, 1978).

The SAR data can also be digitally processed. This is done in a series of software steps that involves, among other things, a two-dimensional Fourier transform of the data. There is a trade-off between optically and digitally processed data. Optical processing is inexpensive and fast. Digital processing is time consuming, but the final product is amenable to quantitative analysis and is completely reproducible.

C. The Seasat SAR

The Seasat SAR consisted of a planar array antenna, sensor electronics, and a data link to the ground. The antenna was deployed after launch; it was 10.74 m long by 2.16 m wide (Figure 1-4). The antenna was oriented with the long dimension along track, which resulted (Equations 4 and 5) in a ground swath 19 km (along track) by 100 km (cross track). The center of the ground swath was 270 km to the right of the subnadir point. Table 1-1 summarizes the important Seasat SAR parameters.

Table 1-1. Parameters of the Seasat SAR

Parameter	Text Symbol	Value
Cross-track antenna length, m	d_R	2.16
Along-track antenna length, m	d_{AZ}	10.74
Radar wavelength, m	λ	0.235
Signal bandwidth, MHz	f	19
Pulse length, μs	–	33.8
Pulse repetition frequency, pulses/s	PRF	1464 to 1647
Transmitted peak power, W	–	1000
Orientation, Position, and Velocity		
Antenna look angle, deg from vertical	–	20
Incidence angle, deg across swath	i	23 ± 3
Altitude, km	–	800
Velocity, spacecraft, km/s	v	7.5

The SAR on Seasat used the satellite's orbital motion to synthesize a large aperture and to achieve good azimuthal resolution. Parameters from Table 1-1 can be inserted into the equations of the preceding section to obtain the characteristics of the data. The theoretical range resolution with a 19-MHz-signal bandwidth is about 8 m (Equation 1) in slant range. The ground range resolution is thus 8/sin i (i = 20 to 26 deg, the incidence angle) or 18 to 23 m. To calculate the azimuthal resolution, the slant range and the target illumination time are needed. The midswath slant range is approximately the altitude divided by cos i, or about 850 km. The dwell or target illumination time is equal to the time it takes the satellite to move through the 19-km along-track dimension of the ground swath, or about 2.5 s. This yields an azimuthal resolution of 6 m (Equation 2). However, rather than coherently processing all the Seasat data from a given ground swath to achieve this resolution, it was decided to divide the

ORIGINAL PAGE IS
OF POOR QUALITY

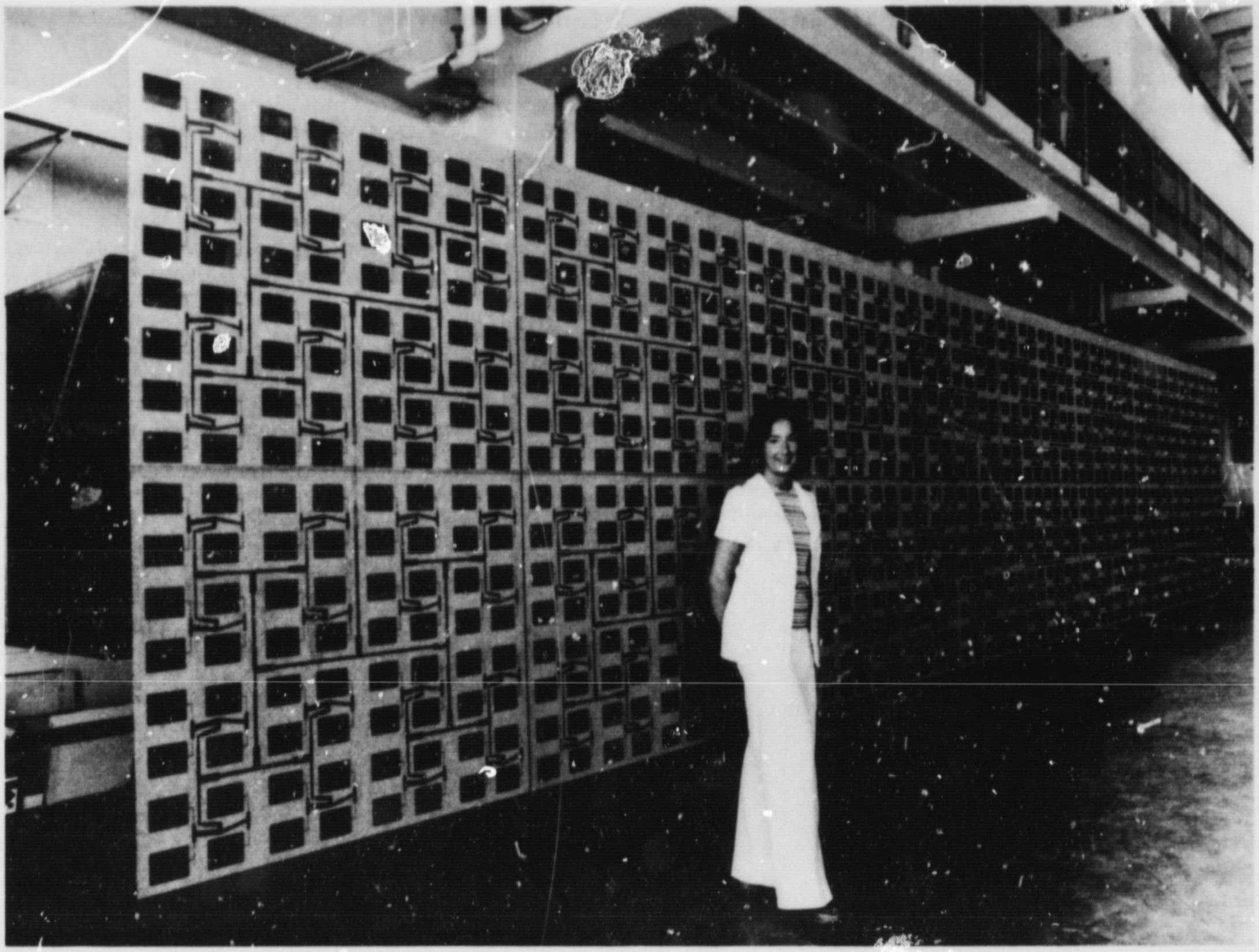

Figure 1-4. Seasat synthetic-aperture radar antenna

illumination time or aperture into four separate "looks," and sacrifice a factor of 4 in the resolution to obtain a better signal-to-noise ratio in each resolution element. The final attained resolution for the production data is about 25 m by 25 m. In certain test cases, imagery has been correlated to the full 6-m azimuthal resolution.

The radar echo amplitude will vary across an image swath as a function of range. As the range increases in the cross-track direction, the echo is attenuated. The Seasat SAR receiver provides a dynamic altering of the gain in the inter-pulse period to coarsely compensate for the peaked antenna gain pattern in this direction. This feature is called the sensitivity time control (STC), and is designed to flatten the echo amplitude response across the image swatch.

D. SAR Data Overview

Data obtained with the Seasat SAR were transmitted to the ground via an analog data link and subsequently digitized and stored on tape at a rate of approximately 110 Mbits/s during the course of each 10-min ground-station pass. Since there were no onboard storage facilities for this data, the areas covered were necessarily in the vicinity of one of the five receiving ground stations. These were located at Goldstone, California (GDS); Merritt Island, Florida (MIL); Shoe Cove, Newfoundland, Canada (SNF); Oakhanger, U.K. (UKO); and Fairbanks, Alaska (ULA).

Timing for the SAR data was provided by a stable local oscillator within the SAR transmitter. The timing information

was included in each major frame of SAR data, which consists of 13,680 range samples taken at a rate of 45.53 MHz or 300.5 μs of data. This information together with orbital ephemeris data on an engineering tape was used to convert the SAR data from a line/pixel representation to the output map projection coordinates.

Approximately 2500 min of SAR data were received and stored on magnetic tapes. Almost all data were optically processed while a small fraction (~3%) were also digitally processed. Appendix A presents computer-generated plots showing the areal coverage of all data of sufficient quality to have been optically processed. The ground swaths illustrated in Appendix A have a width of about 100 km determined by the cross-track beam width. The swath lengths are determined by the satellite velocity and the length of the ground station passes. For a 10-min data pass, the swath length can attain ~4500 km. The image scale for optically processed data is approximately 1:500,000, although it does vary as a function of range. Appendix A also gives tables of orbital information for both optically and digitally processed data.

Seasat SAR data covers in total about 100 million km^2 of the Earth's surface. Oceanographic studies using images of the oceans were the main experiment objective (e.g., Fu and Holt, 1982). However, approximately 65% of the data covers land areas in North America, the Caribbean, and Western Europe, with applications to geology, hydrology and water resources, urban land cover, and agriculture (e.g., Ford et al., 1980).

E. The User's Manual

This concludes the introduction to the Seasat SAR and its data. The succeeding sections discuss the use of SAR data (Section II), more details concerning optically processed (Section III) and digitally processed (Section IV) data, some problems and features that may appear in the data (Section V), and the scope of Seasat SAR observations (Section VI).

Section II
Using Seasat SAR Data

A. Distribution of Seasat SAR Processed Data

The Seasat SAR data were optically processed at JPL. A small fraction of the data were also digitally processed at JPL. These "production" data were provided to the National Oceanographic and Atmospheric Administration (NOAA).

The images from the Seasat SAR that were optically or digitally processed at JPL (Appendix A) are archived at the Environmental Data and Information Service (EDIS) of NOAA. They are available in the form of photographic prints, negatives, and transparencies; digitally processed data are on 9-track, 1600-bit/inch magnetic tapes. For information regarding public sale and distribution of these data, contact:

Environmental Data and Information Service
National Climatic Center
Satellite Data Services Division
World Weather Building, Room 100
Washington, D.C. 20233
Phone: (301) 763-8111

Data received at Oakhanger, United Kingdom, (UKO) were processed also in Europe and are available there. The European Space Agency (ESA) disseminates these data and can be contacted at:

ESRIN — Earthnet Programme Office
Via Galileo Galilei
00044 Frascati
Italy
Phone: (06) 94011
Telex: 610637 ESRIN I

Some data were also processed by:

MacDonald Dettweiler and Associates
3571 Shell Road
Richmond, British Columbia VGX 2Z9
Canada

Sixty to seventy images of 40 km × 40 km scenes were created. Photographs and 1600-bit/inch magnetic tapes are archived at:

Canadian Center for Remote Sensing
2464 Sheffield Road
Ottawa, Ontario K1A OY7
Canada
Phone: (613) 993-0121

B. An Example of Seasat SAR Data

Figures 2-1 and 2-2 show a SAR image of the same scene. In Figure 2-1, the data have been optically processed into four ¼ swaths, each with a width of about 30 km. These overlap by 6 to 7 km for a total swath width of ~100 km. The image intensity changes from swath to swath are due to different film exposure levels. The intensity gradient across the entire swath is due to mispositioning of the sensitivity time control (STC, Subsections I-C and III-D). This causes the attenuation of the antenna gain pattern to be accentuated in the far range where the echo appears weaker. Lesser gradients within a ¼ swath are caused by uneven illumination in the optical processor. Note the white dots that run along the edge of each ¼ swath. These 1-s tick marks represent the time code (see below) annotated every 10 s.

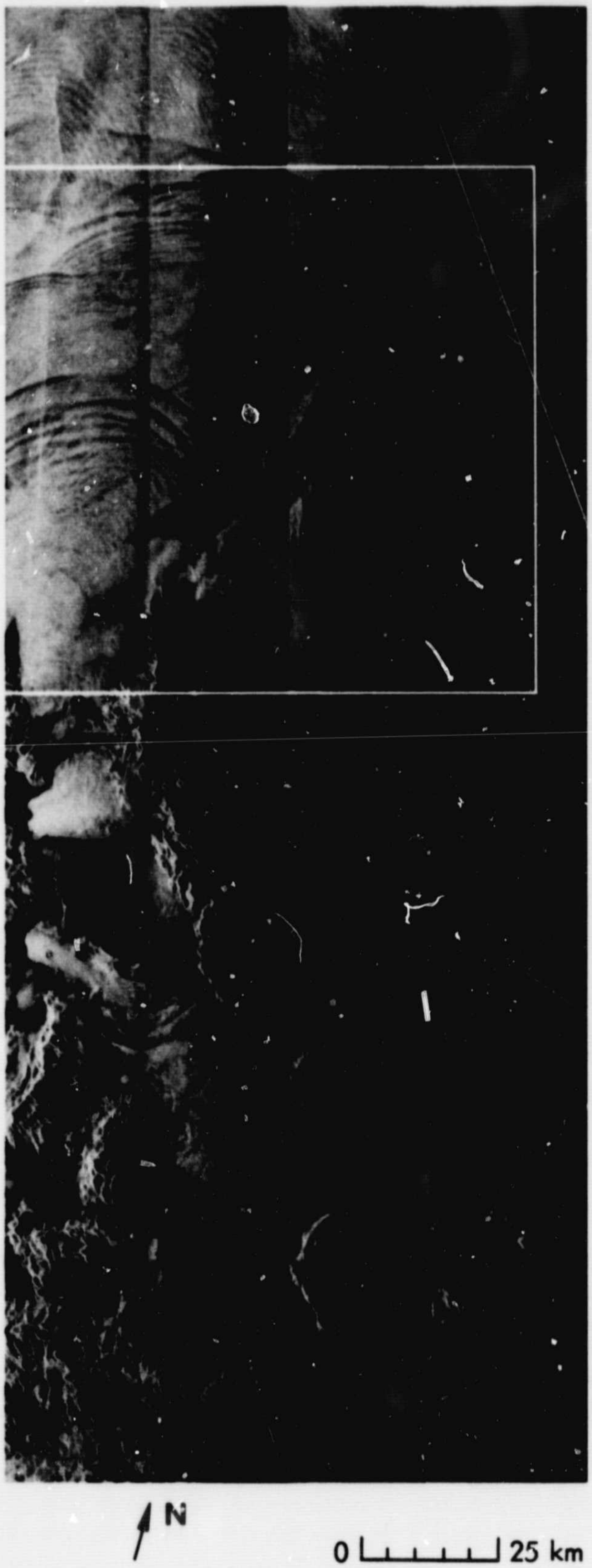

Figure 2-1. Optically processed image

Figure 2-2 is the result of digitally processing the data for the 100 km by 100 km subsection indicated in Figure 2-1. This image does not exhibit those artifacts that are the result of processing individual ¼ swaths. However, the intensity gradient across the entire image is still apparent. Section IV discusses the digital processing in more detail. As discussed therein, some progress has been made in the reduction of the gradient effect.

The scene in Figures 2-1 and 2-2 is in the Gulf of California and shows a number of features identifiable from SAR data. In Figure 2-1, the land mass (identified by the rough texture) in the southwest corner is part of the Baja California peninsula. The large island near the middle of the image is Angel de la Guarda. In the digital image, Figure 2-2, only the northern tip of this island is visible near the bottom. Northwest of Angel de la Guarda, a large number of internal ocean waves are apparent (Elachi, 1980). The wave pattern at the western edge of the image is particularly regular with a wavelength of about 5 km. The radius of curvature for these waves is almost 25 km.

This data was received by the GDS ground station during Revolution 1183. By consulting Appendix A, one can discover some relevant information. For example, the node value for this revolution is 256.01, and Figure A-7 (Appendix A, Figure A-7) shows the areal coverage for this pass labeled by this node value (rounded off to the nearest tenth). The total ground swath stretches from Alaska to south of the Gulf of California.

C. Finding Data

The plots and tables in Appendix A are useful in determining the availability of Seasat SAR data for a particular target on the ground. For an example, consider the Gulf of California discussed above. We wish to find all passes, including Revolution 1183, that make up the total coverage of this area. First we determine the longitude and latitude of the target. It is located at about 248°E and 28°N. Next we look at the summary plots of areal coverage. These are found in Figures A-2, A-8, A-13, A-14, and A-24. Each of these five figures shows the superposed ground swaths obtained at each of the five ground stations. The area covered from one ground station rarely overlapped that covered by another. The figures show that only Goldstone (GDS) passes (Figure A-2) viewed these particular coordinates.

Figures A-3 through A-7 illustrate the individual GDS passes identified either by integer revolution numbers or by real node numbers. Revolution 193 in Figure A-3, Revolution 387 in Figure A-4, Revolution 631 in Figure A-5, Revolutions

ORIGINAL PAGE
BLACK AND WHITE PHOTOGRAPH

Figure 2-2. Digitally processed image

681 and 882 in Figure A-6, and, of course, node 256.0 in Figure A-7 all contain observations of this scene. The orbital information for each of the revolutions can be found in Table A-1 (organized in the order of increasing revolution number), and for each of the nodes in Table A-2 (organized in the order of increasing node number).

Let us look in more detail at Revolution 193. From Table A-1, the node time is 12:15:09 (JLN NODE TIME). The swath went from north latitude 21.1 (LTON) to north latitude 53.6 (LOFF); therefore, it was an ascending node. Table A-3 shows that in an ascending node, spacecraft travel time from the equator to 28°N (TA) is 00:08:00. Thus the time for data acquisition over the scene of interest is approximately 12:23:09, or about 2 min after the start of imagery (TIME ON).

With these aids, the user can determine if SAR data exists for his area of interest; if it does, the swaths can be identified and the data (images or tapes) ordered from NOAA.

ORIGINAL PAGE IS
OF POOR QUALITY

Section III
Optically Processed Data

A. Introduction

Optical processing is an efficient method of turning SAR data into images. Optically produced images are suitable for qualitative and quick-look analysis. The optical processor is an analog-optical computer called a "correlator," which performs a series of analog and sometimes nonlinear functions to produce image film. Figure 3-1 shows a block diagram of this system.

Two digital tape inputs are required to convert SAR data into images. The first is a very-high density digital tape (HDDT) that contains the radar data, time code (Greenwich Mean Time (GMT)), and certain telemetry information. The second tape (SAR Sensor Data Record (SDR)) contains sensor status and orbit information. These digital inputs are converted by an "optical recorder" to an analog signal with which a "signal film" is exposed in a step labeled "tape-to-film conversion" on Figure 3-1. In addition, the time code is converted to a binary-coded decimal (BCD) code of hours, minutes, and seconds of day and transferred from the HDDT to the signal film every 10 s. The signal film is then run through the optical processor to produce image film.

There are two outputs for the user. The first is a computer printout called the Auxiliary Data Listing upon which orbit information (such as velocity and velocity rate), sensor status,

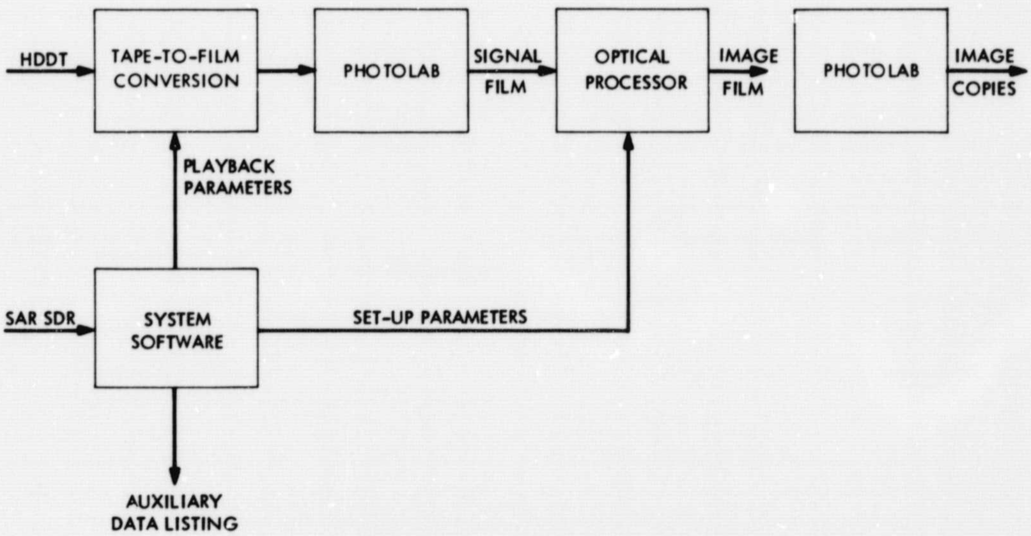

Figure 3-1. Seasat SAR optical data processing system

ORIGINAL PAGE IS
OF POOR QUALITY

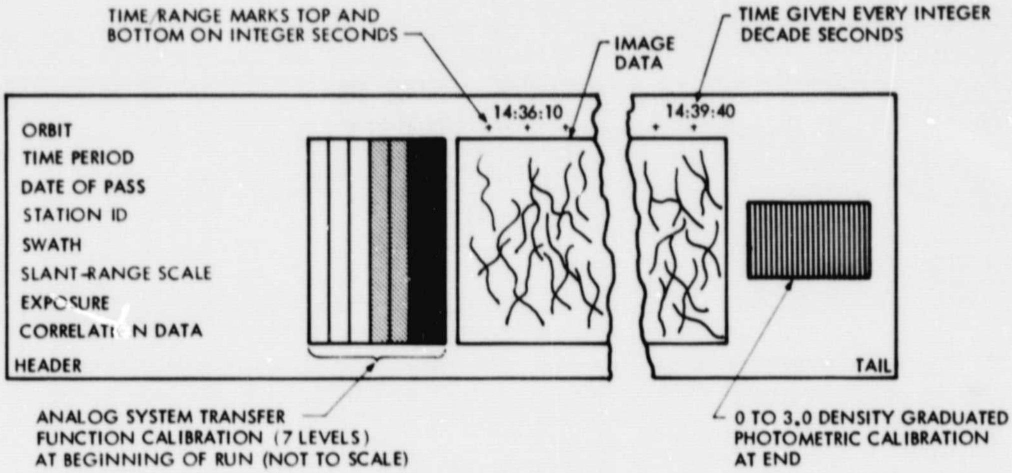

Figure 3-2. Schematic of the optically processed film output

and image parameters have been recorded every 30 s. Appendix B lists the entries in this output. The second is film imagery, which includes negatives, positives, and prints. Positives and prints have clear light areas where the radar signal is strong; negatives are dark in these areas. All products distributed to users are copies: the positives and prints are generated from the original negative, and negatives are generated from a positive copy.

The image is on 70-mm film, 60 mm of which are imagery corresponding to a 30-km, ¼ swath. A single pass is divided into four ¼ swaths, as mentioned in Section II. The total swath is about 100 km wide. The length of the run varies from the whole recorded ground station pass down to 2 min of selected data. In addition to the imagery, each film has tick marks every second at near and far range and, every 10 s, the GMT appears at near range. An amplitude calibration step wedge (each step is 3 dB) is located at the beginning of each ¼ swath and occupies about 0.6 m of film. At the end of the imagery is a 21-step sensitometric wedge, which is used primarily for photographic processing control. A label at the beginning of each ¼ swath identifies the run by station and orbit number, and includes time information and processing date. Figure 3-2 illustrates the optically processed image film format.

B. Method of Production

The signal-film-to-image-film conversion is performed by the optical correlator. Its functions include range and azimuth frequency filtering, range corrections, azimuth scaling for unity aspect ratio, and image scaling for a 1:500,000 scale. In addition, it transfers the time code from the signal film to the image film.

The data flow for the correlation process is shown in Figure 3-3. The input signal film is illuminated by a collimated laser beam. A spherical lens (range lens 1 in Figure 3-3) forms a two-dimensional Fourier transform of the data at its back focal plane. At this plane, frequency filtering is performed by a rectangular aperture that passes the range bandwidth corresponding to the chirp (frequency-modulated) spectrum and azimuth bandwidth corresponding to the Doppler spectrum. In addition, a narrowband block (50 Hz) in azimuth is located at zero Doppler to eliminate low-frequency and coherent noise.

Range migration corrections are performed by a set of three cylindrical lenses. A second spherical lens (range lens 2) retransforms the data back to image space. The output image is filtered, range corrected, and focused in range and azimuth, but the focus of each dimension occurs in a different plane. A cylindrical lens (azimuth telescope), which operates only on the azimuth focus, is adjusted to bring the azimuth focal plane into coincidence with the range focal plane. The telescope also adjusts the azimuth scale factor so that it equals the ground-range scale factor at the center of the swath. A relay lens magnifies this intermediate image onto the output film drive. The magnification factor is adjusted so that the output scale factor is 1:500,000.

The output film drive contains raw film to be exposed by the aerial image. The input and output film drives must have a very precise speed ratio so that the output film speed will match the image speed well enough to prevent blurring. In actual operation, the speeds are slightly mismatched to create a desired blurring that is actually an integration in the azimuth dimension. In this way, 25-m resolution in four looks is created from data that has an inherent resolution of 6 m in one look.

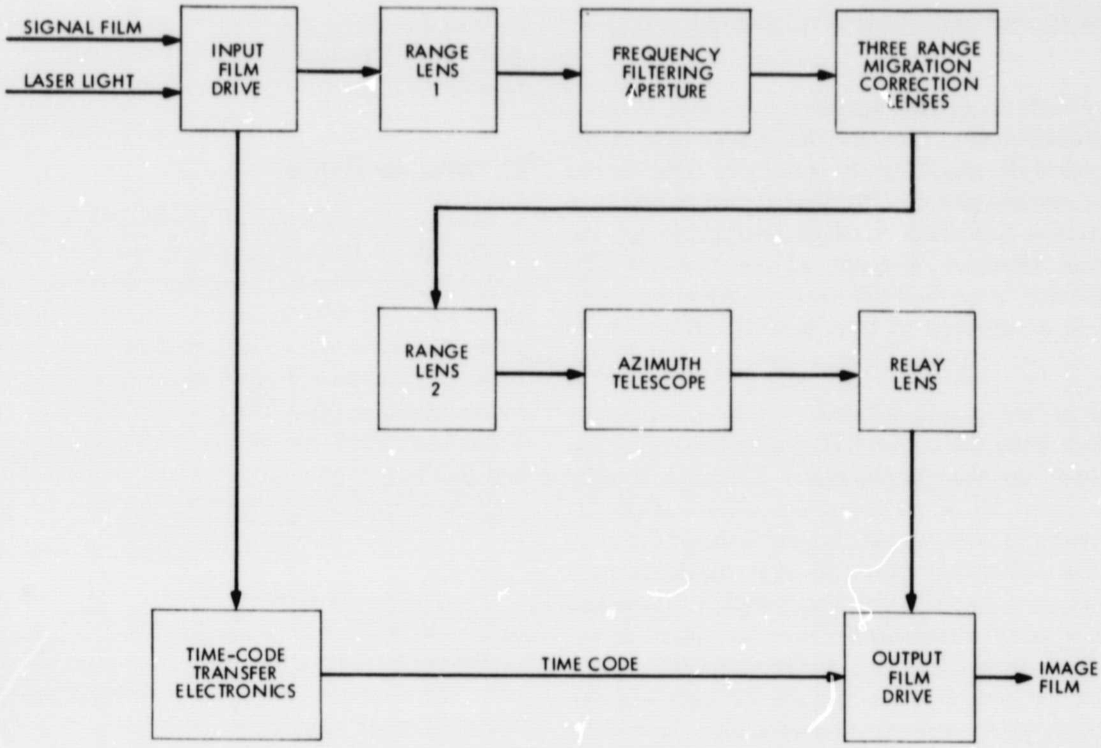

Figure 3-3. Data flow for the correlation process

C. Image Degradation

Several potential sources of image degradation occur in the correlator. Relative amplitude accuracy is affected by non-uniform illumination of the signal film during a run. Azimuth resolution can be degraded by tracking errors created by a speed difference between the input and output film drives. Position accuracy is greatly affected by the time-code transfer system and adjustments of the mirrors; these mirrors are uncalibrated and can produce large image position offsets.

There are two ways in which the correlator can cause resolution degradation. First, lens misalignment or component mispositioning can cause the image to be out of focus at the output film plane. Misfocusing is characterized by a speckle width smaller than the width of an actual point target, which might be broken up into two or more spots. Second, degradation can be caused by mistracking between the output image motion and the output film motion. Some film-drive along-track tracking error is deliberately introduced to accomplish speckle integration for multiple looks. Inadequate control of mistracking leads to azimuth resolution degradation.

The effect of film-drive jitter on resolution is determined by measuring point-target widths at the output of the correlator. Typical jitter values range from 12 to 20 m (unfortunately, film-drive jitter is not consistent), but the average value is about 15 m. This value must be added to the correlator film-drive tracking error (or integration) to determine image-film resolution.

Occasionally, range resolution may have been broadened up to 60 or 70 m by incomplete range corrections. Azimuth resolution rarely exceeded 25 to 50 m. Digital processing eliminates many of these sources of resolution degradation (see following section).

D. Image Intensity Calibration

Absolute radiometric calibration of Seasat data is very difficult. There is no reliable, absolute signal that can be used to establish an absolute reference. The receiver noise is used as a reference and is probably stable to within a decibel or two on the spacecraft. Before the tape-to-film conversion, the video gain is adjusted so that the receiver noise level driving the optical recorder is 95 mV. This value is used because most of the data is then at a level appropriate to adequately modulate the optical recorder with little saturation occurring. The receiver noise immediately preceding the transmitter turn-on is used as the evaluation point. Occasionally, there is no gain setting that will allow the noise to reach 95 mV, or there is no recorded receiver noise. In these cases,

the gain is set to some nominal level to achieve a reasonable video level.

One of the most significant obstacles to making accurate backscatter measurements, even for the relative case, is the change in signal level caused by the sensitivity time control (STC) and the antenna pattern. The STC was incorporated to change the system gain cross track to compensate for the antenna pattern. However, in nearly all the data, the STC started considerably later than the ideal compensation point; this resulted in a gain drop of from 6 to 10 dB across the swath.

Part of the processing includes estimating the gain function across the swath using the known STC position and roll information (to obtain antenna pointing angle). The gain is actually calculated for about 20 points across the 100-km swath. Its value at the center of each ¼ swath is used to adjust the video gain during tape-to-film conversion. The adjustments are made relative to the first ¼ swath gain setting, which is determined by the receiver noise measurement. However, there is still as much as 2 dB of residual gain variation across a single ¼ swath since the compensation is fixed for each ¼ swath while the actual system gain varies continuously across the swath. An estimate of the residual gain can be obtained from the values in the auxiliary data listing. The 20 points where the net antenna/STC gain are evaluated are given as part of the auxiliary data listing for every time listing (usually every 30 s). These values can be used to determine relative gain changes cross track and along track. Their accuracy is limited primarily by the roll-angle accuracy. Roll errors can contribute 1 or 2 dB of error near the swath edges.

Any calibration is also limited by the dynamic ranges of the signal and image films. The signal film has a dynamic range of 12 to 15 dB, and the observed dynamic range of distributed target imagery is 10 to 15 dB. The image film has a useful dynamic range of about 20 dB. This dynamic range rarely, if ever, limits the dynamic range of distributed targets. The primary limitation of the image film's dynamic range is on the range of point targets or partially compressed signals. Many targets of interest, such as fields, have dimensions smaller than the 15-km azimuth and 15-km range dimensions that correspond to a target of no significant compression. Targets with dimensions smaller than these values have an output dynamic range greater – by the dimension ratio – than the distributed target dynamic range. For example, a target with dimensions of 30 km by 7.5 km will be distributed in one dimension, but have a compression gain of 3 dB in the other. This 3 dB must be added to the observed 15-dB dynamic range of the signal film to estimate potential dynamic range for targets of this size. Similarly, a target 5 km by 5 km would have nearly 10 dB of compression gain, and its potential dynamic range (25 dB) would exceed the image film capability.

Unfortunately, quantitative analysis cannot be reliably performed with these data due to the many sources of calibration error.

E. Image Scale

The azimuth scale factor is affected primarily by two parts of the optical processing system, the tape-to-film conversion and the signal-film-to-image-film conversion. In both cases, the output film velocity must be carefully controlled to match either the spacecraft velocity relative to the image point (tape to signal film) or the input signal film speed (signal film to image film). A scale factor of 1:500,000 is maintained to about 0.3% after the effects of spacecraft velocity changes and film-drive mistracking are taken into account. Some passes may have larger errors than this, but most of them are closer to 0.1 to 0.2%.

The range scale factor is nominally 1:500,000 at the center of each ¼ swath, with a variation from near range to far range of about +3½% to -3½%. The assumption of a linear ground-range scale change across each ¼ swath will give good accuracy. The slant-range scale factor for each ¼ swath is given in the auxiliary data listing and expressed as slant-range m/mm of film. The ground-range scale factor at any point is determined by dividing the slant-range scale factor by the sine of the incidence angle. Incidence angles are listed for the near-range cross marks in each swath.

Another change in the ground-range scale factor occurs as a function of time. Although the slant-range scale factor remains constant for a pass, the incidence angle changes because of changes in the altitude and digitization window. A measure of this effect is given in the listing as "ground-range coverage." This value is the number of kilometers that actually occurred between the two range cross marks (assuming the image had been perfectly located). At some point near the pass center, these values will be very close to 25 km because that is where the calculations are made to set up the scale factors. The values change continuously as the altitude changes, and then make a step when the digitization window (or STC position) changes.

Geometric distortion is caused by data skew in the azimuth. A rectangle on the ground whose sides are parallel to the range and azimuth dimensions becomes a parallelogram on the image, a parallelogram whose range-direction sides are rotated with respect to the swath perpendicular. The primary cause of this effect is the Earth's rotation (and lack of compensation for it in the processing). Pitch and yaw errors also introduce this effect and may add to or subtract from the Earth's rotational effect. The angle of data skew can be as high as 3 or 4 deg.

Thus, significant errors in image scale, as well as geometric distortions, are present in optically processed data. These errors can be corrected in digitally processed images.

F. Summary

Optically processed data (e.g., Figure 2-1) provide images suitable for only qualitative analysis because of the problems listed above – resolution degradation, difficulty of intensity calibration, image scale variations, and geometric distortions. Many of these problems are alleviated by the digital processing methods discussed in the following section.

One should not, however, overlook the fact that optically processed data provides a fast, inexpensive method of surveying large data sets. It is ideal for scanning data quality, intercomparing data sets, and recognizing large-scale phenomena. Once a specific area of interest has been identified from the optically processed data, it can be digitally processed and quantitatively analyzed.

Section IV
Digitally Processed Data

A. Introduction

The digital processing technique converts SAR data into images that are both reproducible and suitable for quantitative analysis. This section discusses two general methods used to digitally process Seasat SAR data. Approximately 3% of all the data were "routinely" processed with the Interim Digital Processor (IDP), a software-based SAR processor developed at JPL (Wu et al., 1981). The products from this processor are the "production" images and tapes available from NOAA (Subsection II-A). These are listed in Table A-4 of Appendix A. While these products are superior in quality to the optically processed data also from NOAA, they do not optimally utilize the resolution, pixel location accuracy, and intensity calibration of the Seasat data. Furthermore, the NOAA digital products have not been geometrically rectified (Subsection III-E and below). The second general method for digital processing was used for a small sample of data in the course of research projects to determine the ultimate capabilities of the data set in producing the characteristics mentioned above. These "research" processors (RPs) were developed at JPL and at MacDonald Dettwiler and Associates, Ltd. High-quality images from the RPs are, however, not generally available at this time.

Both the digital processors and the optical processor use the Seasat SAR high-density digital tape (HDDT) as an input. In addition, the IDP uses the sensor status and orbital information tape (SAR SDR), while the RPs had alternative sources for orbital data (see below).

The IDP consists of a SEL computer and three array processors. It can produce one Seasat SAR frame, a 100-km by 100-km image scene, in about 2.5 h. There are approximately 5800 range data lines and 6140 pixels per line in each frame. The RP at JPL consists of a VAX 11/780 computer with one array processor, although the location and rectification steps at JPL are performed on the SEL. Depending upon the type of processing done, the RPs can produce a frame in between 1 and 10 h.

The products of the IDP are 9-track, 1600-bit/inch tapes. Tables 4-1 and 4-2 provide the format for these tapes. Photographic images (negatives) are then made from the tapes.

Table 4-1. Seasat image tape format

(File 1)	
HEADER	Record
DATA LINE 1	Record
DATA LINE 2	Record
DATA LINE 3	
.	
.	
.	
.	
LAST DATA LINE	Record
END OF FILE	
(File 2)	
HEADER	Record
DATA LINE 1	Record
.	
.	
.	
.	
END OF FILE	
.	
.	
.	
.	
(Last File on Tape)	
HEADER	Record
DATA Line 1	Record
.	
.	
.	
.	
END OF FILE	
END OF FILE	

ORIGINAL PAGE IS
OF POOR QUALITY

Table 4-2. Header record format

Item	Description	Bytes	Location	Remark
1	Title: "JPL DIGITALLY PROCESSED SEASAT RADAR IMAGE"	44	1–44	
2	Data tape ID code: xxxxyyyy	8	45–52	xxxx = orbit number (REV) yyyy = tape number
3	Frame starting time: DDD:HH:MM:SS	12	53–64	Actual time of data taken
4	Receiving station identification: SSS	4	65–68	Where SSS is three characters of station ID: ULA = Alaska GDS = Goldstone MIL = Merritt Island UKO = Oakhanger SNF = Shoe Cove
5	Processing date: DA-MON-YR	12	69–80	
6	Processing run: rrrr	4	81–84	rrrr = processing run number (begin with 1)
7	Latitude of target area: xxx:yy:N(or S)	8	85–92	xxx degree yy second N = north S = south
8	Longitude on target area: xxx:yy:W (or E)	8	93–100	xxx degree yy second W = west E = east
9	Site: (name of target area)	24	101–124	
10	Number of samples/line N_S	2	125–126	$N_S \leq 6144$
11	Total number of lines N_L	2	127–128	$N_L \leq 6144$
12	Pixel spacing in azimuth M_A	2	129–130	Typically $\simeq$ 16 m
13	Pixel spacing in range M_R	2	131–132	Typically $\simeq$ 18 m
14	Resolution in azimuth R_A	2	133–134	Typically 25 m
15	Resolution in range R_R	2	135–136	Typically 25 m
16	Blanks	6008	137–6144	

Before November 1980, the negatives (10 by 13 cm) were produced with a Dicomed Model D47 that averaged 3-pixel by 3-pixel arrays from the tape. This resulted in an image resolution of about 75 m. Since November 1980, the negatives are produced with an Optronics Photowrite System 1500. These are 20- by 25-cm negatives that feature the maximum resolution of approximately 25 m in both the range and azimuth directions. A label placed on the near-range side of each image contains the information listed in Table 4-3.

Table 4-3. IDP image label format

Label	Description
1. NASA JPL Seasat SAR image	Standard
2. Digitally correlated	Standard
3. Spacecraft track ← XXX.X deg 0 to 360 deg indicates spacecraft flight direction based on clock angle orientation with 0 deg being north and 180 deg being south.	
4. ASC or DSC	ASC: ascending revolution DSC: descending revolution
5. Number of pixels XXXX azimuth XXXX range	 Roughly 6144 pixels Roughly 5800 pixels
6. Pixel size center of image 16-m azimuth 18-m range	Standard
7. Rev. XXXX AAA	Revolution number, receiving station abbreviation GDS: Goldstone, CA MIL: Merritt Island, FL ULA: Fairbanks, AK UKO: Oakhanger, United Kingdom SNF: Shoe Cove, Newfoundland
8. Site	Nominal site name at center of image
9. LAT XX°XX' LON XXX°XX' W or E	Latitude degrees, minutes, north Longitude degrees, minutes, west or east
10. XXX	Number of Julian day, 1978
11. XX H XX M XX S	Time of center of image in hour, minute, second
12. Processed XX AAA XX	Day/month/year
13. File No. XXXXXXXX	IDP reference tape file
14. GRID – azimuth and range image borders	Pixel spacing in 100-pixel increments
15. Grey scale – top of image	16 divisions of 256 pixel values
16. JPL logo	

The following subsections describe the characteristics of digital products obtained with the various digital processors. Table 4-4 summarizes several key parameters of the images produced by the IDP.

Table 4-4. Parameters of IDP images

Parameter	Value
Input raw data, bits/sample	4
Range resolution, m	25
Azimuth resolution, m	~25
Range peak sidelobe ratio, dB	–15
Azimuth peak sidelobe ratio, dB	–6 to –9
Number of looks	4
Pixel dynamic range	Selectable 48 dB in 8 bits amplitude (over 70 dB total)

B. Resolution

The IDP processing algorithm is capable of achieving an image resolution of about 25 m in both range and azimuth, although a routinely processed image may have a resolution slightly worse than 25 m due to an error in estimating the focusing parameters. The resolution was measured by examination of the SAR responses from an array of corner reflectors located near the Goldstone Tracking Stations. Figure 4-1(a) shows one of these. Each corner reflector appears as a distinct point in the SAR image (Figure 4-1(b)). The intensity distribution of pixels around the peak responses of the reflectors was measured and indicated a 3-dB resolution of about 25 m.

Another way to characterize the resolution is by the integrated sidelobe ratio (ISLR), or the ratio of energy in an image sidelobe to that of the mainlobe. For the IDP, this quantity has a value of –6 to –9 dB. Figure 4-2 shows an optical and a digital image of the same scene near the Goldstone Tracking Station. The star-like object near the lower center of the images (arrows) is the SAR reflection from a 26-m antenna. It is clear that the digital processing reduced the ISLR at least in the along-track direction, since the reflected image is significantly smaller in the lower picture. Note that the corner reflector array is evident as a row of bright dots to the lower left of the antenna.

As discussed in Subsection I-C, the Seasat synthetic aperture was generally divided into four looks. Thus a factor of four was sacrificed in resolution (resulting in the 25-m azimuthal resolution discussed above) in exchange for a reduction in the complexity of image production and a better signal-to-noise ratio in the resultant image. Figure 4-3(a) is an image created from one of the four constituent looks; Figure 4-3(b)

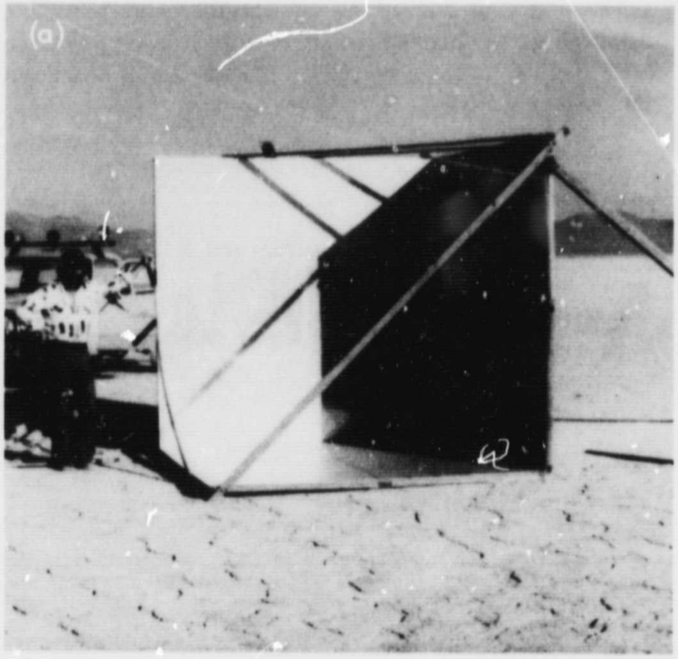

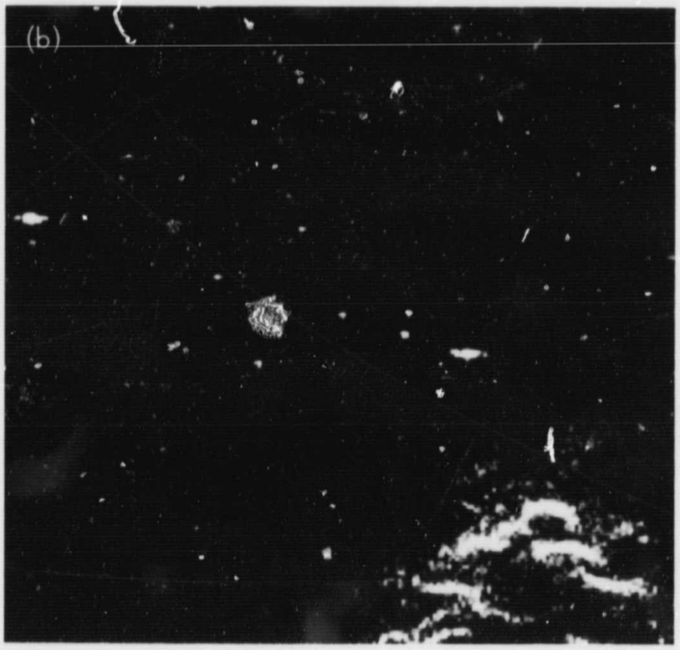

Figure 4-1. Corner reflector: (a) 2.6-m cubic corner reflector; (b) corner reflector array in a Seasat SAR image

is the summed four-look image. The bands in the one-look image are due to antenna gain differences that are essentially averaged out in the four-look image.

Alternatively, if the entire aperture is used for one look, the theoretical azimuthal resolution of the Seasat SAR is about 6 m (Subsection I-C). This resolution has been demonstrated in practice with an algorithm called the "hybrid processor" developed for the RP at JPL (Jin, 1981). This algorithm uses exact range and azimuth reference functions that allow the image sidelobes to be significantly suppressed by weighting. The ISLR can be reduced to as small as −24 dB. Figure 4-4 shows plots of the compressed and weighted corner reflector waveforms in the azimuth and range dimensions, employing the full aperture. The resulting resolution is 6 m in azimuth and 25 m in range. In principle, all Seasat SAR data can be processed in this manner.

C. Pixel Location Accuracy

A pixel in a SAR image can be located accurately in terms of its longitude and latitude on the Earth's surface, provided the location of the spacecraft and the sensor operation parameters are known exactly (e.g., Curlander, 1982a). However, the IDP products available at NOAA are not suitable for precise pixel location for two reasons. First, these digital images have not been geometrically rectified. Second, the only absolute references given to ground positions for these images are the latitudes and longitudes of the swath centers. These coordinates were not intended for ultimate accuracy and can be offset by as much as 5 km from the actual position. The process of geometric rectification includes a conversion from slant range to ground range, and the removal of data skew. In the azimuthal dimension, image pixels of the same along-track position (a column in the Seasat SAR image) are produced from targets on the Earth's surface that respond to the sensor with the same instantaneous Doppler frequency. This column of pixels traces a curvilinear path on the Earth's surface. To be directly comparable to a surface map, the curvilinear paths must be straightened (i.e., the data skew must be removed; see also Subsection III-E). Since the effects mentioned above are not corrected in the NOAA digital imagery, only approximate comparisons can be made with surface maps.

The IDP in conjunction with an additional software package (Curlander and Pang, 1982) can produce digital images that are geometrically rectified with pixels absolutely located to within 50 m, using only the spacecraft ephemeris data and the characteristics of the data collection and processing system. This capability can be used to mosaic disjointed data sets without the aid of ground reference points. Figure 4-5 shows an example of a mosaic produced in this manner.

The precise location of pixels in the Seasat SAR imagery has been studied with RPs by Curlander (1982b) and MacDonald Dettwiler (1982). Given the position of the satellite at the time the radar data are acquired, the range of the pixel, and the Doppler parameter used in the image reduction process, the location of the pixel is determined by the

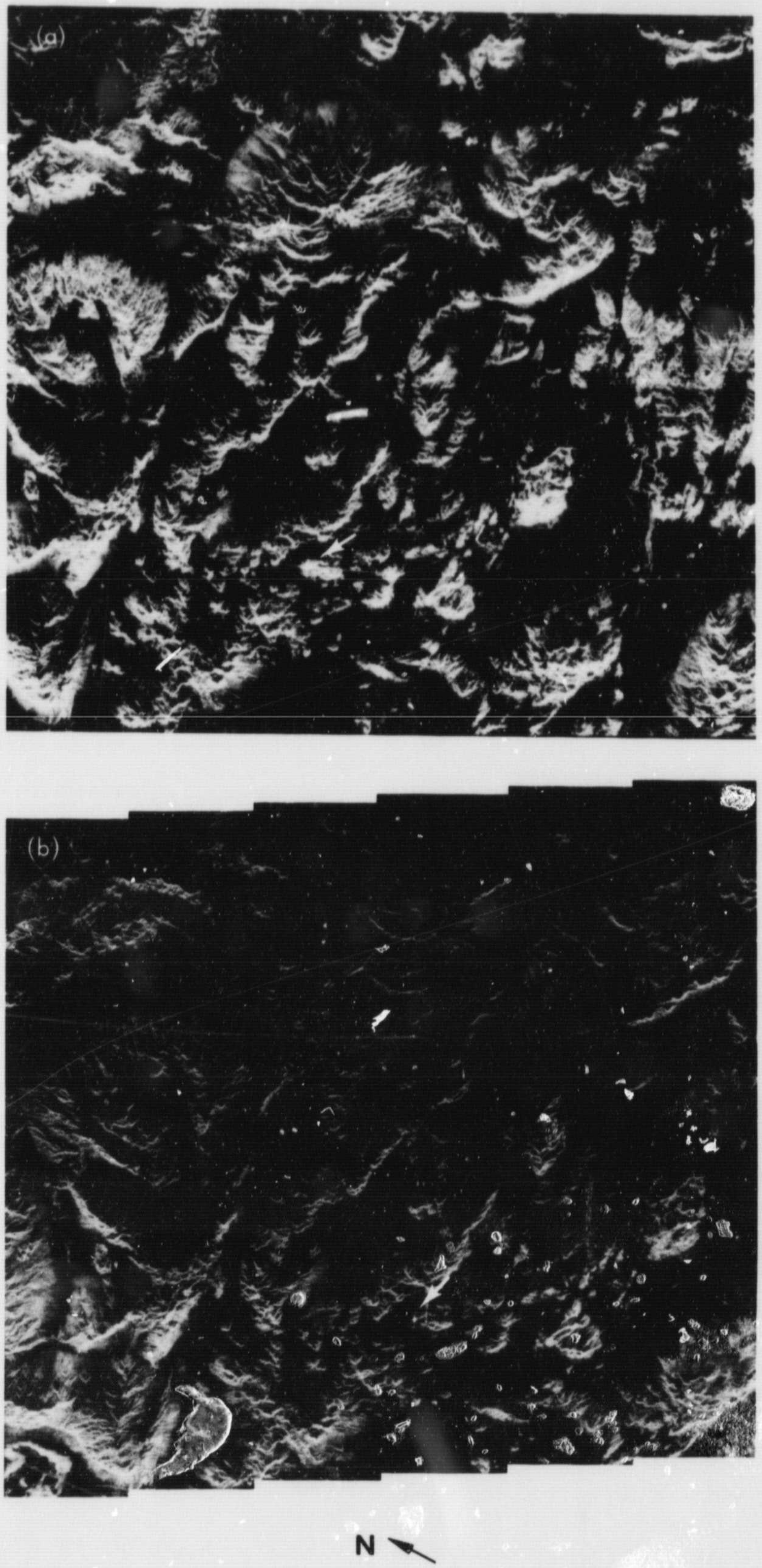

Figure 4-2. Images of Goldstone: (a) optically processed; (b) digitally processed

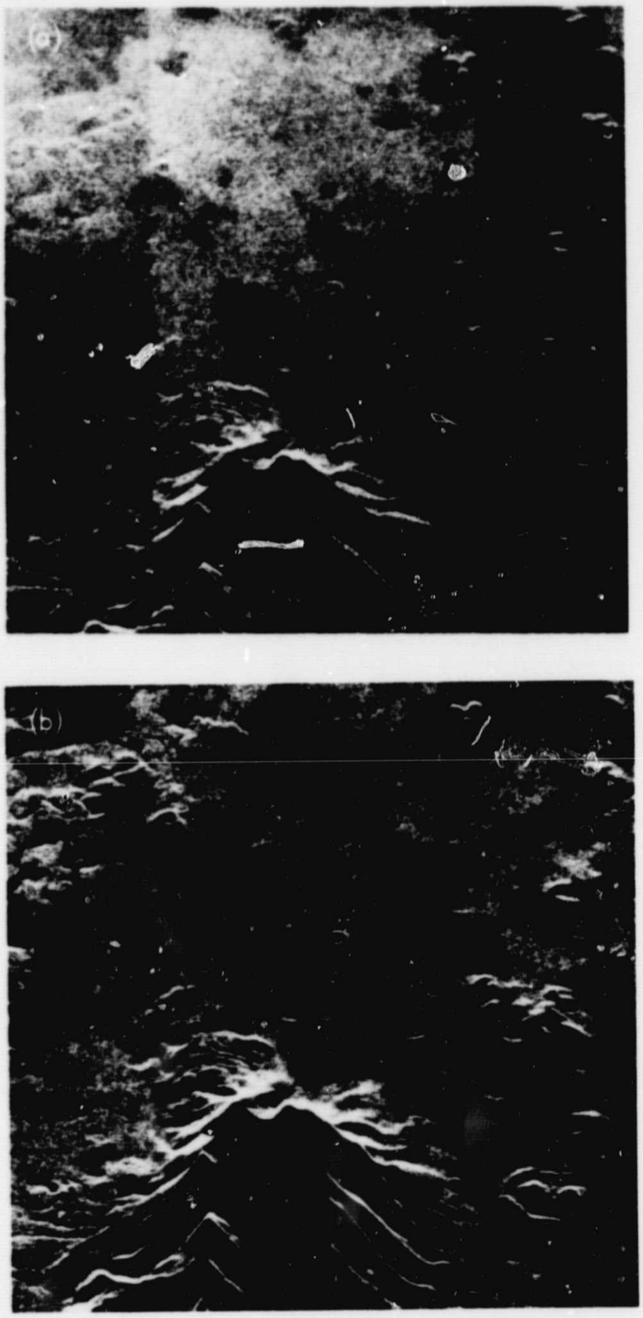

Figure 4-3. Seasat SAR imagery (1024 × 1024 pixels): (a) single-look; (b) four-look

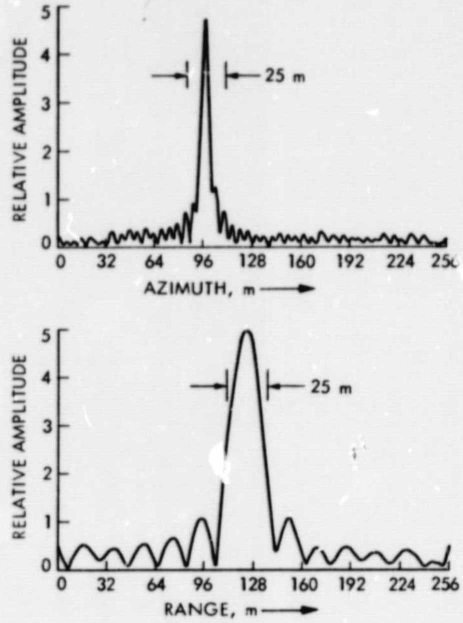

Figure 4-4. Seasat SAR resolution with the hybrid processor

intersecting point of three planes. These are the spherical plane of constant range to the spacecraft, the conic iso-Doppler plane (on which the target will respond at a constant Doppler frequency to the SAR sensor), and the plane of the Earth's surface. The coordinates of the target can be obtained by solving the three simultaneous equations that describe these three curved planes.

Several potential sources of error are:

(1) Inaccuracies in the spacecraft ephemeris data.

(2) Deviation of the geoid from an assumed model (e.g., an ellipsoid).

(3) Missing data lines.

(4) Map location interpretation error.

The major source of location error is due to inaccuracies in the spacecraft ephemeris data. Curlander (1982b) compared the results of pixel location using the ephemeris data on the SAR SDR tapes with the results obtained using high-precision orbit data (10-m, 3-σ accuracy in each of three axes) from Code 900, Goddard Space Flight Center. An absolute location error of as much as 250 m based upon the SAR SDR ephemeris data was reduced to less than 50 m in both range and azimuth with the high-precision data (Curlander, 1982b). The two ephemerides agreed to within 20 m in spacecraft location, but the SAR SDR spacecraft velocity values apparently had an average error of nearly 1 m/s, which accounted for the larger location error.

Another key parameter included with the emphemeris data is the ground clock time. Synchronization between the clocks in the data formatting process and the orbit tracking and determination process is extremely important. While the MacDonald Dettwiler analysis obtained a pixel location accuracy of better than 50 m in several cases, they also analyzed data in which a bias of 6 km was introduced by apparent time-code errors (MacDonald Dettwiler, 1982).

ORIGINAL PAGE IS
OF POOR QUALITY

Figure 4-5. Mosaic of Seasat SAR digital images

Errors in the modeled target range can also degrade position location accuracy. These can arise from deviations in the assumed shape and radii of the Earth (geoid) or from imprecisely known target elevations. Curlander (1982b), for example, employed a 25th-order polynomial for the geoid with a resolution of approximately 100 km. MacDonald Dettwiler (1982) found that hilly areas could increase the position-location error to as much as 80 m.

The spacing between raw data lines corresponds to about 4 m on the Earth's surface. Data lines were sometimes "lost" during the recording or playback processes (e.g., due to loss of synchronization). Since there were typically 50 to 75 data lines lost over all the processing stages for each 100-km IDP image frame, a significant position error could accumulate if the missing lines were not taken into account. This error was eliminated in the processing method of Curlander (1982b). The last of the possible sources of error listed above (map error) is simply a reminder that a reliable ground survey is necessary for comparison with the satellite results.

D. Radiometric Calibration

The amplitude information available on the IDP-generated imagery at NOAA is of a limited usefulness with regards to radiometric calibration. An 8-bit integer, equivalent to a dynamic range of 48 dB, describes the amplitude of the radar echo in each pixel. However, essentially no calibration was performed for these products. In addition, the effect of the mispositioned STC (Subsection I-C), which introduces a large, spurious gain change across the image, is present. In fact, the limits of the 48-dB range were arbitrarily chosen for each image from a total input data range of 70 dB to maximize a more-or-less subjective appearance for the image.

Other positive features of the data (e.g., linearity and stability), however, indicate that an effort to provide this calibration would be worthwhile. Measurements have shown that the Seasat SAR system exhibits near-linear gain performance below an 8-bit saturation level. MacDonald Dettwiler (1982) carried out an experiment to test this linearity with imagery of the Goldstone target array described above (Subsection IV-B). They found that after corrections, the theoretical backscatter amplitudes and the measured backscatter amplitudes were well correlated (linear regression correlation coefficient of 0.970 and a slope of 0.954). Single-pass linearity was good despite considerable saturation in the signal data, and pass-to-pass stability was maintained with only a 1.1-dB gain variation.

A calibration experiment was performed at JPL (Croft, 1982) and analyzed on an RP. The data were acquired in ten passes over the Cottonbaii Basin area of Death Valley. Within the basin, eleven sites were selected to represent a range of backscatter intensities, and the measured values at the sites (9-pixel by 9-pixel or 144-m × 144-m area) were calculated for each pass. A largely automatic technique was developed that made a series of gain corrections (before correlation) for the STC waveform, target range variations, changes in antenna gain, and gain variations in the data link. In addition, a thermal noise component was subtracted from the data. The results indicated that, aside from passes with saturated data, Seasat SAR images can be calibrated to an interpass variation of 1 to 2 dB, a considerable reduction from an uncorrected value of about 4 dB. Figure 4-6 shows a linear regression plot of these data. The passes that show variations greater than 2 dB

ORIGINAL PAGE IS
OF POOR QUALITY

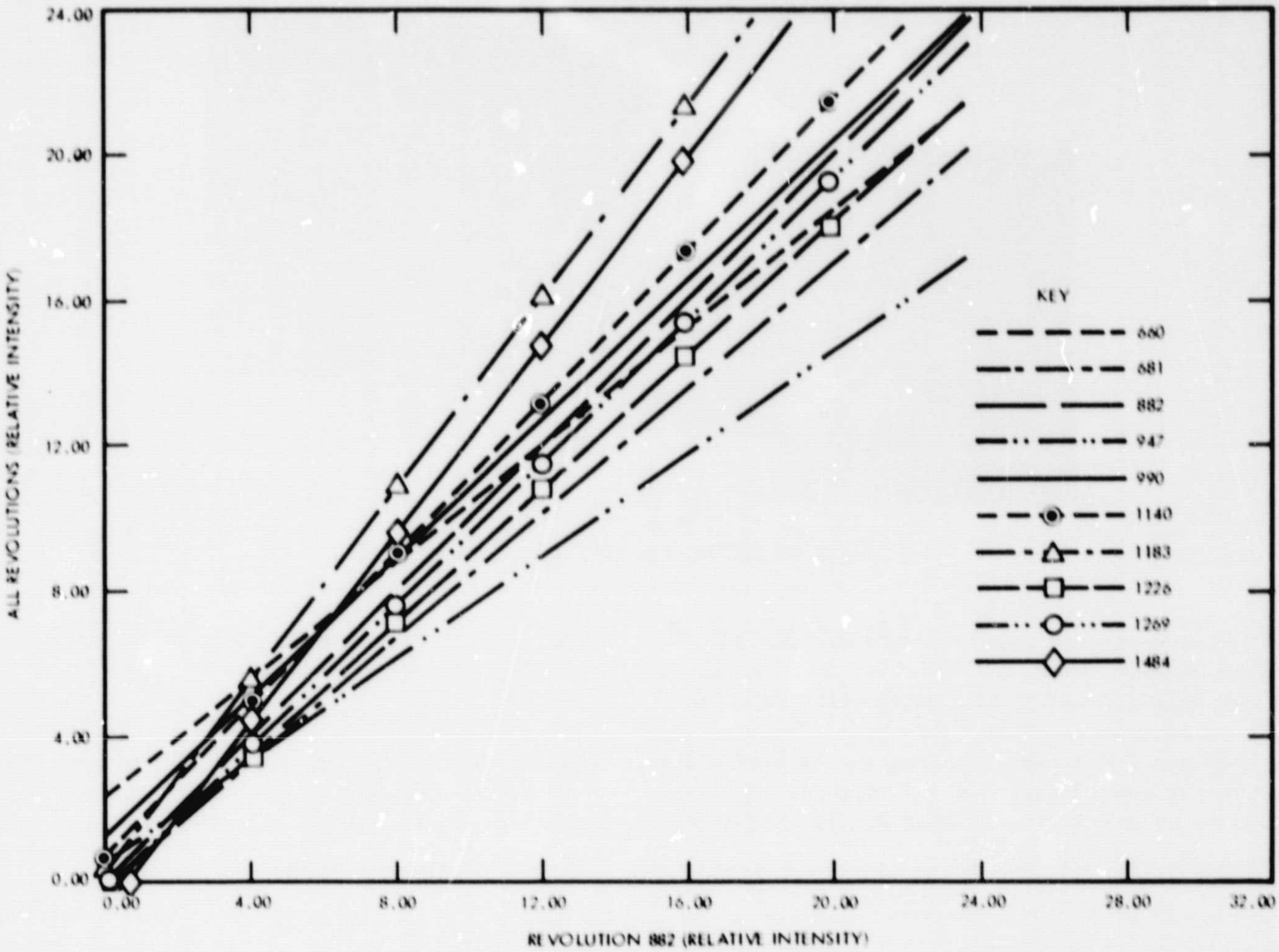

Figure 4-6. Intensity after all corrections

(Revolutions 947, 1183, and 1484) contain either known or suspected cases of saturation (see Subsection V-A).

Although the calibration procedure described by Croft (1982) is largely automatic, the fact that data screening is necessary precludes its use on a production basis. The possibility of undetected saturation in a data set also limits the accuracy of radiometric calibration. However, it was demonstrated that a significant improvement can be achieved in this data set, and that with a similar effort it is likely that a typical Seasat image can be comparably calibrated.

E. Summary

We have discussed in this section the characteristics of digitally processed Seasat SAR data. Improved algorithms, developed after the digital data at NOAA were processed, result in imagery with 6-m by 25-m resolution, better than 50-m position location accuracy, and 2-dB relative amplitude calibration for unsaturated data. While the NOAA data set is the best currently available for the general user, the possibility that selected data can be reprocessed with the above improvements should be noted.

Section V
Problems, Artifacts, and Peculiarities of SAR Data

This section will illustrate with processed images a number of features that could be present in Seasat SAR data. Some features arise from hardware problems (e.g., the previously discussed mispositioning of the sensitivity time control – STC), others from transient outside effects such as the weather, and some are simple geometric effects inherent in SAR data.

A. Saturation

A major difficulty with Seasat SAR data is caused by the limited dynamic range in many parts of the system. Saturation can occur in the analog-to-digital signal conversion, the data link, the SAR processor, or any combination of these. Figure 5-1 shows an example of saturation of the data link in both the raw and processed data. The white streaks in the image and the striped patterns in the raw data are due to retriggered chirp pulses that were to have been used for image calibration. However, because of a hardware failure in the flight electronics, the pulses exceeded the dynamic range of the data link. (See Subsection V-D.)

Another result of signal saturation is weak-signal suppression. In this case, the signal from a dim target appears to be suppressed by a very bright target in proximity. Furthermore, the suppression is stronger as the distance between a dim target and the bright target is reduced. This effect is due to limited quantization of intermediate products in the IDP and causes a nonlinear loss (more for dimmer targets) in detectability due to saturation of the partially correlated radar signals. An example is shown in Figure 5-2. The horizontal linear feature in the upper half of the picture is the Santa Ana River. The dark bands (arrows) next to several bright features right above the river are oriented in the azimuth direction, and are due to weak-signal suppression.

B. Azimuth Ambiguities

Ambiguous target responses are mainly due to sidelobes in the antenna radiation pattern. In the azimuth dimension, the target Doppler spectrum corresponds to the antenna response in that direction. The finite radar PRF sampling in azimuth results in the foldover of Doppler spectral energy from the sidelobes into the mainlobe. This aliasing effect produces ambiguous target response in the azimuth dimension. The PRF ambiguities normally do not produce visible effects because of the predominance of the mainlobe. However, strong targets such as the one illustrated in Figure 5-3 will produce ambiguities. The brighter features (A) in this image of Lake Pontchartrain, New Orleans, are caused by the ambiguous response of the very bright area (B) located 6 km southeast of the eastern shore.

Range ambiguities are more difficult to verify because the targets responsible are located outside the imaging swath and cannot be referenced without using another image.

ORIGINAL PAGE IS
OF POOR QUALITY

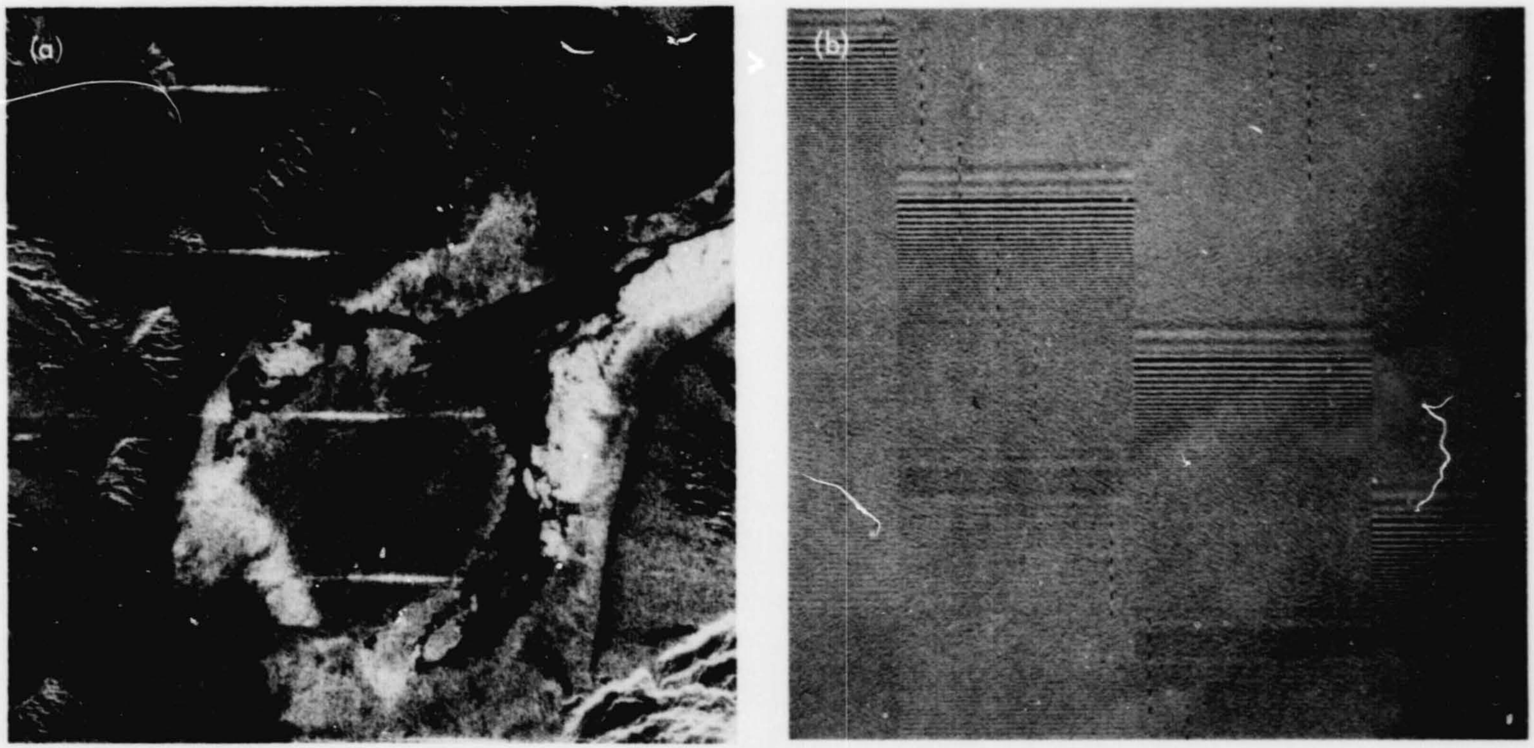

Figure 5-1. Saturation in Seasat SAR data link: (a) image; (b) raw data

ORIGINAL PAGE IS
OF POOR QUALITY

Figure 5-2. Azimuth weak-signal suppression effect

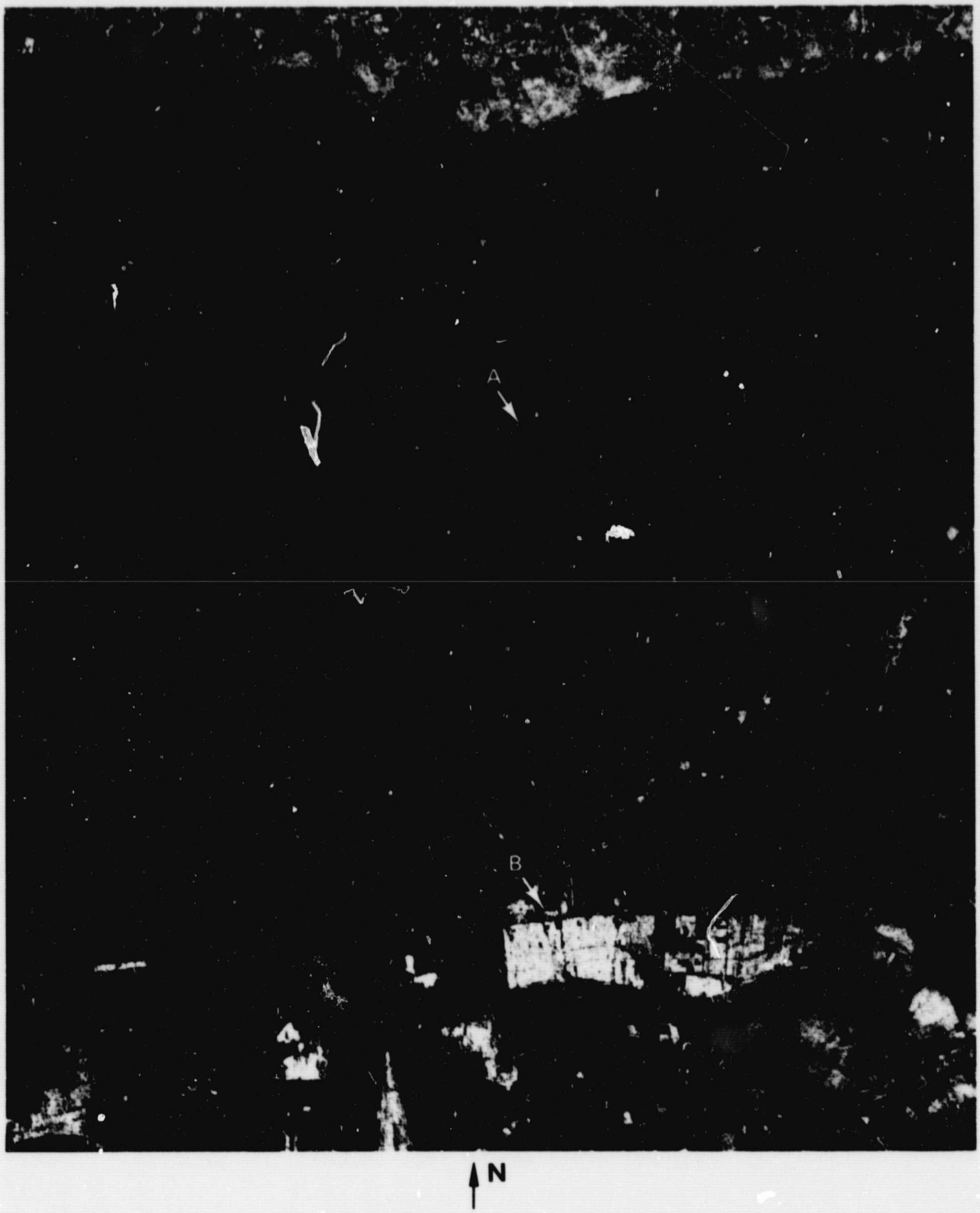

Figure 5-3. False features induced by azimuth ambiguity

The centroid of the azimuth spectrum varies across the track since the Doppler frequency is a function of the look angle. If the processor sets the azimuth frequency window for center swath, the ambiguity level increases and the azimuth resolution degrades at near and far range. Because the azimuth Doppler frequency changes with latitude, the spectrum can move out of the frequency window if the processor does not employ Doppler tracking during a pass. This loss of window results in increased ambiguities and degraded azimuth resolution. Figure 5-4 shows an optically processed image for which the azimuth spectrum has shifted out of the azimuth frequency window at the end of the pass. The true features at A are repeated as false features (ambiguities) at B. Note that the lower image is significantly out of focus, a problem unrelated to ambiguities.

C. Atmospheric-Related Features

For Seasat SAR, performance degradation is expected to be worse in the auroral geomagnetic regions. These are areas surrounding the north and south geomagnetic poles within which intense auroral activity occurs. Many Seasat SAR passes are 3000 km to 4500 km long; ionospheric scintillation effects can vary significantly along track, and thus azimuthal resolution can vary during the pass. In particular, the ULA ground-station antenna coverage pattern can accommodate SAR data from ground latitudes of about 48°N to 74°N over the same pass. During such a pass, the spacecraft passes from a region of low geomagnetic activity into a tansitional region and finally into the auroral region, within which intense auroral activity may occur, degrading azimuthal

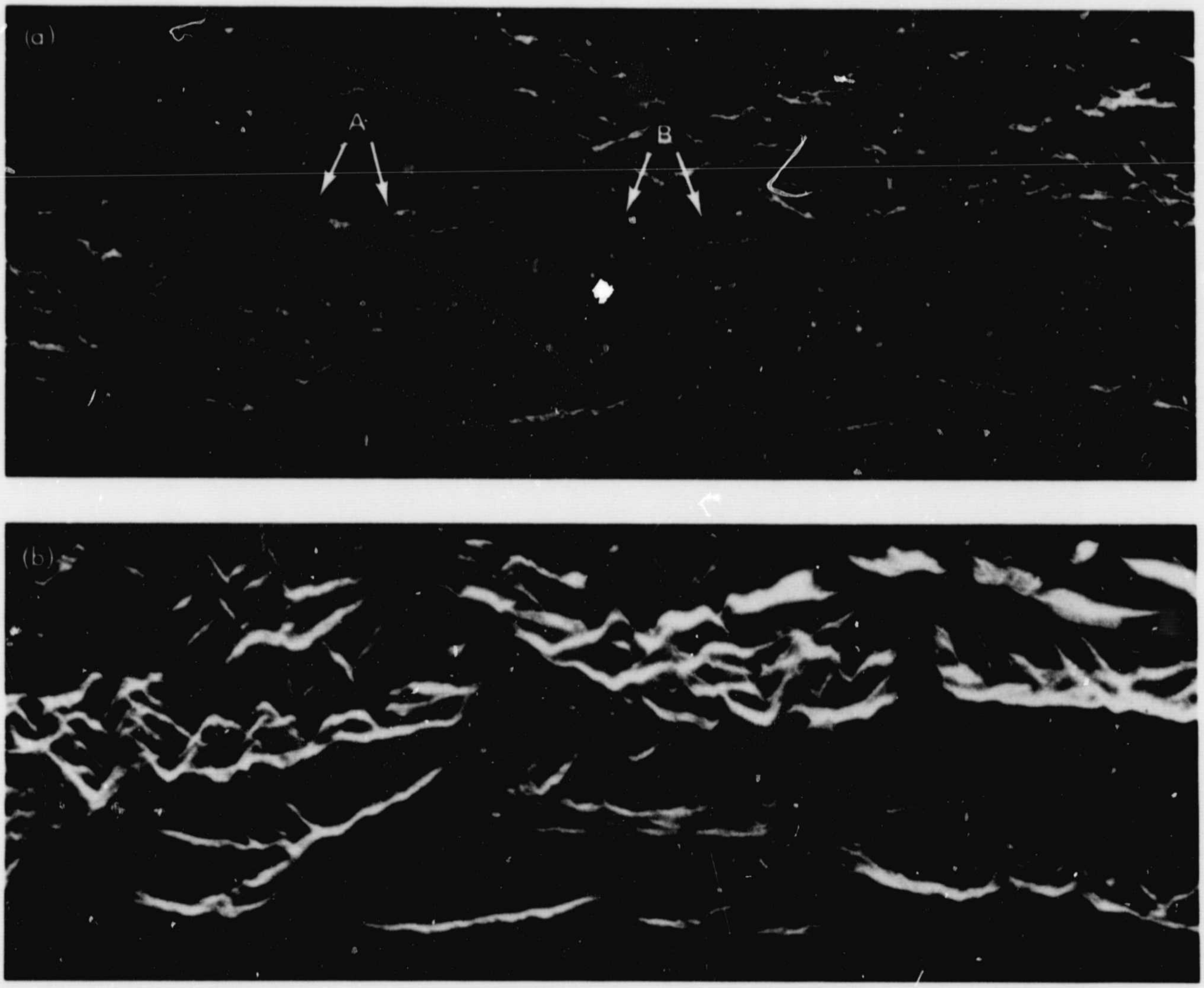

Figure 5-4. Ambiguities in SAR imagery of Juneau, Alaska: (a) azimuth ambiguities in GDS image; (b) ambiguities absent in ULA image

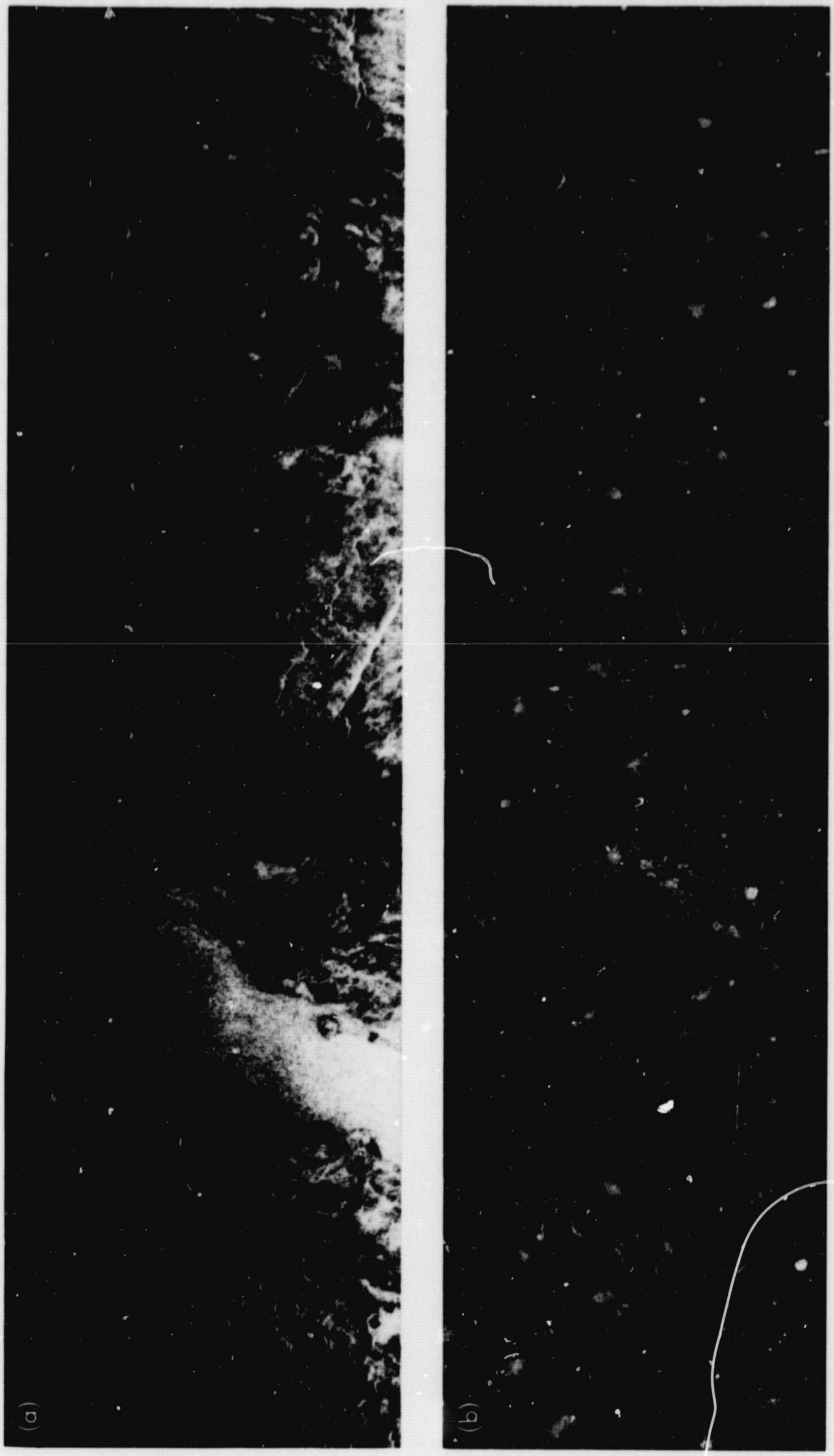

Figure 5-5. Banks Island radar images: (a) high geomagnetic activity for Revolution 894, ULA; (b) low geomagnetic activity for Revolution 1023, ULA

resolution. Figure 5-5 shows images of the Banks Island area for two different passes. The first pass (upper picture) occurred during a time when the geomagnetic activity was reported to be high; the second pass (lower picture) when the activity was low. Since the two images were recorded about two weeks apart and were both optically processed, real changes on the ground (ice melting) and differences in the processing parameters contributed to the differing appearances of the images. In fact, the effect of enchanced geomagnetic activity on Seasat SAR images has never been measured in a controlled experiment. However, these images are at least illustrative of the possibility, as mentioned in Subsection I-B, that magnetic storms, which cause ionospheric irregularities, may degrade image quality.

Weather can also create features that appear on both land and ocean imagery. The scene of Ames, Iowa, shown in Figure 5-6, contains a number of bright streaks running from the upper right to the lower left of the image. These are caused by rain-soaked ground, which exhibits high reflectivity (Ford et al., 1980). Other atmospheric phenomena are discussed and illustrated by Fu and Holt (1982).

Figure 5-6. Ames, Iowa, with bright streaks due to rain-soaked ground

D. Sensor-Related Artifacts

The Seasat SAR had a built-in test signal intended to aid in data processing and calibration. However, a prelaunch failure occurred in the circuitry responsible for the precision level of the pulse. In early SAR imaging passes, the calibrator was commanded on for the entire duration of the pass. However, since the images showed a bright line down the center (Figure 5-7), the calibration pulse was commanded off for the later imaging passes. Notice the small circular feature near the calibration pulse in the center of Figure 5-7. This is the famous Barringer Meteorite Crater located near Winslow, Arizona.

During several passes, the gain state of the SAR receiver was changed while transmitting. This resulted in image intensity variations and caused an abrupt phase change in point-target echoes at the instant of gain change. Figure 5-8 shows an optically processed image during which a gain change was made, and a comparison image of the same scene when the gain was not changed.

The sensitivity time control (STC) function was initiated by stored commands in the satellite at times based upon predicted variations in slant range (Subsections I-C and II-B). Sometimes a jump in the STC position, the "digitization window," occurred during data acquisition for a particular image. In these cases, the portion of the image obtained after the jump was shifted relative to those portions obtained before the jump. Figure 5-9 illustrates a particularly egregious example of this in which the lower quarter of the image is shifted almost 20 km to the left relative to the upper part. The arrows mark the location of the shift.

E. An Inherent SAR Feature

Not all effects are caused by sensor malfunctions or vagaries of the weather. Figure 5-10 illustrates an effect due to the physics of radar wave interaction with the ground scene. These images are from two different passes over the same urban scene but with different radar aspect angles. In the upper image, the radar line of sight was along a direction preferred for reflectively of the targets contained in the bright rectangular section; in the lower image, the radar illumination is not along this preferred direction.

ORIGINAL PAGE IS
OF POOR QUALITY

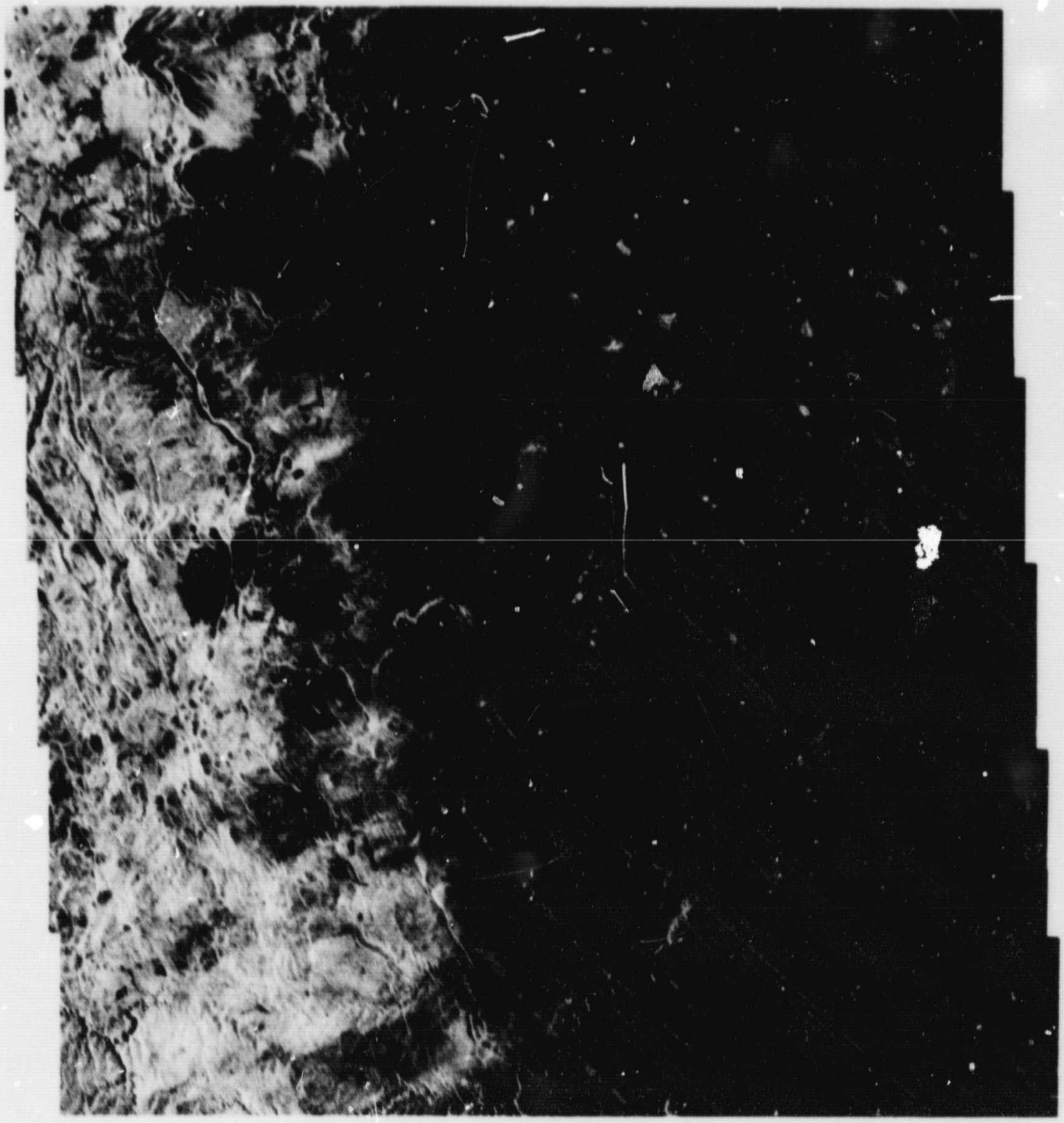

Figure 5-7. Imaged calibrator pulse

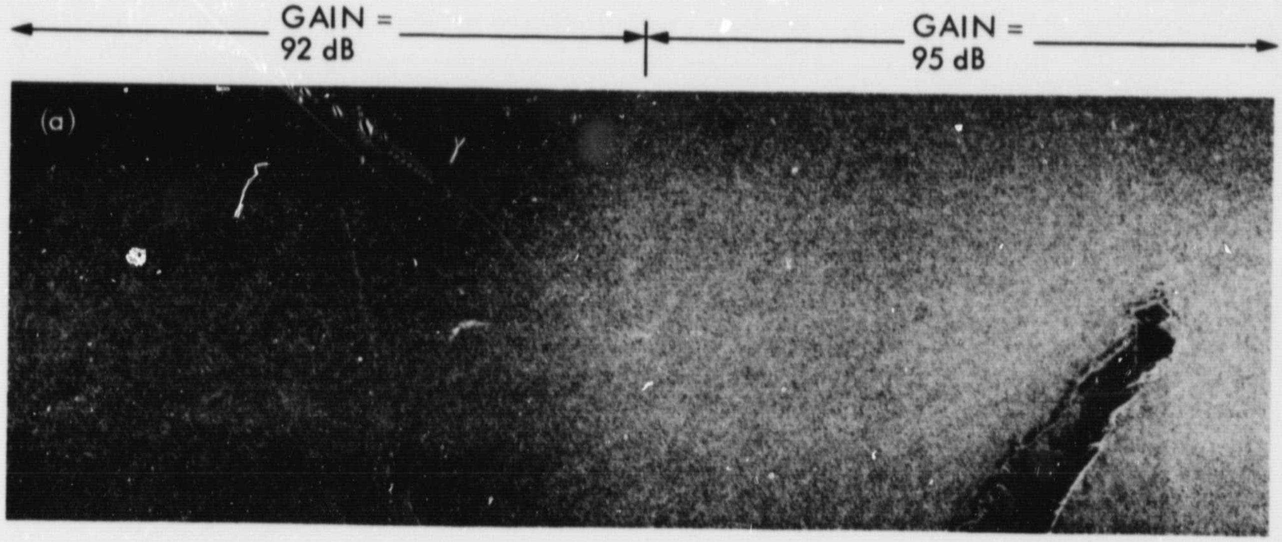

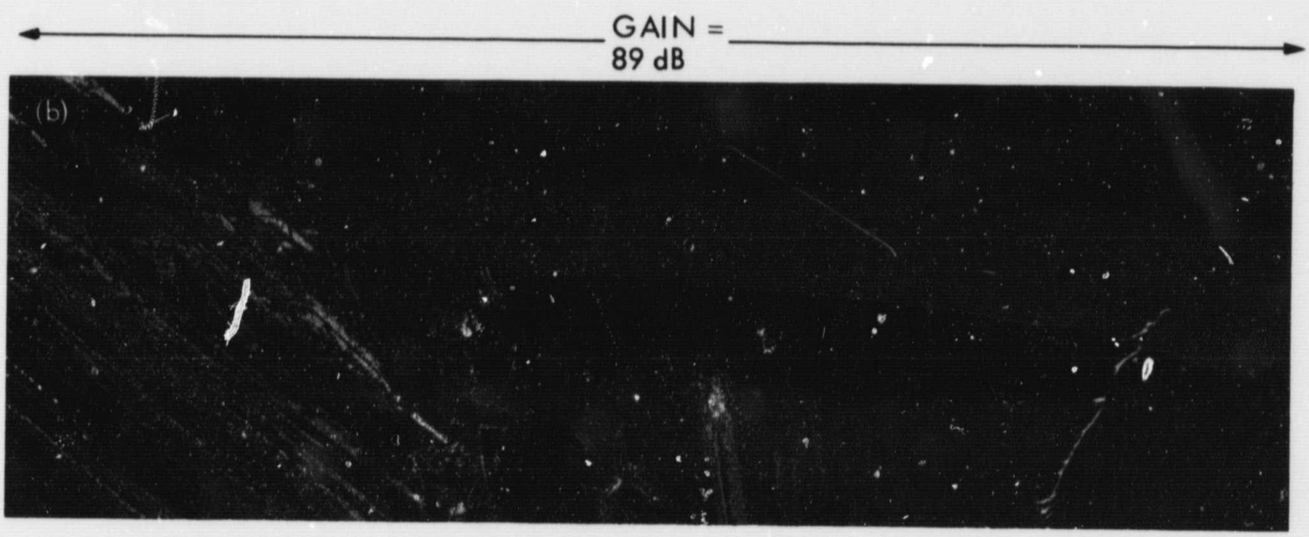

Figure 5-8. Receiver gain: (a) change in Revolution 416, GDS; (b) no change in Revolution 1205, GDS

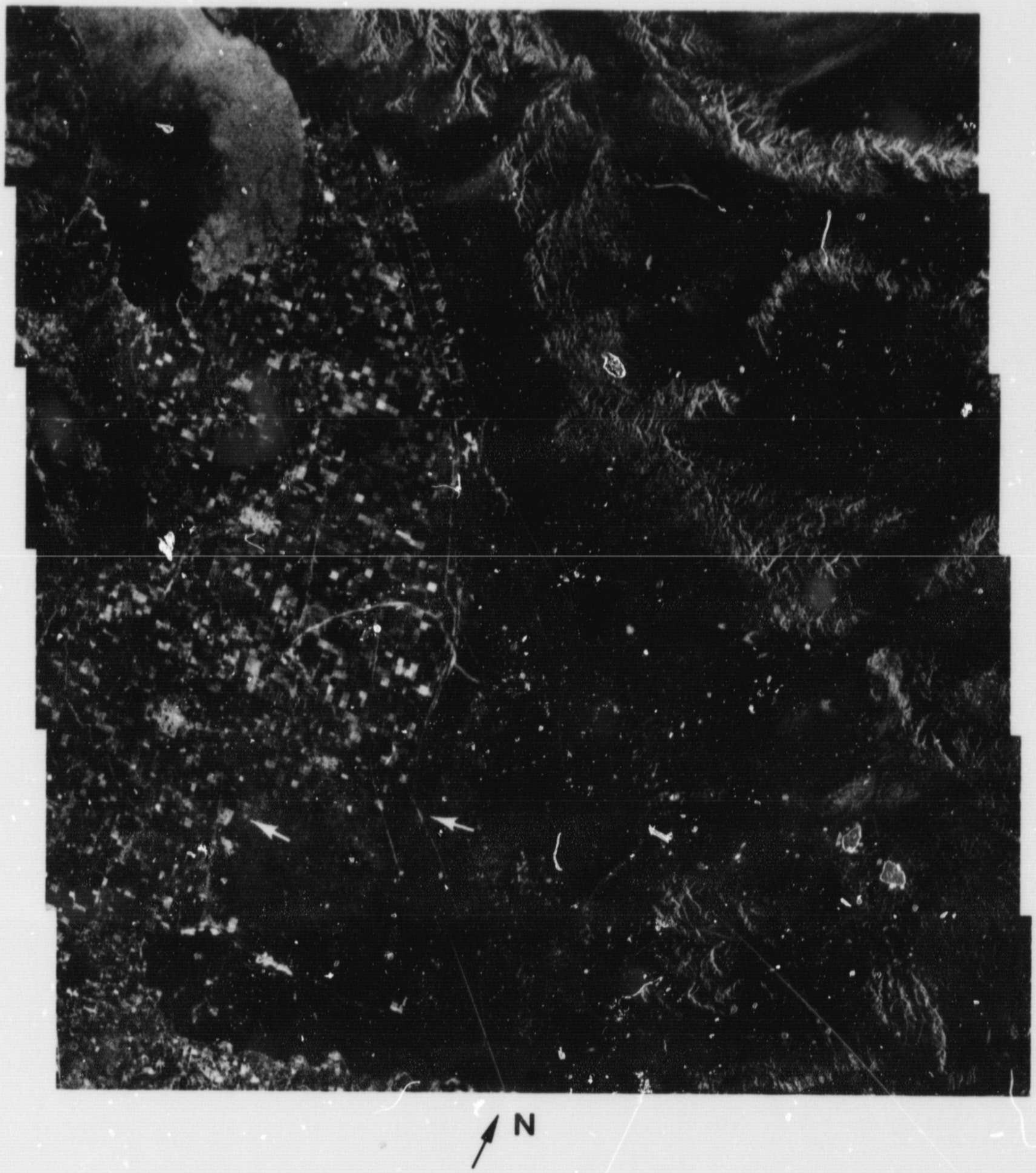

Figure 5-9. STC change during a pass

ORIGINAL PAGE IS
OF POOR QUALITY

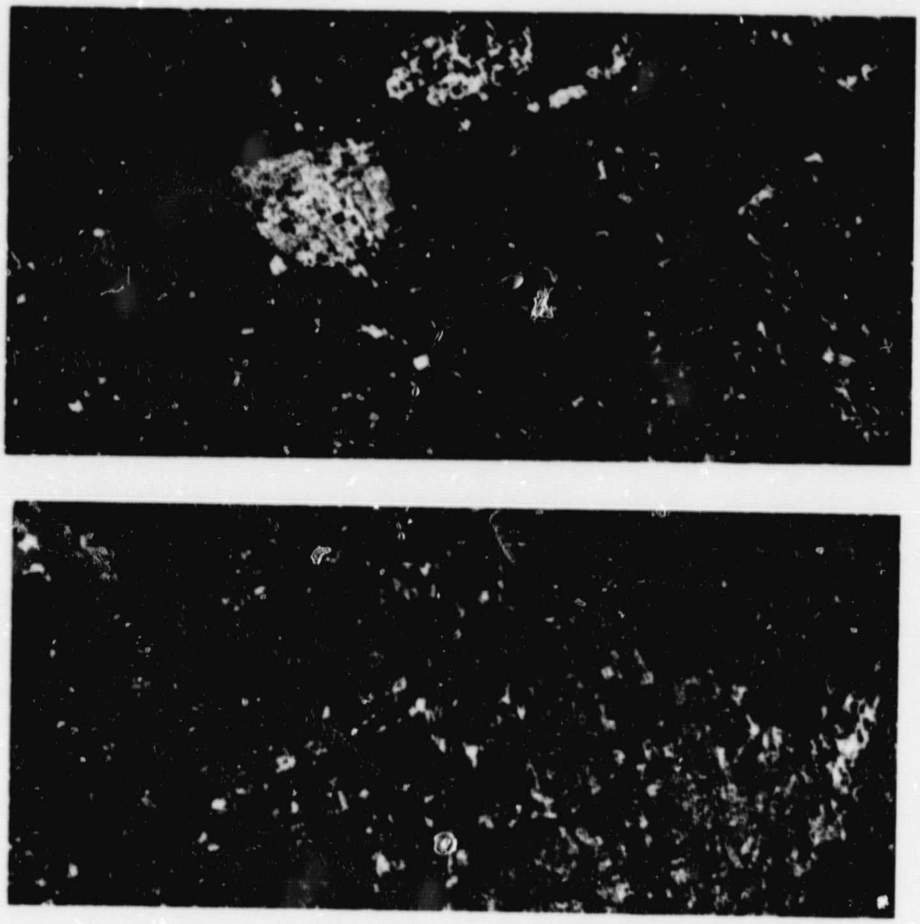

Figure 5-10. Effect of radar aspect angle on the apparent target reflectivity

Section VI
Scope of Seasat SAR Observations

A. Pictorial Outline

The following images (Figures 6-1 through 6-14) are illustrative of the types of targets viewed by Seasat. Many more scenes with detailed captions can be found in the geographic atlas of Ford et al. (1980) and the oceanographic atlas of Fu and Holt (1982). Some of the images contained herein also appear in these references. The first seven figures are land targets while the others are over water and ice.

B. Seasat SAR Data Base: Past and Future Uses

Many scientific results have been extracted from the Seasat SAR data. Comparisons between it and data from other satellites (e.g., Landsat) have proven to be quite revealing. The atlases of Ford et al. (1980) and Fu and Holt (1982) give particularly striking examples of such comparisons. Appendix C gives a partial listing of Seasat SAR scientific publications.

Much analysis, however, remains to be done. Quantitative analysis using digitally processed data is still in its early stages. It is complicated by the problems discussed in earlier sections as well as incomplete understanding of, for example, ocean phenomena and their interpretation with the SAR technique. Nevertheless, the interactive process of data analysis and theoretical development promises to be rewarding.

The Seasat SAR data is an archival record (see Section II for details). Future SAR observations, such as those with the Shuttle Imaging Radar (SIR) series, will provide a time series of data so that temporal trends can be investigated. The authors hope that this report will allow the Seasat data to be meaningfully employed for these purposes.

ORIGINAL PAGE
BLACK AND WHITE PHOTOGRAPH

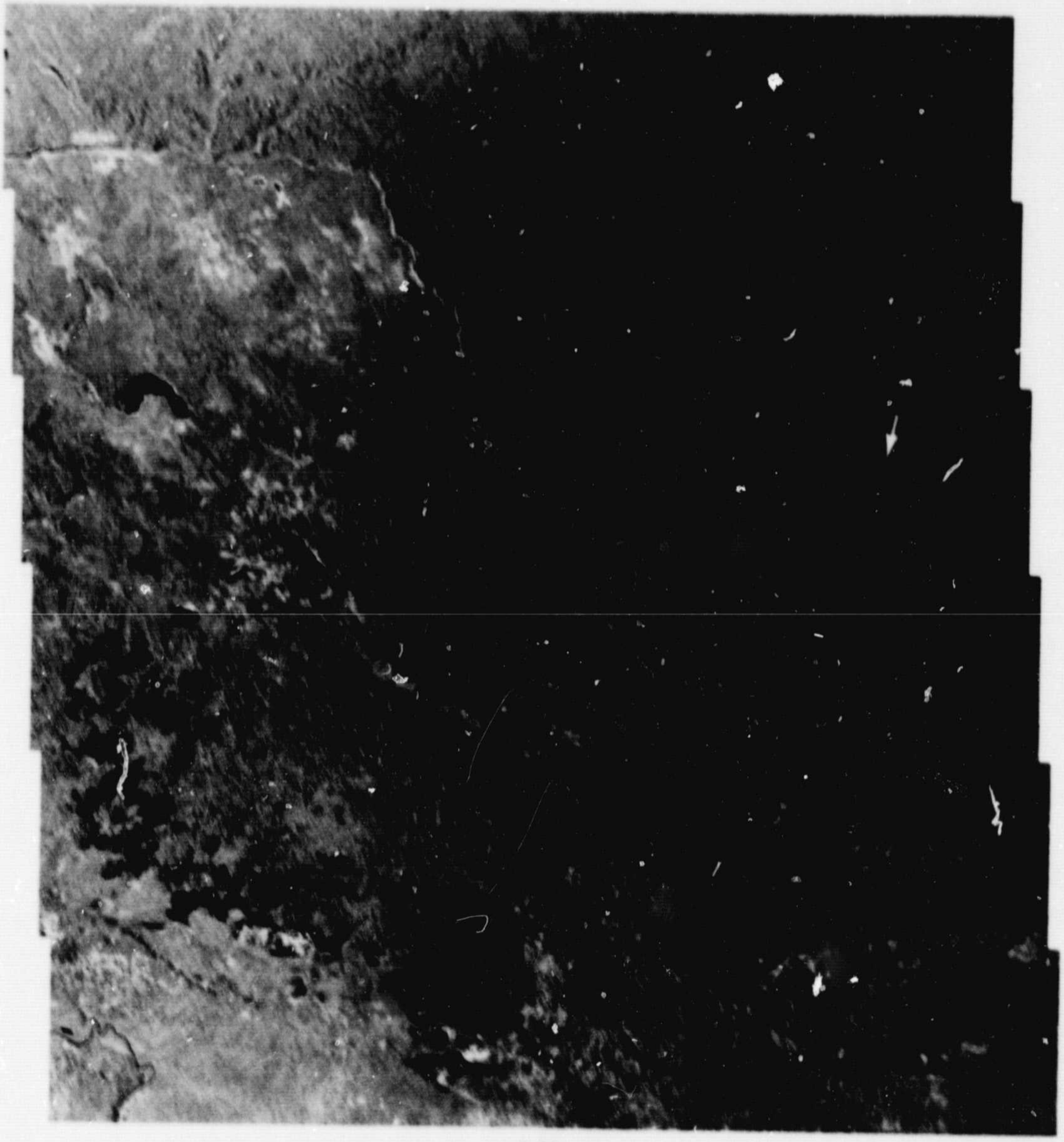

N

Figure 6-1. Tikal, Guatemala. This scene, obtained on July 29, 1978, shows an undeveloped land area containing ruins of the ancient Mayan city of Tikal. The dark linear feature (arrow) is an airstrip near the bright ruins. Seasat Revolution 465, MIL site.

ORIGINAL PAGE
BLACK AND WHITE PHOTOGRAPH

N

Figure 6-2. Biskra, Algeria. Northeastern Algeria contains the city of Biskra (bright area at arrow), which was observed on August 21, 1978. Note the retriggered chirp pulses in the lower left of the image. Seasat Revolution 791, UKO site.

ORIGINAL PAGE
BLACK AND WHITE PHOTOGRAPH

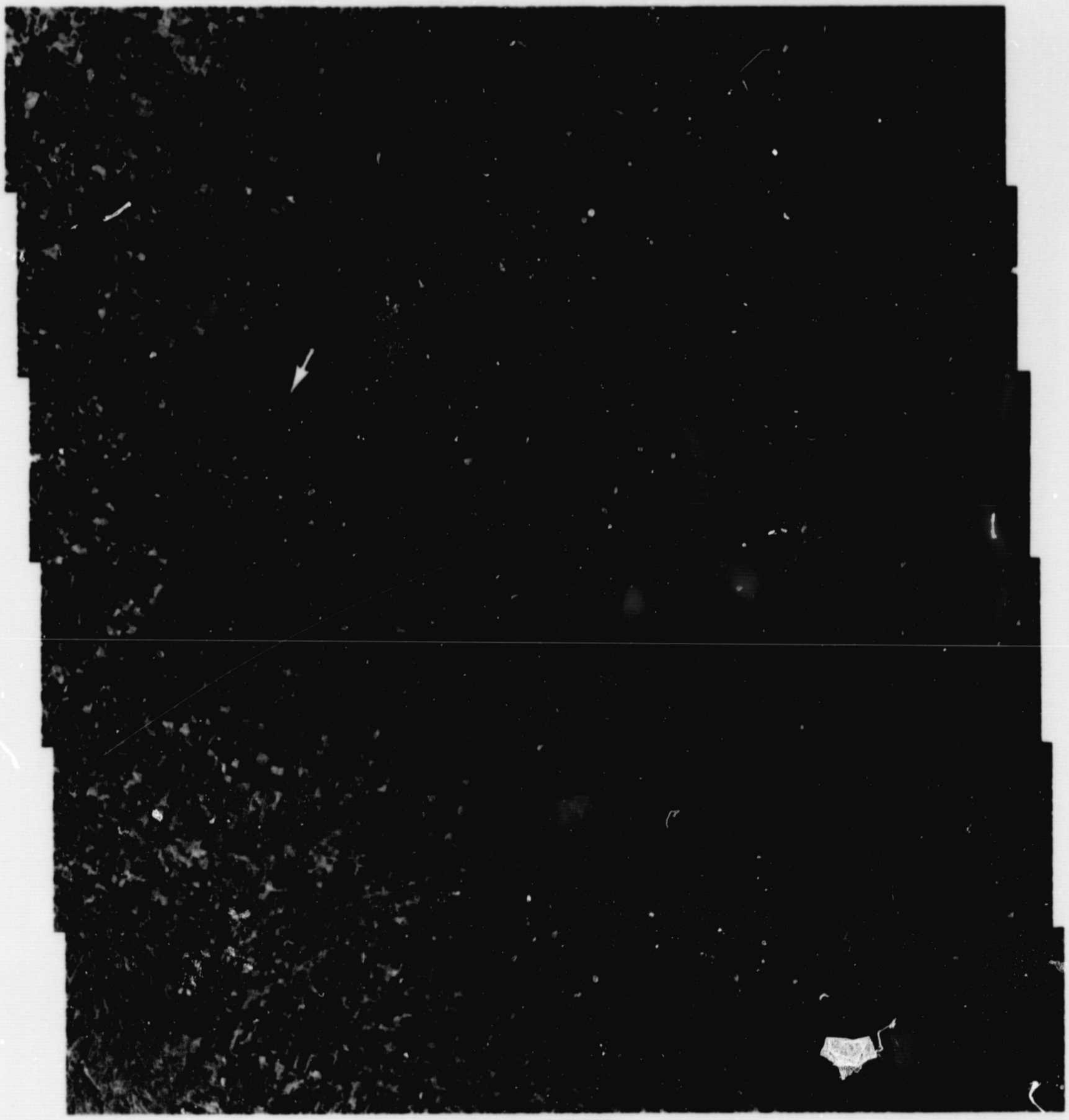

N

Figure 6-3. Indianapolis, Indiana. Indianapolis (arrow) and its environs are shown in this observation of July 25, 1978. Notice the contrast between the regular features in this developed area and the absence of such features in the preceding two images. Also note that the horizontal roads are mainly bright while the vertical roads are mainly dark, a result of differing radar aspect angles. Seasat Revolution 407, MIL site.

ORIGINAL PAGE
BLACK AND WHITE PHOTOGRAPH

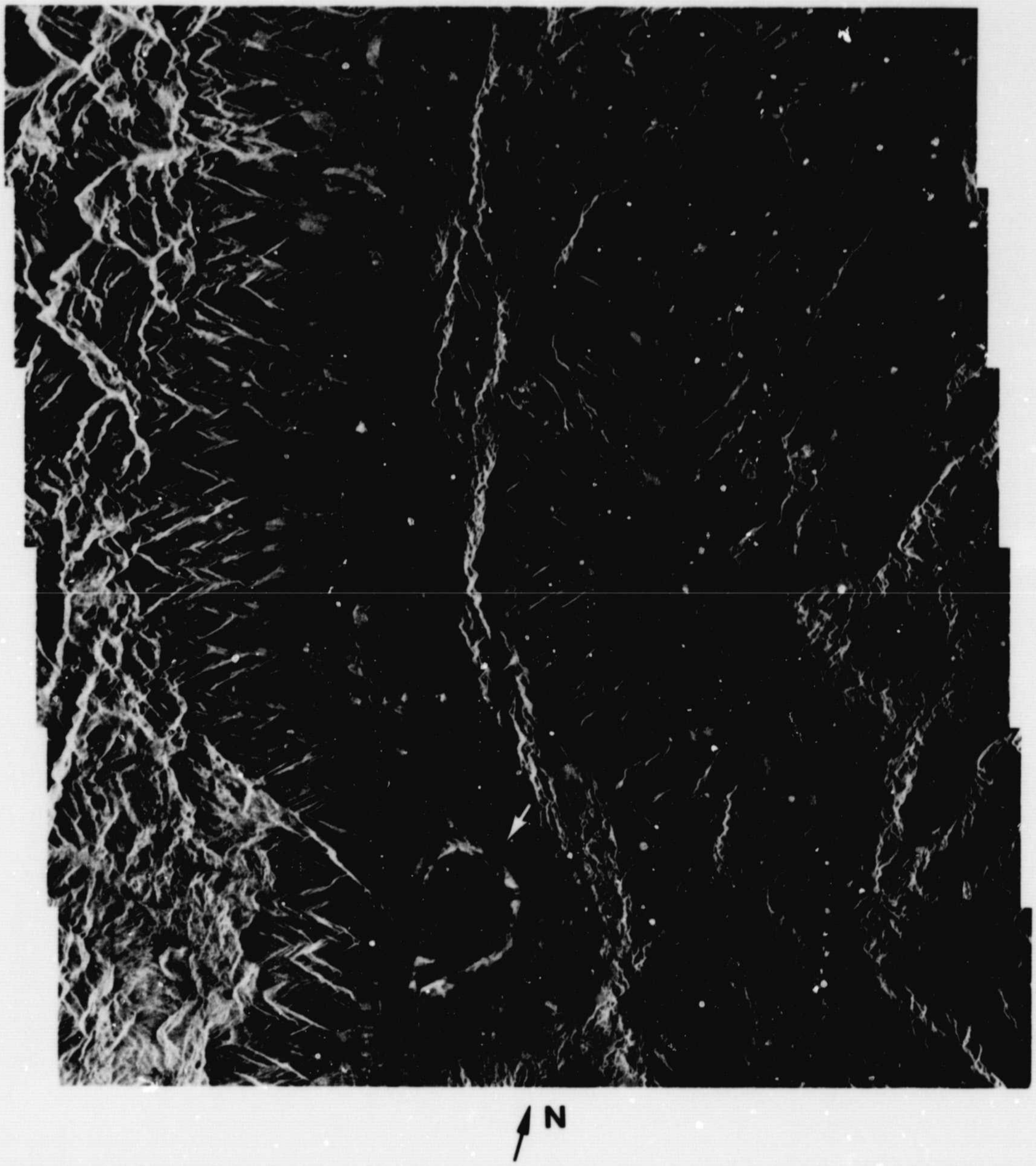

Figure 6-4. Owens Valley, California. In this scene, taken on July 24, 1978, Owens Lake appears at the arrow. The bright sawtooth patterns are due to mountain slopes inclined toward the SAR. The Panamint Mountains are toward the north. Bright linear features that run horizontally in the center of the image are power lines. Seasat Revolution 394, GDS site.

ORIGINAL PAGE
BLACK AND WHITE PHOTOGRAPH

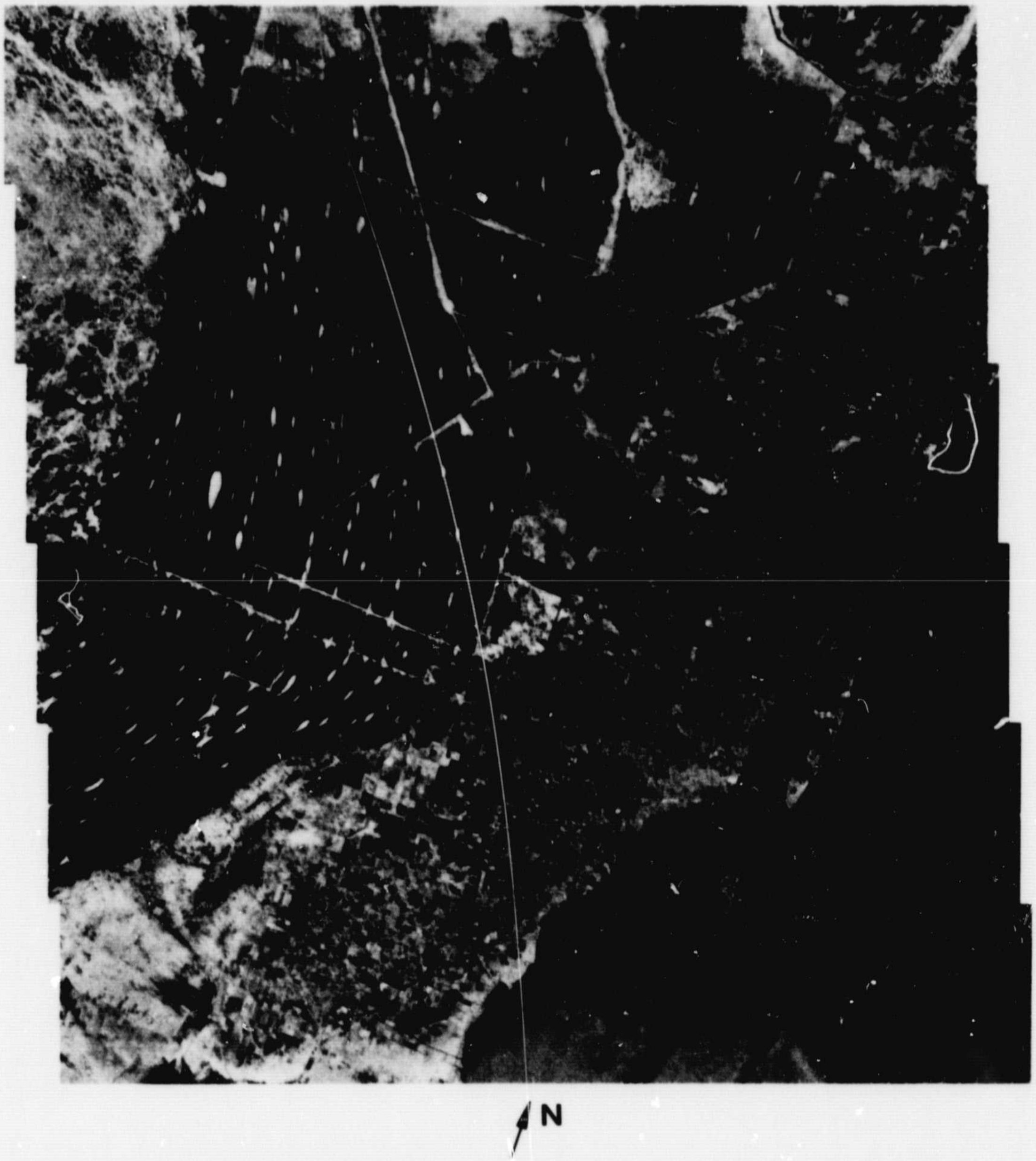

Figure 6-5. Miami, Florida. The coast off Miami, the city of Miami, and the Everglades were observed on August 8, 1978. Bright specks on the oceans are ships. Bright teardrop shapes in the Everglades are hardwood "hammocks" formed by the buildup of rafted vegetation during repeated drying and flooding cycles (Ford et al., 1980). Seasat Revolution 608, MIL site

ORIGINAL PAGE
BLACK AND WHITE PHOTOGRAPH

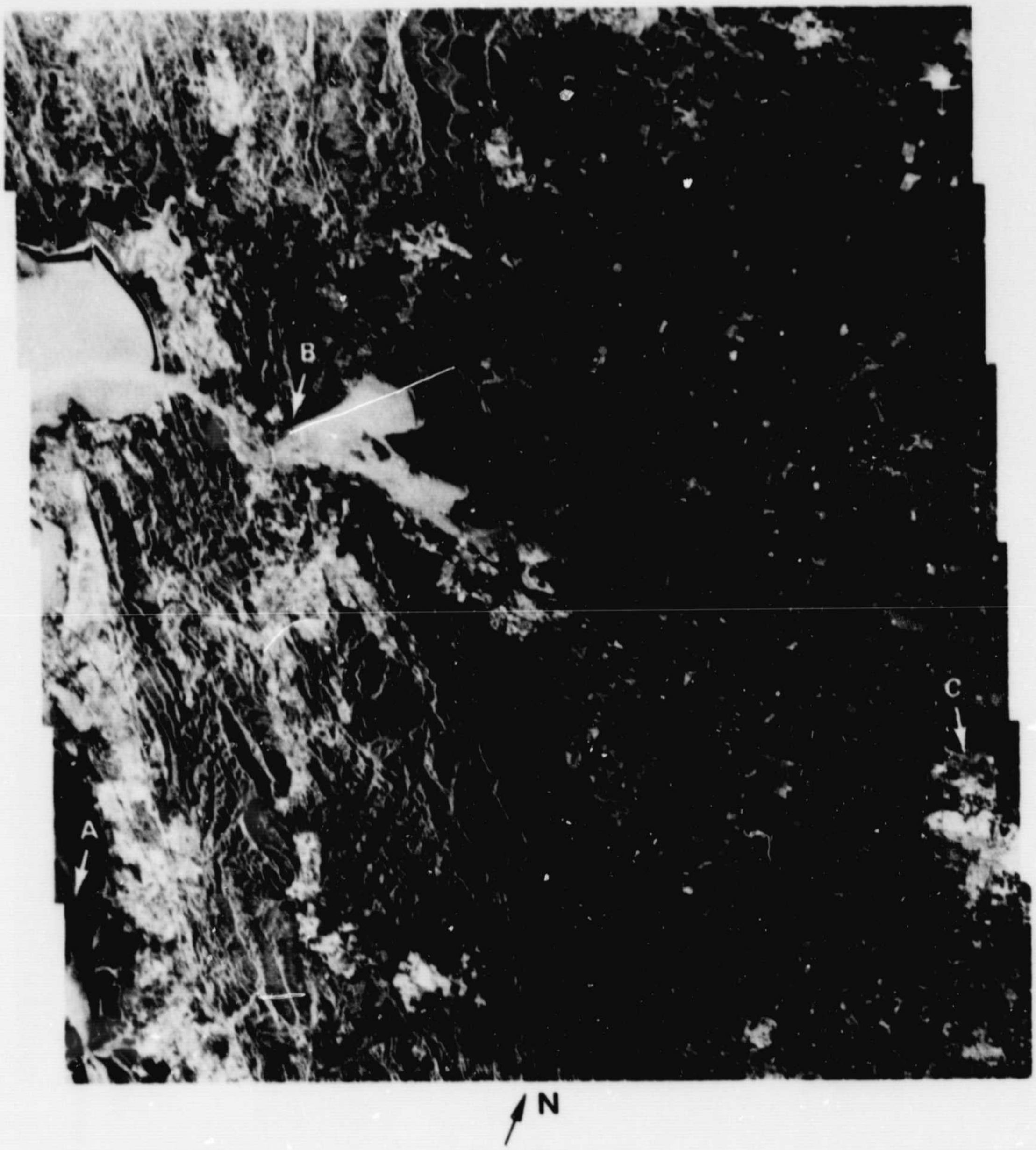

Figure 6-6. Sacramento River Delta. The river runs horizontally through the center of this picture, which was taken on August 4, 1978. Features include the San Mateo Bridge (A), the naval fleet on the north shore of Suisun Bay (B), and Stockton (C). Seasat Revolution 552, GDS site.

ORIGINAL PAGE
BLACK AND WHITE PHOTOGRAPH

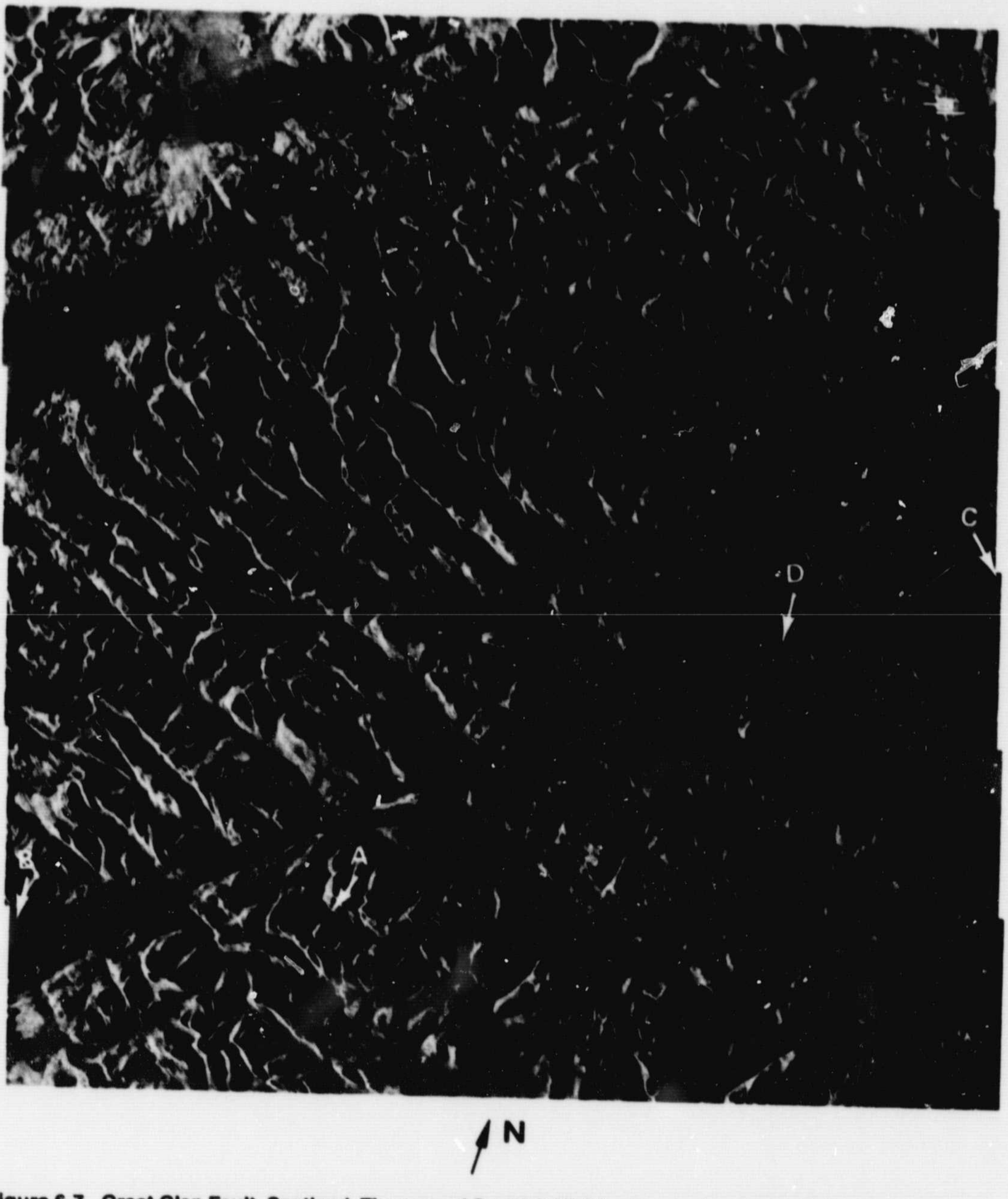

Figure 6-7. Great Glen Fault, Scotland. The rugged Scottish Highlands were imaged on August 16, 1978. The highest point in the British Isles, Ben Nevis (1343 m) in the Grampian Mountains appears at A. The Great Glen Fault (B to C) separates the Grampian Mountains from the Northern Highlands to the north and west. This is a left-lateral strike-slip fault that was active in Paleozoic time. The Great Glen (Glen Mor, C to D) lies along the fault and contains the famous Loch Ness (Ford et al., 1980). Seasat Revolution 719, UKO site.

ORIGINAL PAGE
BLACK AND WHITE PHOTOGRAPH

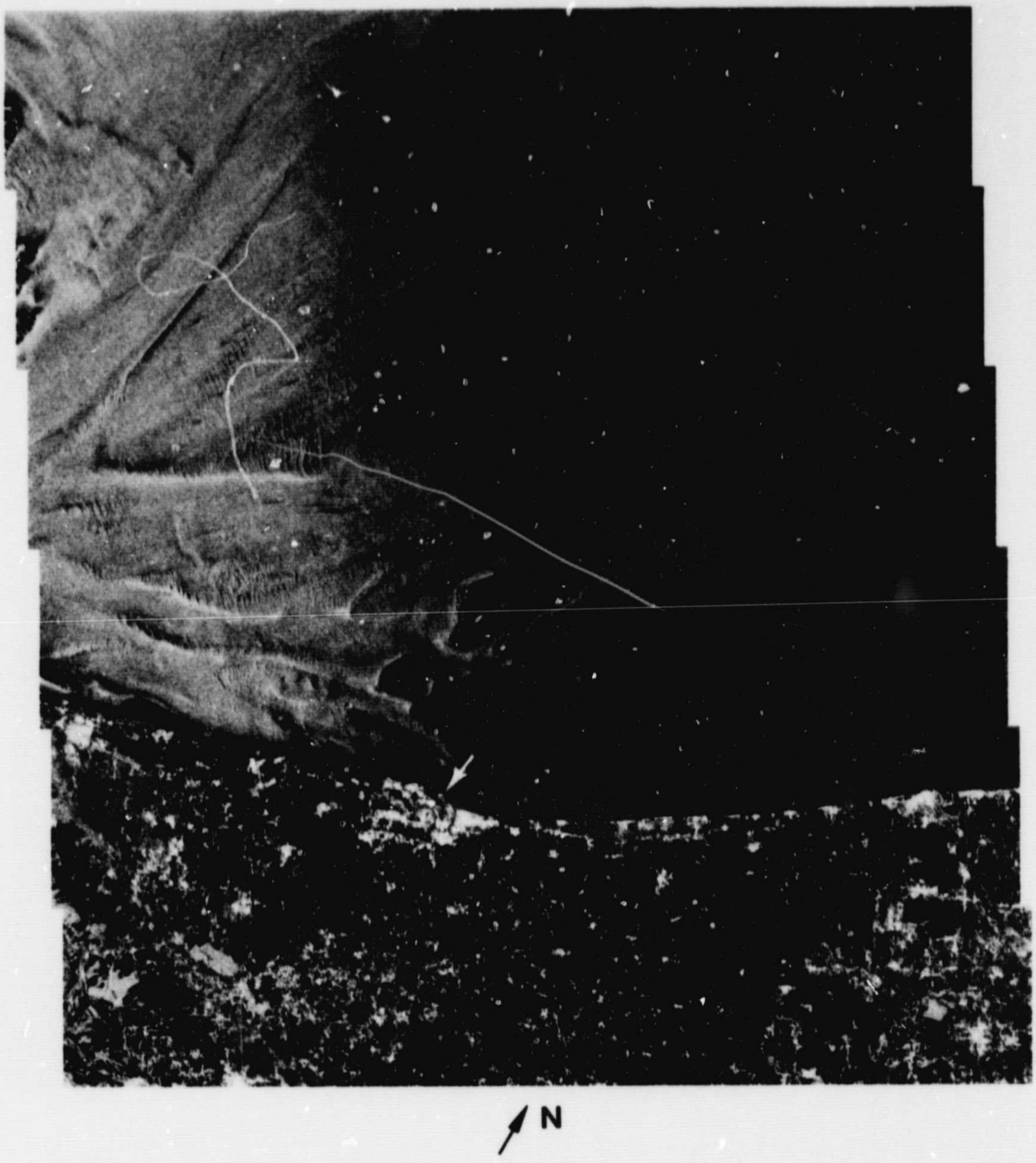

Figure 6-8. English Channel. This scene, near the Straits of Dover, was observed on August 19, 1978. The city of Dunkirk (arrow) is visible near the center of the coast. Notice the filamentary piers off the eastern coast. Long sea surface patterns (10 to 30 km) follow closely the sandbar patterns, which form oblique angles to the coast (Fu and Holt, 1982). Seasat Revolution 762, UKO site.

ORIGINAL PAGE
BLACK AND WHITE PHOTOGRAPH

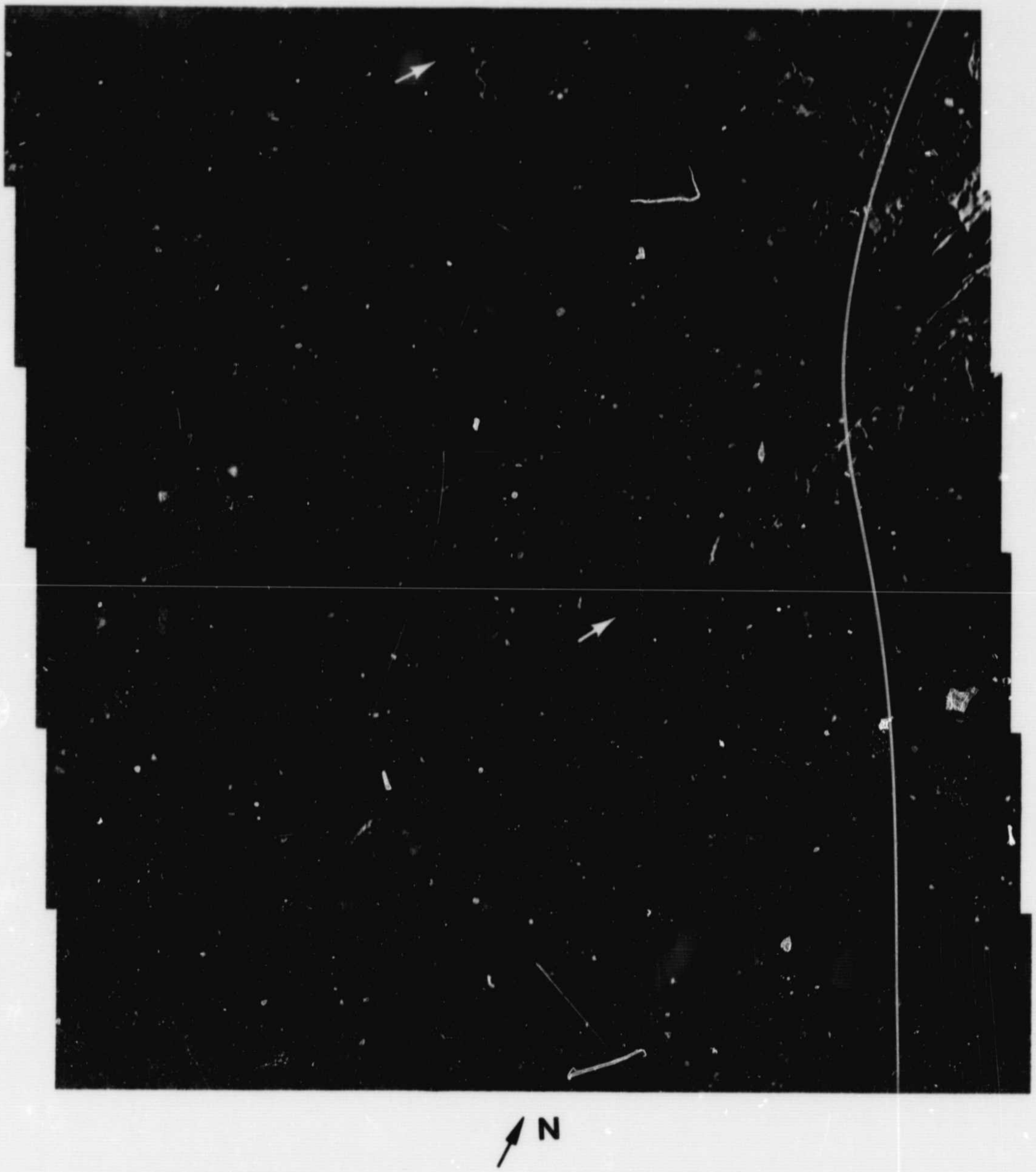

Figure 6-9. Shetland Islands. Seasat observed this scene north of Scotland on September 15, 1978. Little structure is seen in the open sea because of the homogenizing effect of the high winds that were thought to be present. Note, however, the refraction and diffraction patterns (arrows) of the surface waves around the islands. Seasat Revolution 1149, UKO site.

ORIGINAL PAGE
BLACK AND WHITE PHOTOGRAPH

Figure 6-10. Nantucket Shoals. These shallow water areas, observed on August 27, 1978, to the south and east of Nantucket Island, south of Cape Cod, are characterized by ridges and shoals separated by deeper channels. The brighter patterns occur over areas shallower than 18 m (e.g., at the arrow). Seasat Revolution 880, MIL site.

ORIGINAL PAGE
BLACK AND WHITE PHOTOGRAPH

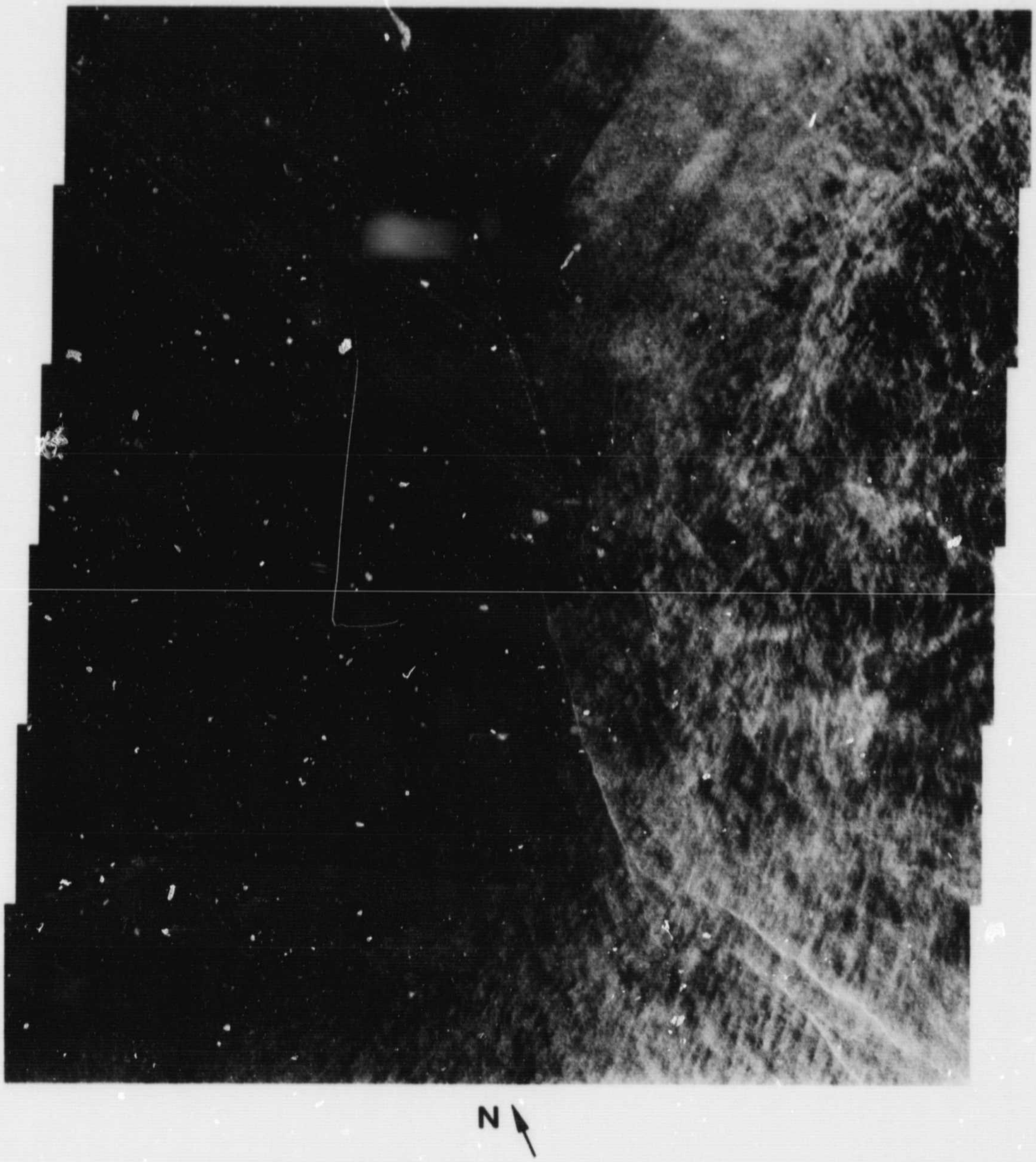

Figure 6-11. Warm Ring in the Atlantic Ocean. On the right is the western portion of a warm-core ring about 100 km southeast of Delaware Bay, observed on September 21, 1978. The area within the ring generally has a higher image intensity than the surrounding area. The boundary is characterized by concentric curvilinear lines probably due to shear zones caused by a rotating current (Fu and Holt, 1982). Seasat Revolution 1232, MIL site.

ORIGINAL PAGE
BLACK AND WHITE PHOTOGRAPH

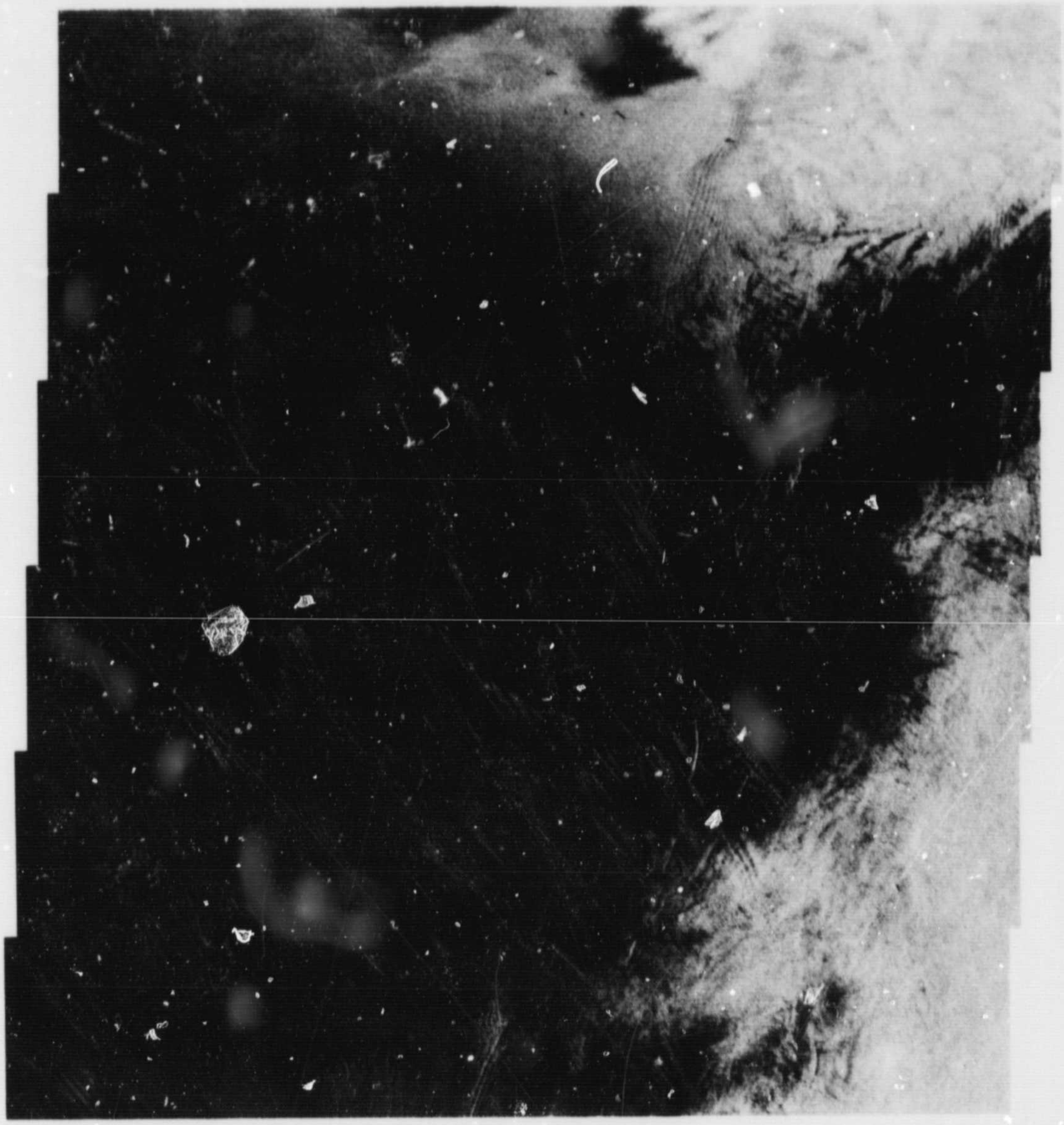

N

Figure 6-12. Mid-Atlantic Bight. The sharp continental shelf break off the east coast of the United States is well known for the generation of near-surface internal waves. This area of the Mid-Atlantic Bight is southeast of Delaware; it was observed on August 31, 1978. Numerous packets of internal waves with long, linear wave crests can be seen (Fu and Holt, 1982). Seasat Revolution 931, MIL site.

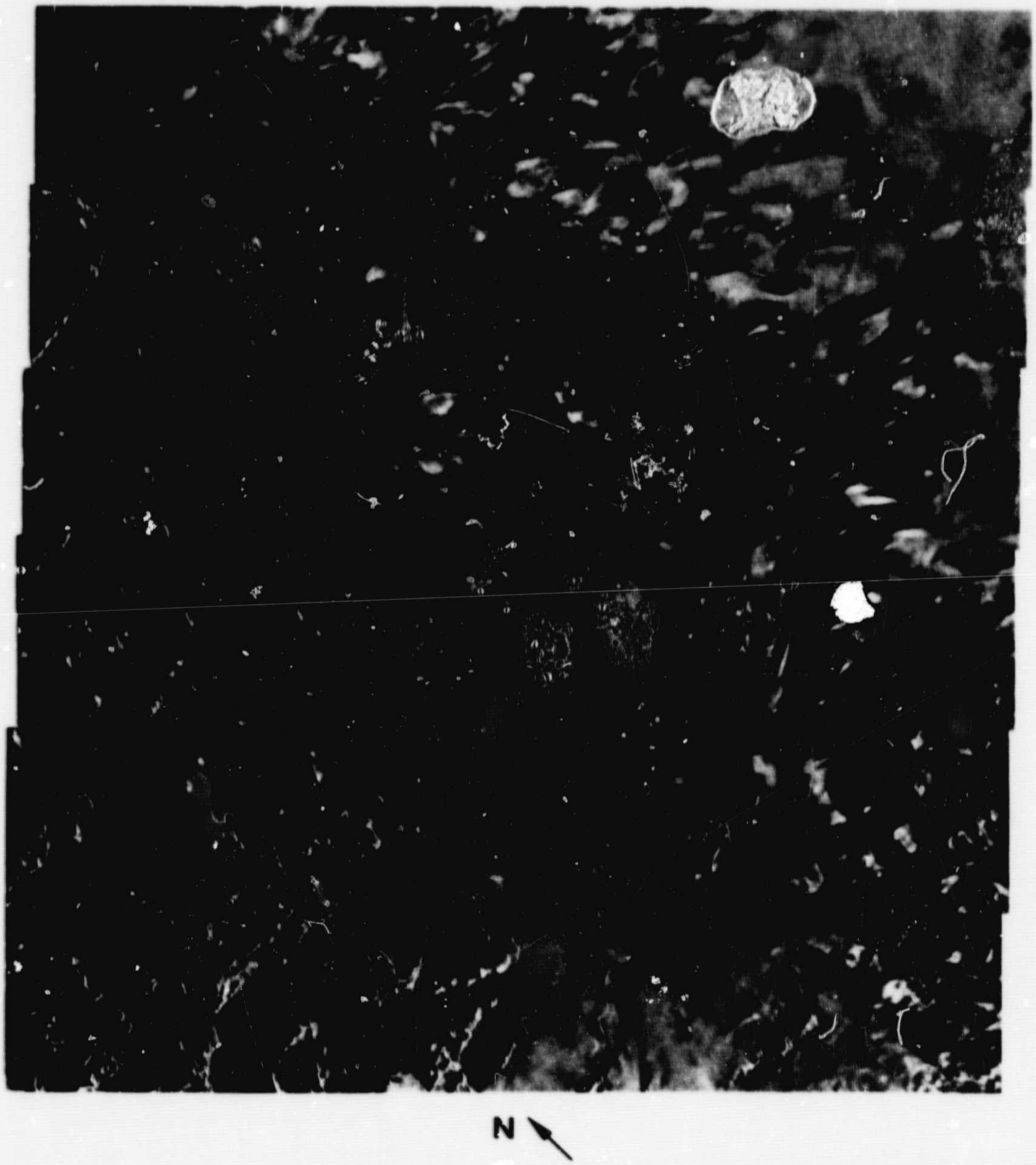

Figure 6-13. Southwest Greenland. The boundary between the inland ice of the Greenland icecap to the east, and exposures of very ancient rocks in coastal and near-coastal areas to the west was seen by the radar on October 9, 1978. Notice the ice flow patterns to the north (Ford et al., 1980). Seasat Revolution 1490, SNF site.

ORIGINAL PAGE
BLACK AND WHITE PHOTOGRAPH

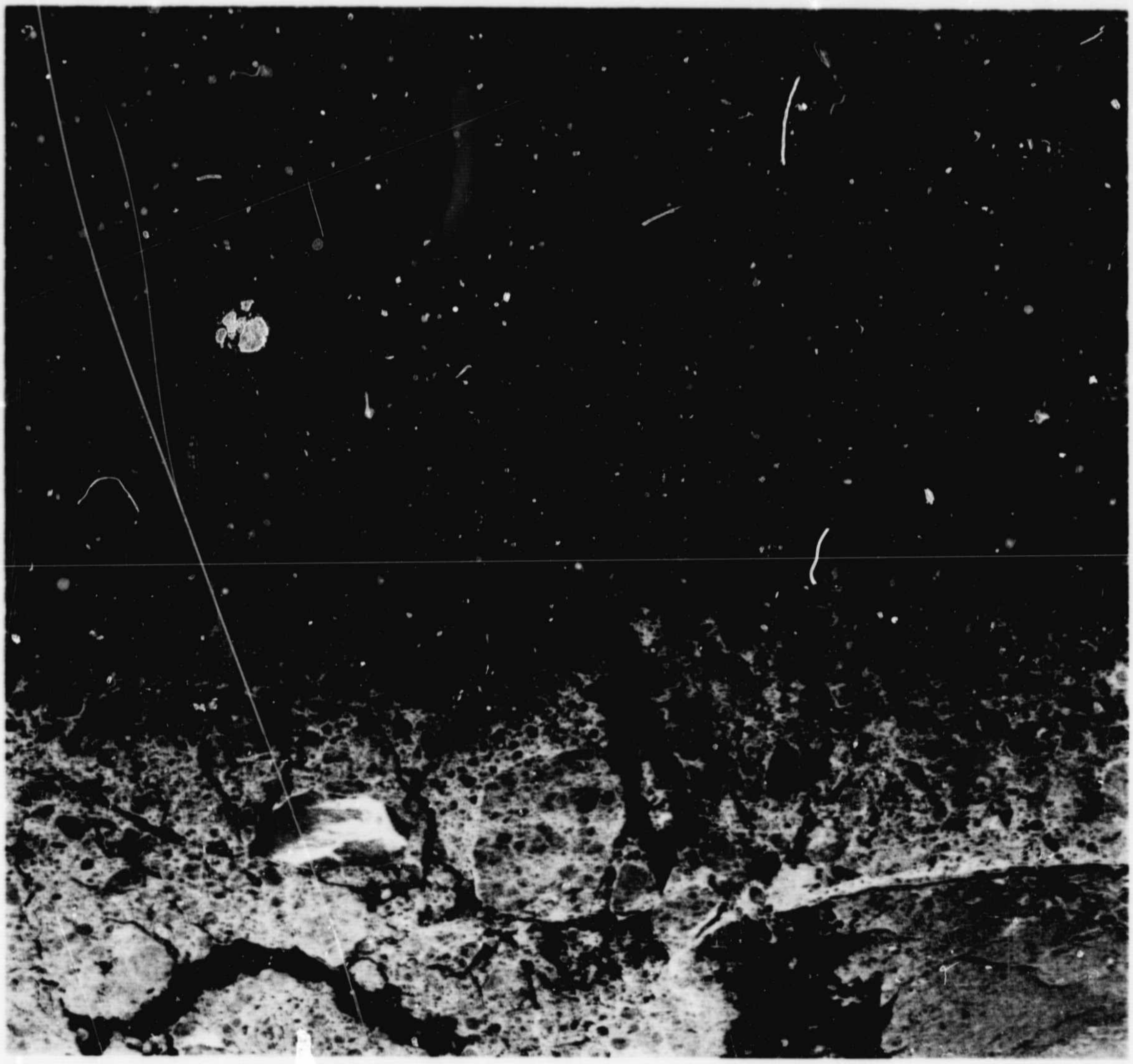

N

Figure 6-14. Ice Pack Northwest of Banks Island. This ice pack is located just northwest of Banks Island, Canada. The northwest corner of the island is in the southeast corner of the image. Fletcher's Ice Island (also known as T-3) is the bright feature located at the arrow. Dark features indicate open water or recently frozen ice (Fu and Holt, 1982). Seasat Revolution 1452, ULA site.

References

Active Microwave Workshop Report, 1975, R. E. Mathews, ed. NASA SP-376, National Aeronautics and Space Administration, Washington D. C.

Born, G. H., J. A. Dunne, and D. B. Lame, 1979, "Seasat Mission Overview," *Science*, Vol. 204, p. 1405.

Burns, A. A., and E. J. Fremouw, 1970, "A Real-Time Correction Technique for Trans-ionospheric Ranging Error," *IEEE Trans. Ant. Prop.*, Vol. AP-18, p. 785.

Carlson, R. J., 1980, *User's Guide for the Satellite Mission Design Program (SAMPD 4.0)*. Engineering Memorandum No. 312/80-106, Jet Propulsion Laboratory, Pasadena, Calif. (JPL internal document).

Croft, C., 1982, *Calibration Progress Report*. IOM 3345-82-029, Jet Propulsion Laboratory, Pasadena, Calif. (JPL internal document).

Curlander, J., 1982a, "Location of Spaceborne SAR Imagery," *IEEE Trans. Geosci. Rem Sens,* Vol. GE-20, p. 359.

Curlander, J., 1982b, *High Precision Pixel Location Study*. IOM 3347-82-021, Jet Propulsion Laboratory, Pasadena, Calif. (JPL internal document).

Curlander, J. C. and S. N. Pang, 1982, "Geometric Registration and Rectification of Spaceborne SAR Imagery," presented at International Geoscience and Remote Sensing Symposium, June 1-4, Munich, FRG. *IEEE Cat. No. 82CH 14723-6*, Vol. II, Session FA-2, p. 5.1-5.5.

Elachi, C., 1980, "Spaceborne Imaging Radar: Geologic and Oceanographic Applications," *Science*, Vol. 209, p. 1073.

Ford, J. P., R. G. Blom, M. L. Bryan, M. I. Daily, T. H. Dixon, C. Elachi, and E. C. Xenos, 1980, *Seasat Views North America, the Caribbean, and Western Europe With Imaging Radar*. Publication 80-67, Jet Propulsion Laboratory, Pasadena, Calif.

Fu, L.-L., and B. Holt, 1982, *Seasat Views Oceans and Sea Ice with Synthetic-Aperture Radar*. Publication 81-120, Jet Propulsion Laboratory, Pasadena, Calif.

Johnson, J. W., L. A. Williams, Jr., E. M. Bracalente, F. B. Beck, and W. L. Grantham, 1980, "Seasat-A Satellite Scatterometer Instrument Evaluation," *IEEE J. Ocean. Eng.*, Vol. 5, p. 138.

Jones, W. L., P. G. Black, D. M. Boggs, E. M. Bracalente, G. Dome, J. A. Ernst, I. M. Halberstam, J. E. Overland, S. Peteherych, W. J. Pierson, F. J. Wentz, P. M. Woiceshyn, and M. G. Wurtele, 1979, "Seasat Scatterometer," *Science*, Vol. 204, p. 1413.

Jin, M., 1981, *Simulation of Weighting Effect on ISLR*. IOM 3347-81-101, Jet Propulsion Laboratory, Pasadena, Calif. (JPL internal document).

Klose, J. C., 1979, *Seasat Node Tables and Osculating Elements*, Report 622-215, Jet Propulsion Laboratory, Pasadena, Calif. (JPL internal document).

Long, M. W., 1975, *Radar Reflectivity of Land and Sea*. D. C. Heath and Co., Lexington, Mass.

MacDonald Dettwiler, and Associates Ltd., 1982, *Seasat SAR Performance Evaluation Study Report*, 00-0676-000. Richmond, B. C., Canada.

McClain, E. P., and R. A. Marks, 1979, "Seasat Visible and Infrared Radiometer," *Science*, Vol. 204, p. 1421.

McClain, P., R. Marks, G. Cunningham, and A. McCulloch, 1980, "Visible and Infrared Radiometer," *IEEE J. Ocean. Eng.*, Vol. 5, p. 164.

Njoku, E. G., J. M. Stacéy, and F. T. Barath, 1980, "The Seasat Multichannel Microwave Radiometer (SMMR): Instrument Description and Performance," *IEEE J. Ocean. Eng.* Vol. 5, p. 100.

SMMR Mini-Workshop III, August 26-27, 1980, Report No. 622-224, edited by R. G. Lipes and G. H. Born. Jet Propulsion Laboratory, Pasadena, Calif. (JPL internal document).

Tapley, B. D., et al. 1979, "Seasat Altimeter Calibration: Initial Results," *Science*, Vol. 204, p. 1410.

Tomiyasu, K., 1978, "Tutorial Review of Synthetic-Aperture Radar (SAR) With Applications to Imaging of the Ocean Surface," *Proc. of IEEE*, Vol. 66, p. 563.

Townsend, W. F., 1980, "An Initial Assessment of the Performance Achieved by the Seasat-1 Radar Altimeter," *IEEE J. Ocean. Eng.*, Vol. 5, p. 80.

Wu, C., B. Barkan, B. Huneycutt, C. Leang, and S. Pang, 1981, *An Introduction to the Interim Digital SAR Processor and the Characteristics of the Associated Seasat SAR Imagery*. Publication 81-26, Jet Propulsion Laboratory, Pasadena, Calif.

Appendix A

Catalogue of Seasat SAR Imagery

This appendix presents the catalogue of synthetic-aperture radar (SAR) imagery acquired by the Seasat satellite. Included are areal coverage plots (Subsection A-I) and tables of key orbital information (Subsection A-II). This information will enable an investigator to identify which revolutions (if any) imaged an area of interest and to determine the dates and times of this imagery. Additonally, tables of digitally processed SAR imagery are provided (Subsection A-III). Parts of this appendix are reproduced from Appendix C of Fu and Holt (1982).

I. Areal Coverage

The following figures (Figures A-1 through A-26) are computer-generated plots showing the areal coverage of all the Seasat SAR data that were of sufficient quality to have been optically processed in a survey mode. The plots have been grouped geographically by the location of the five receiving stations, which are labeled GDS (Goldstone, California); MIL (Merritt Island, Florida); SNF (Shoe Cove, Newfoundland, Canada); ULA (Fairbanks, Alaska); and UKO (Oakhanger, United Kingdom). Each SAR swath is shown by two parallel lines enclosed at both ends and labeled in one of two ways: by revolution number (3 or 4 digits) or by node (1 to 3 digits followed by a decimal). The revolution numbers are used for single swaths; the node numbers are used for two or more swaths with nearly identical ground tracks (i.e., within 0.1 deg). The swaths labeled by node numbers depict the superposed coverage from all the constituent revolutions. For example, the Table A-2 node values from 255.99 to 256.02 constitute the 256.0 swath in Figure A-7 and include Revolutions 1441, 1269, 1312, 1398, 1355, 1226, 1484, 1140, 1183, and 1097. Tables A-1 and A-2 can be consulted for specific orbital information. Note that revolution numbers for swaths labeled by node can be most easily determined from Table A-2. Figure A-1 is a composite plot of the total SAR areal coverage, and Figures A-2, A-8, A-13, -14, and -24 are composite plots* of the total SAR recording activity for each of the five receiving stations and are provided primarily for general interest.

These plots were generated using the Satellite Mission Design Program (Carlson, 1980) with osculating orbital elements taken from Klose (1979).

*The composite plot for Shoe Cove, Newfoundland, is identical to the single period of its areal coverage.

ORIGINAL PAGE IS
OF POOR QUALITY

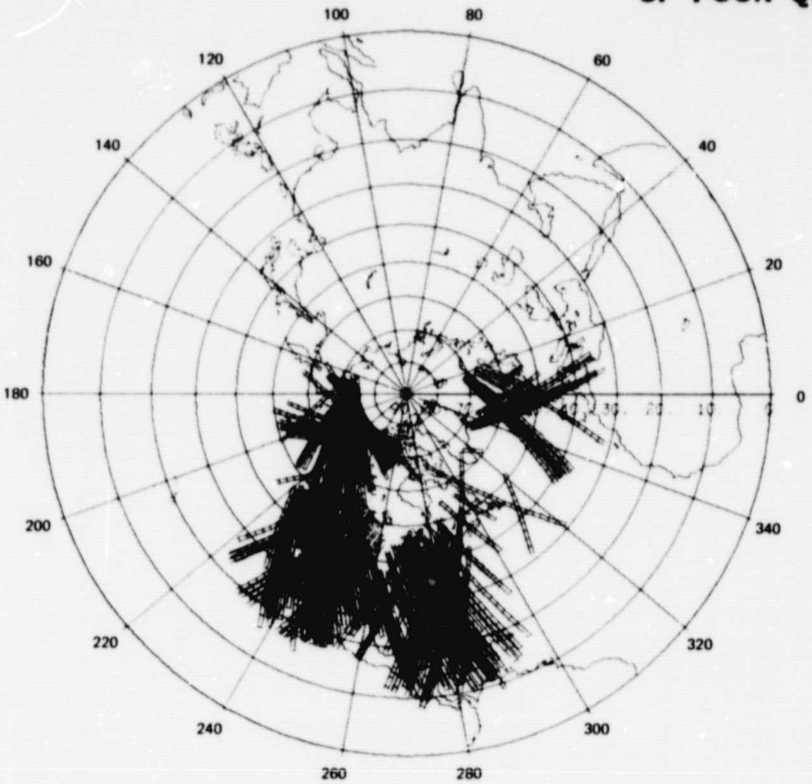

Figure A-1. Composite Seasat SAR areal coverage

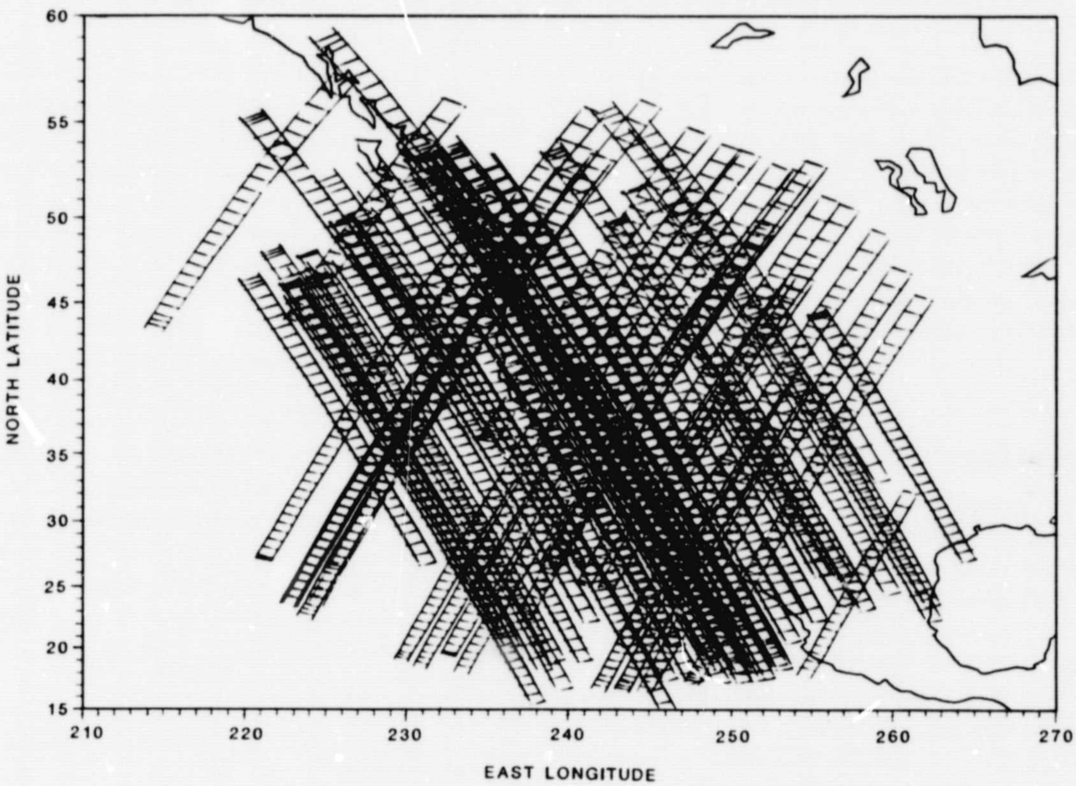

Figure A-2. Goldstone, California: July 4 through October 9, 1978

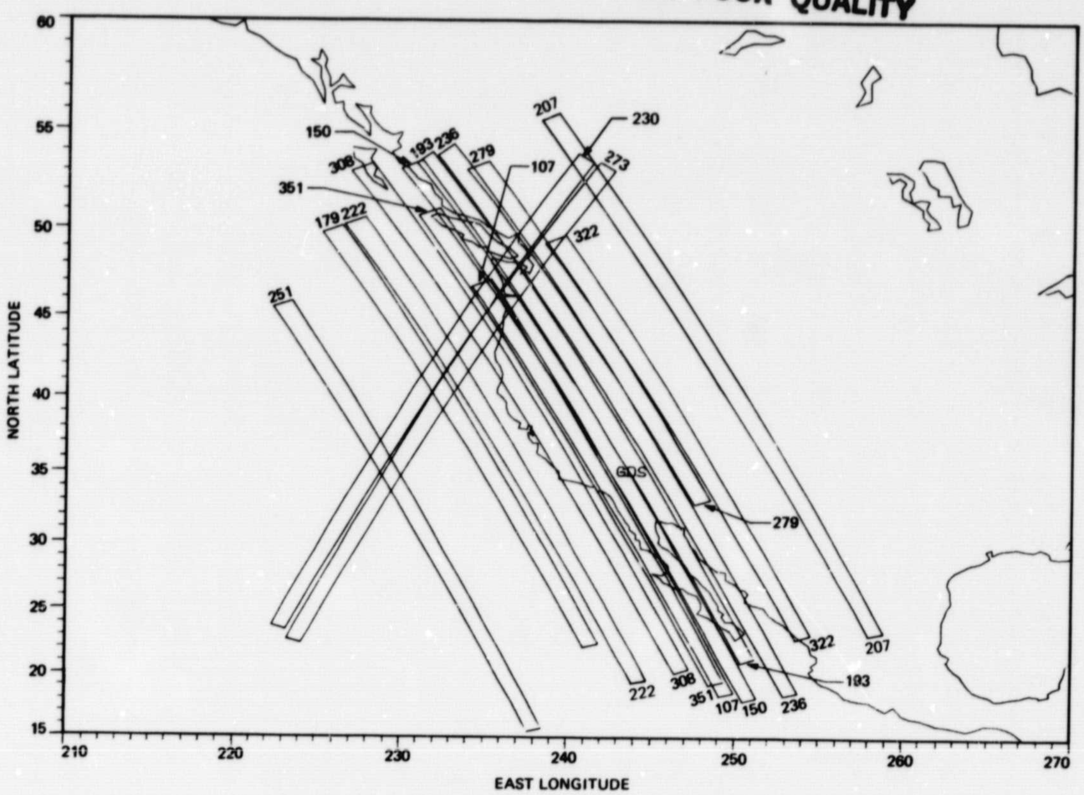

Figure A-3. Goldstone, California: July 4 through July 21

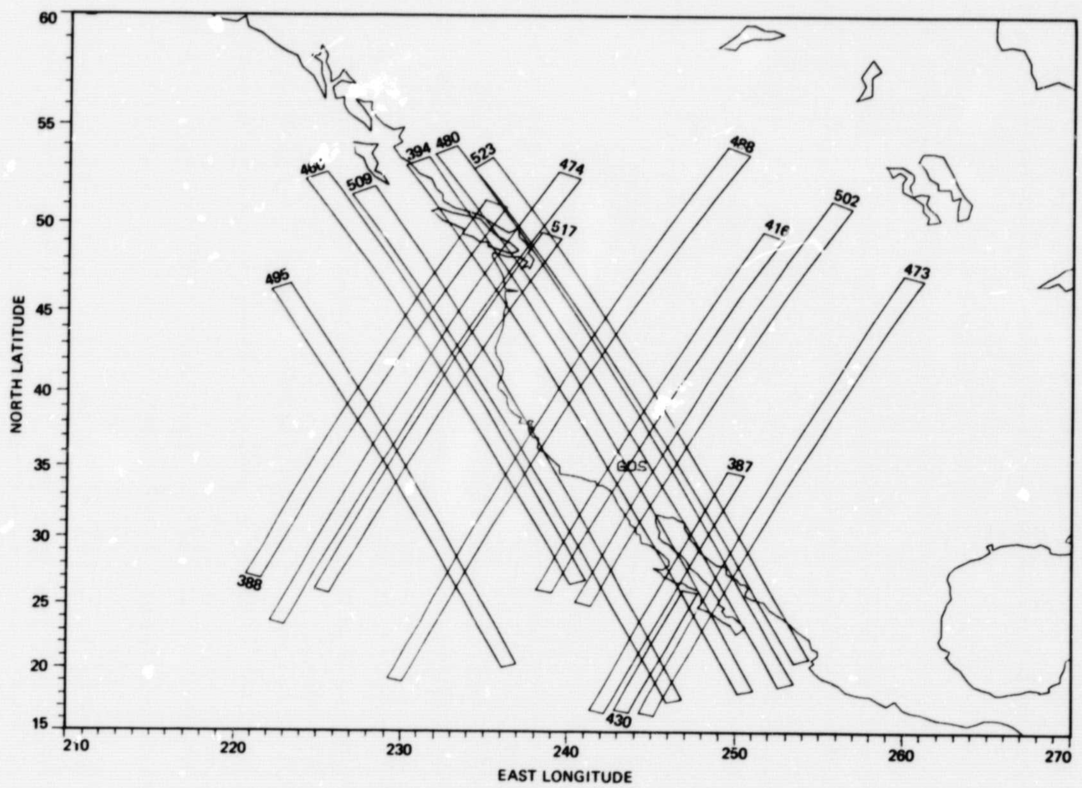

Figure A-4. Goldstone, California: July 22 through August 2

ORIGINAL PAGE IS
OF POOR QUALITY

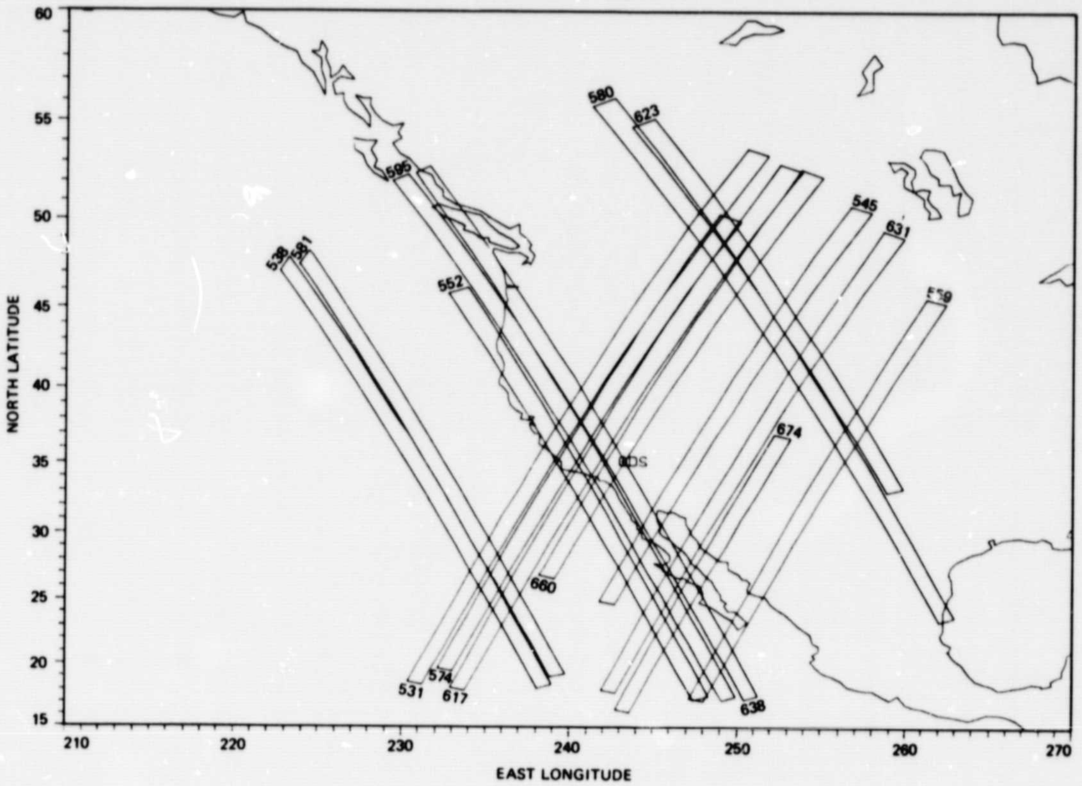

Figure A-5. Goldstone, California: August 3 through August 13

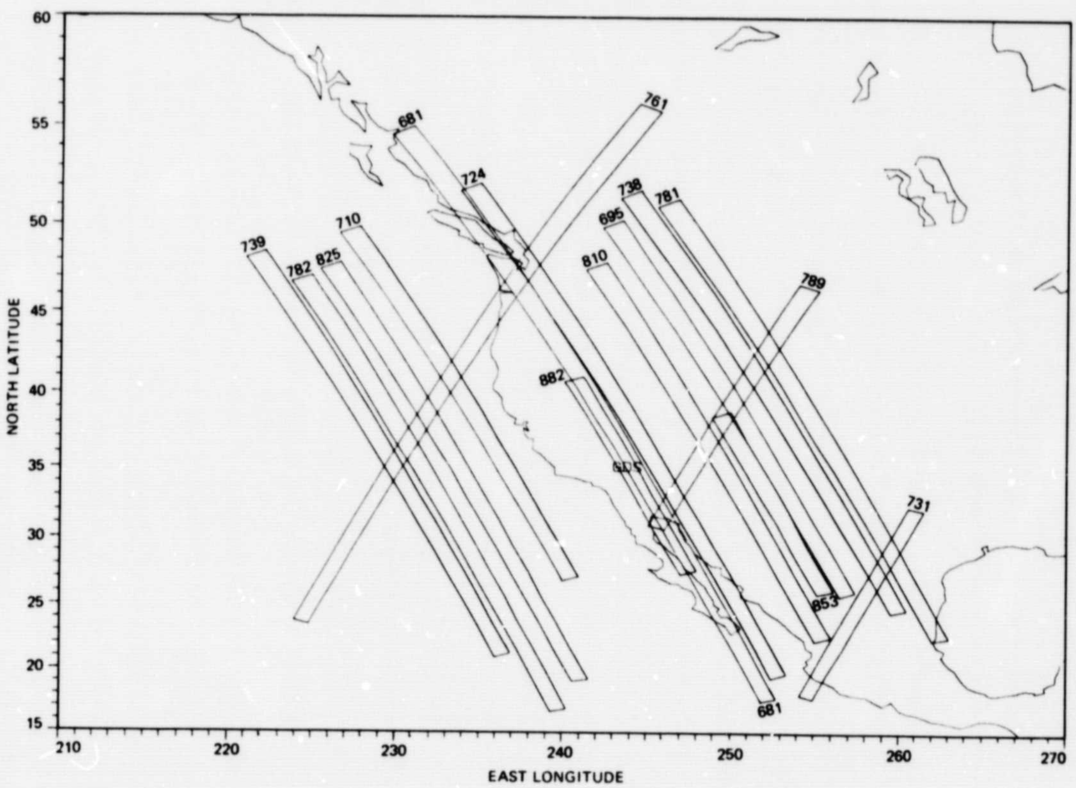

Figure A-6. Goldstone, California: August 13 through August 27

**ORIGINAL PAGE IS
OF POOR QUALITY**

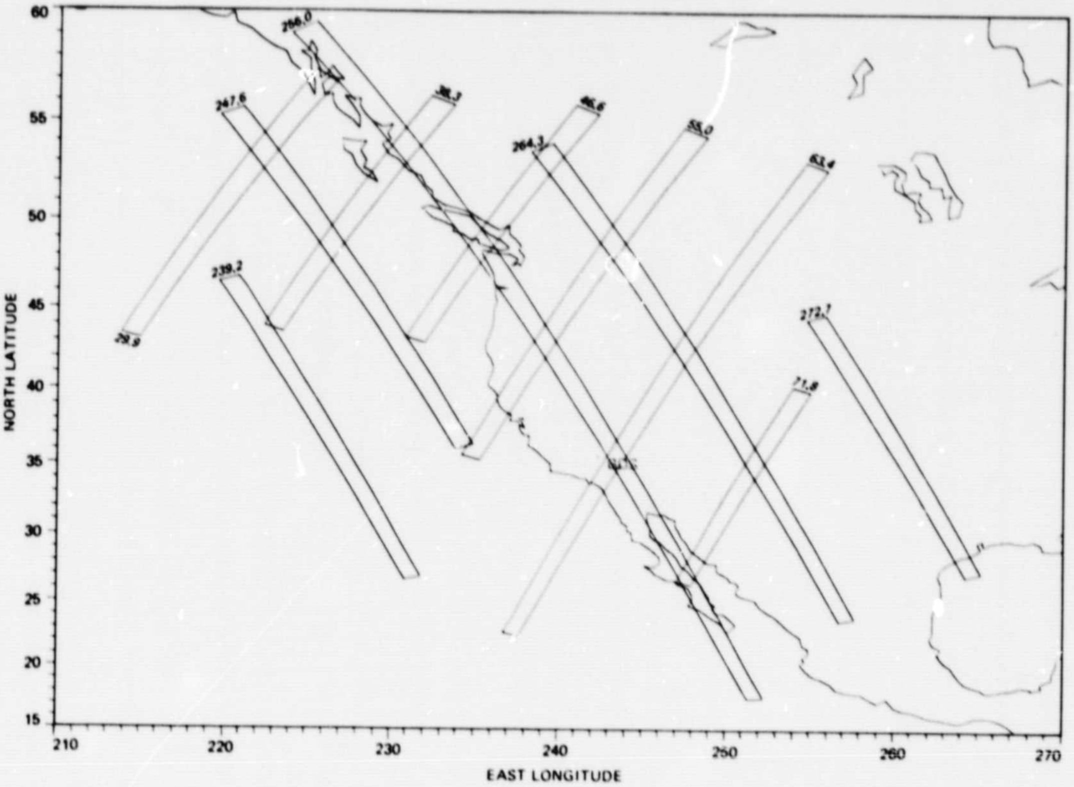

Figure A-7. Goldstone, California: August 28 through October 9

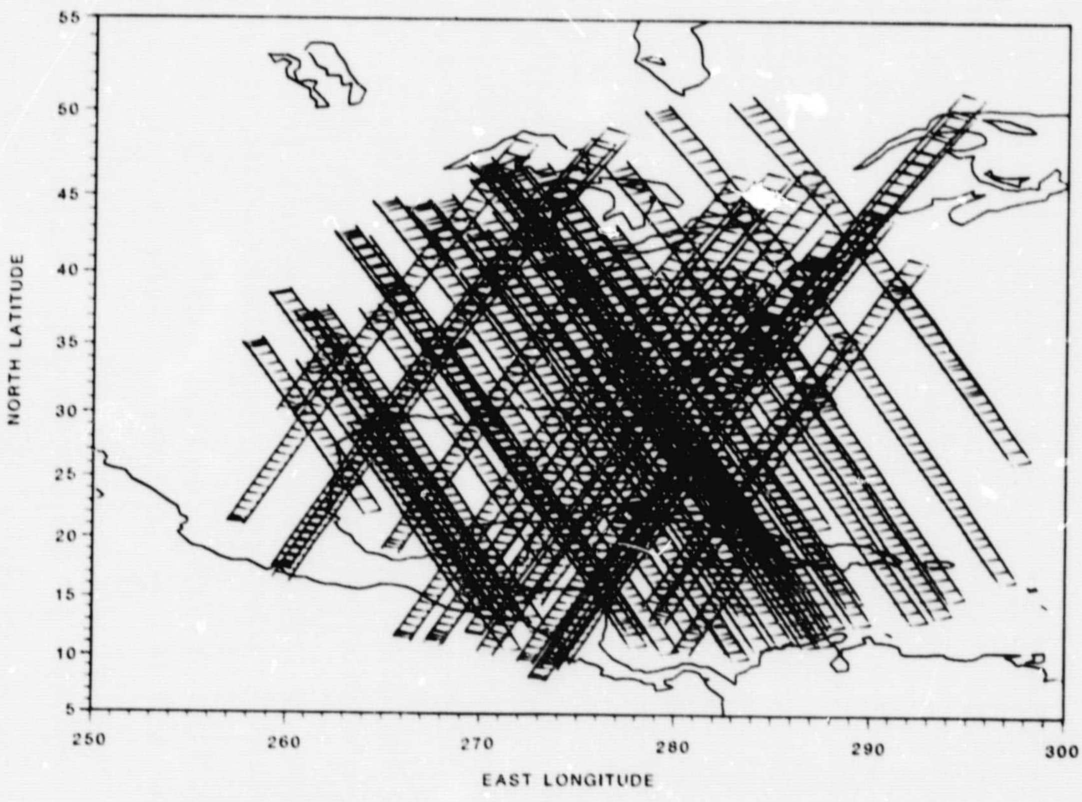

Figure A-8. Merritt Island, Florida: July 8 through October 9, 1978

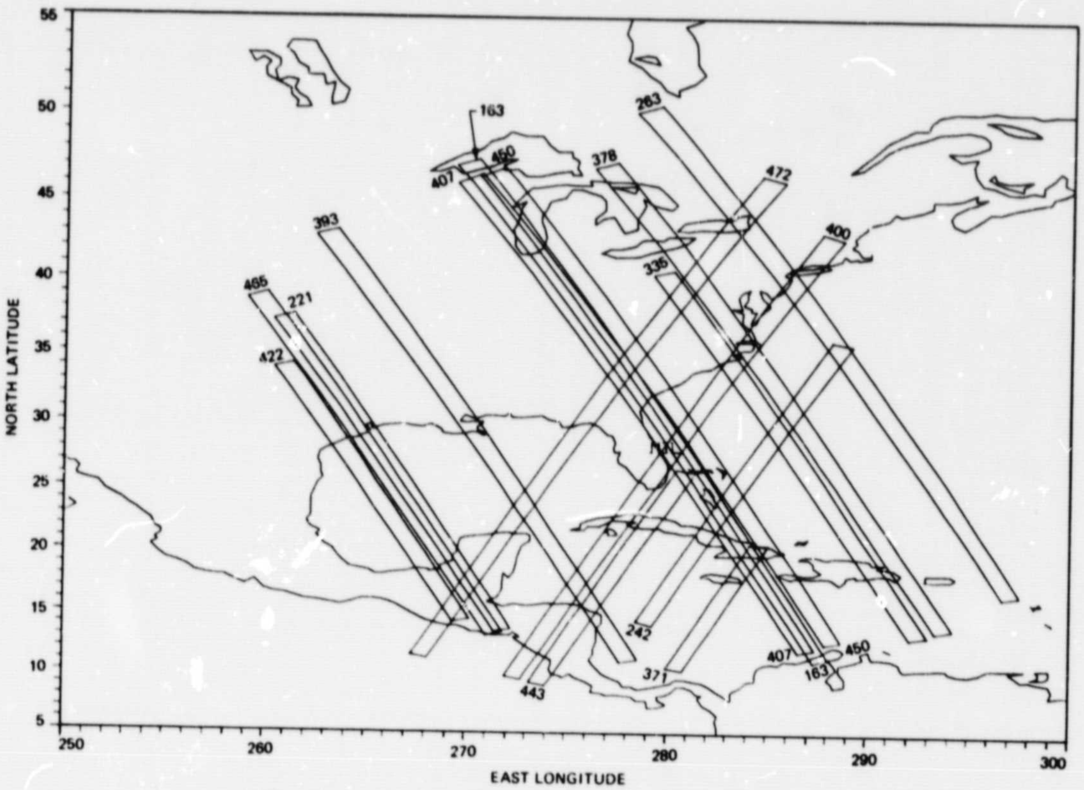

Figure A-9. Merritt Island, Florida: July 8 through July 30

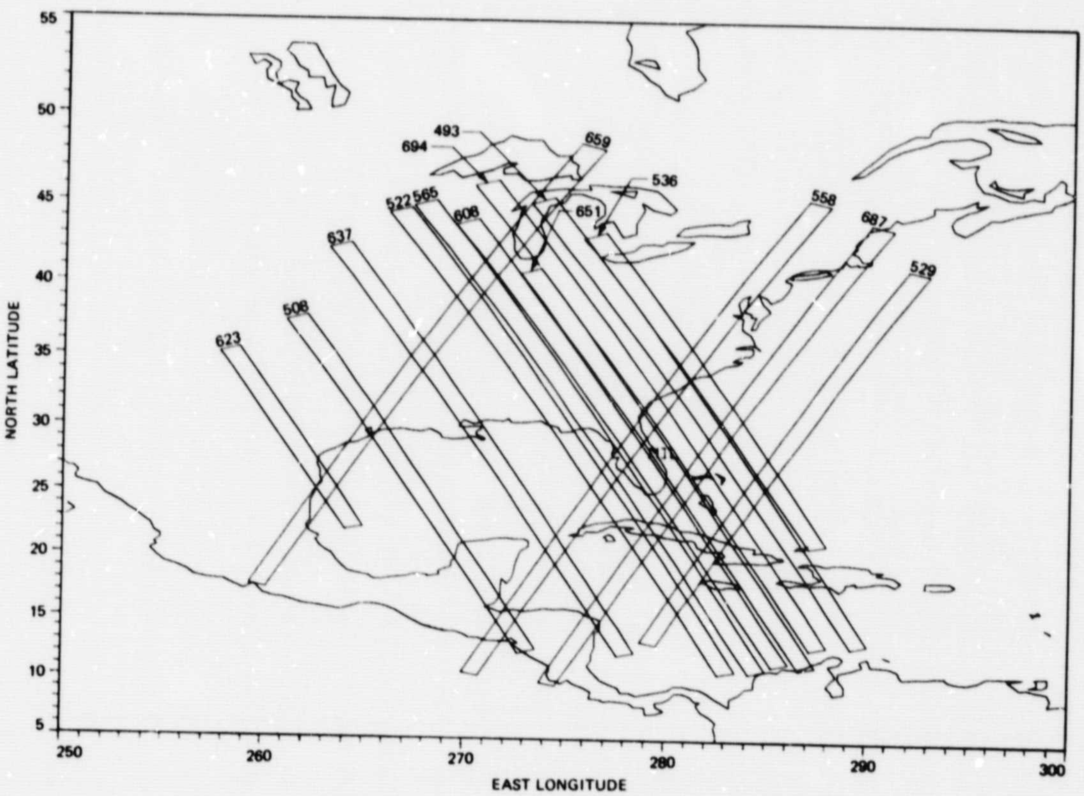

Figure A-10. Merritt Island, Florida: July 31 through August 14

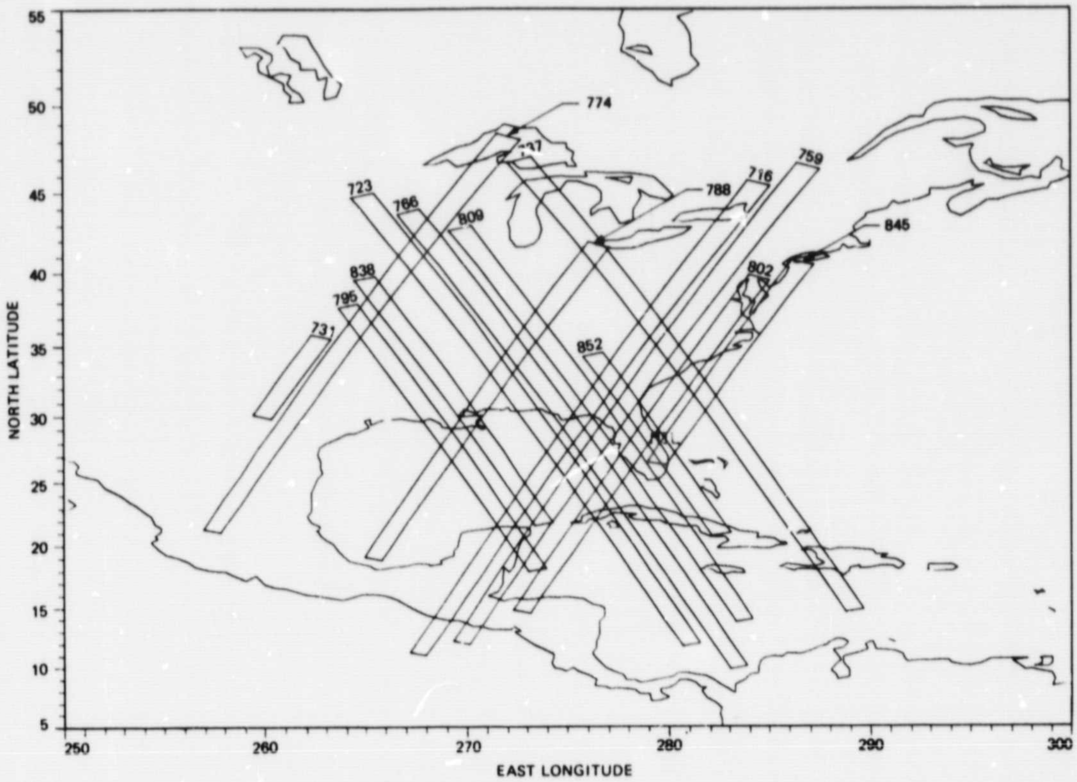

Figure A-11. Merritt Island, Florida: August 15 through August 25

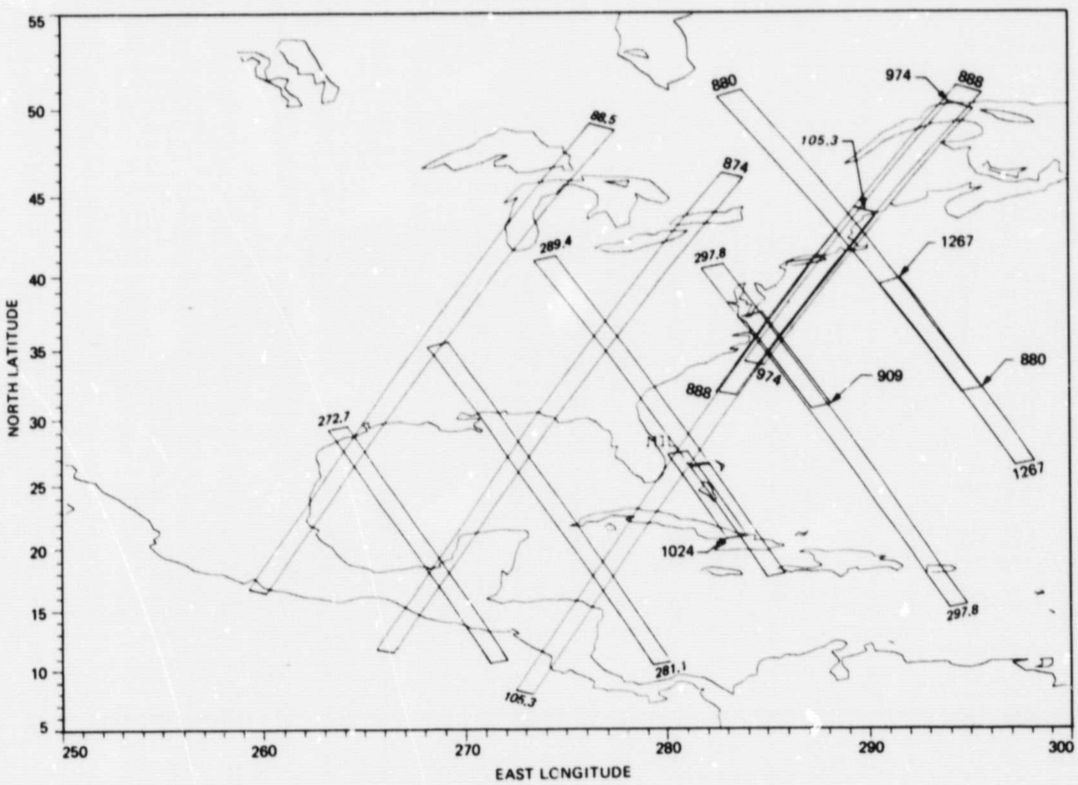

Figure A-12. Merritt Island, Florida: August 26 through October 9

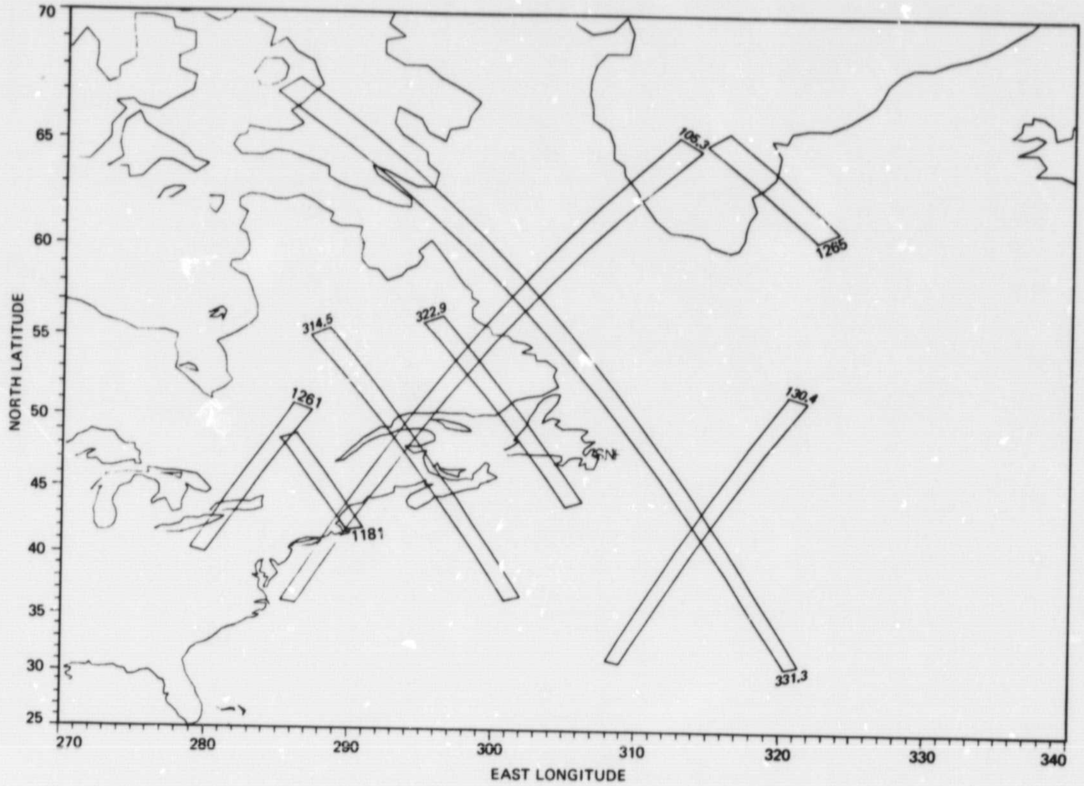

Figure A-13. Shoe Cove, Newfoundland. September 17 through October 9, 1978

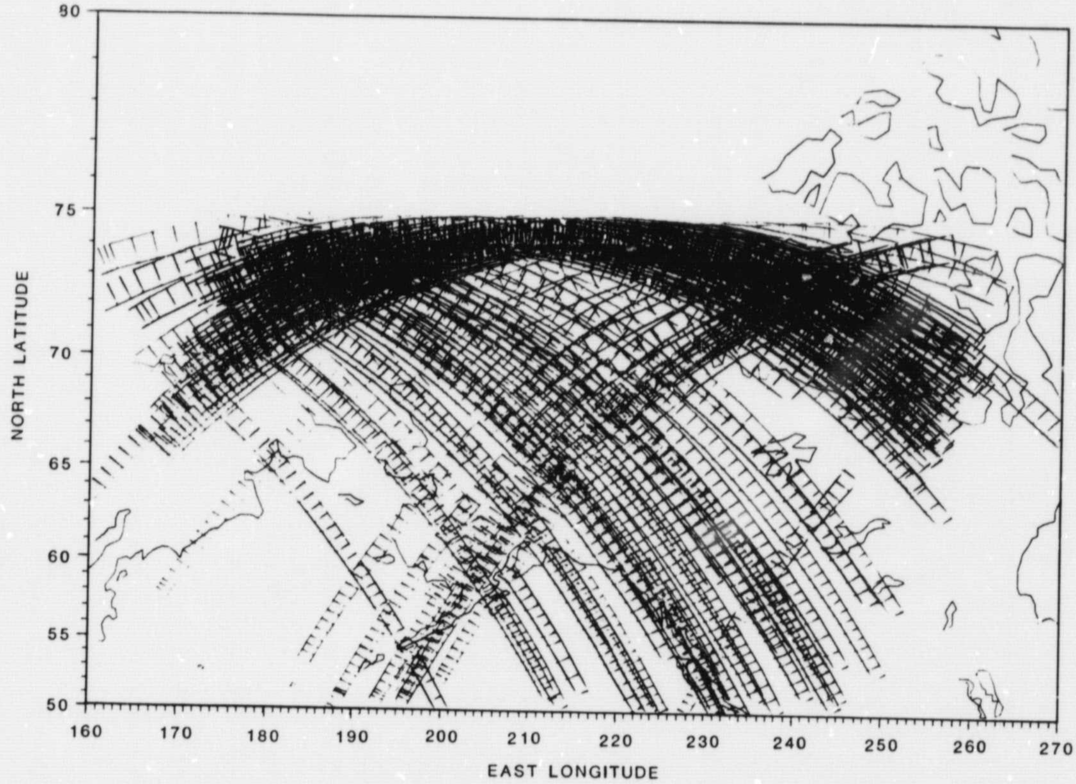

Figure A-14. Fairbanks, Alaska: July 4 through October 9, 1978

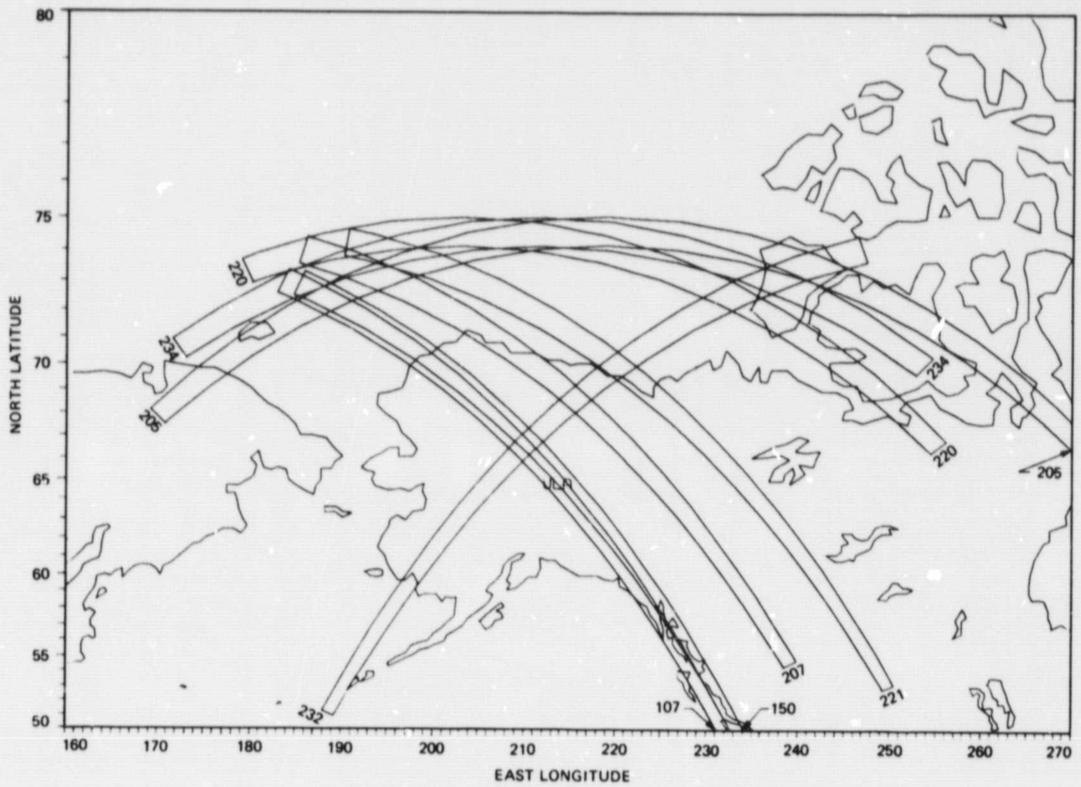

Figure A-15. Fairbanks, Alaska: July 4 through July 13

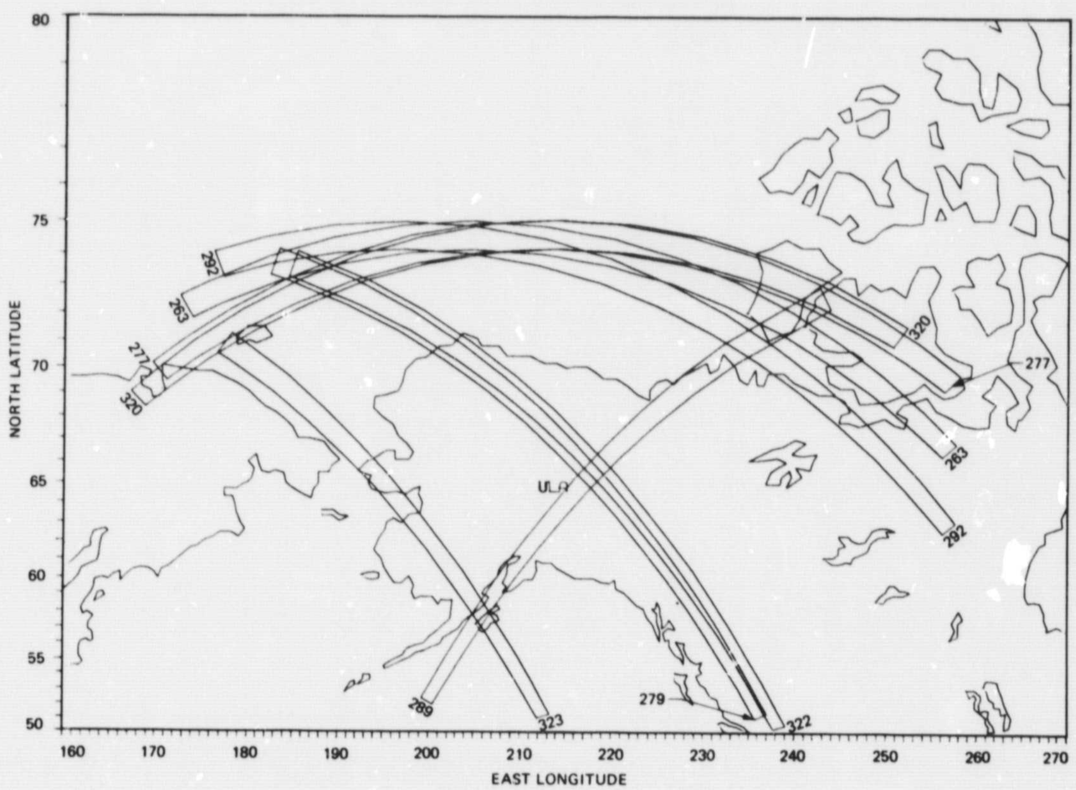

Figure A-16. Fairbanks, Alaska: July 14 through July 19

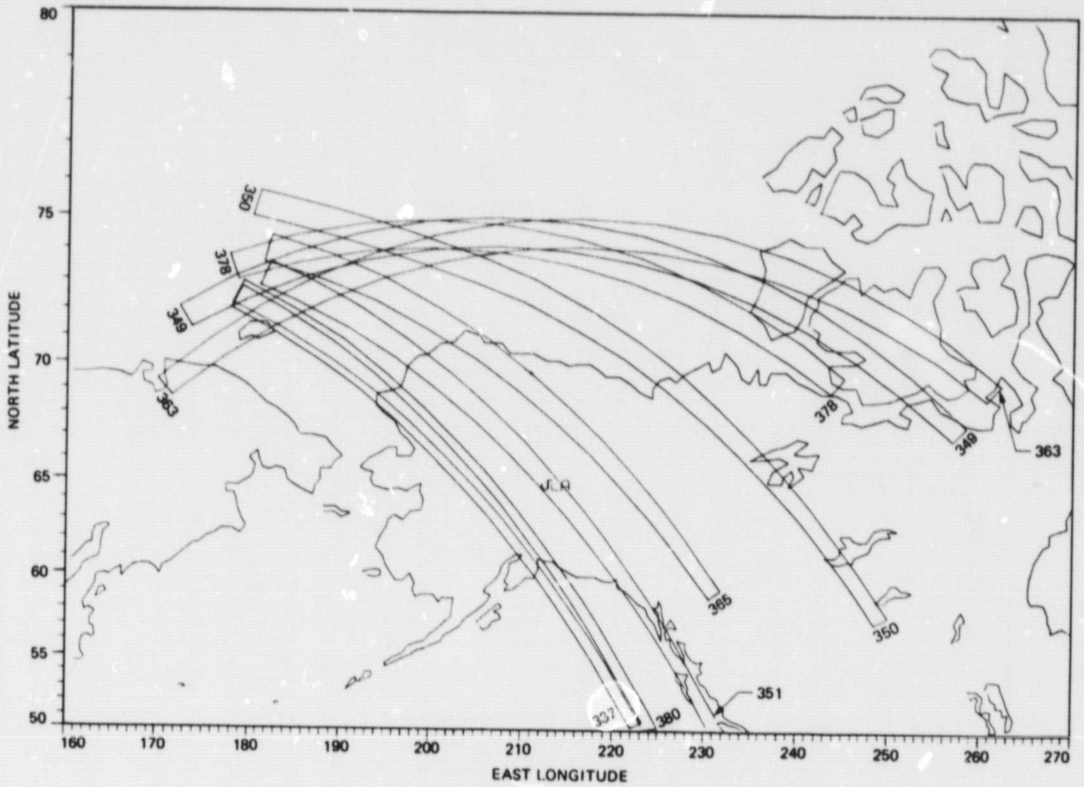

Figure A-17. Fairbanks, Alaska: July [illegible] through July 23

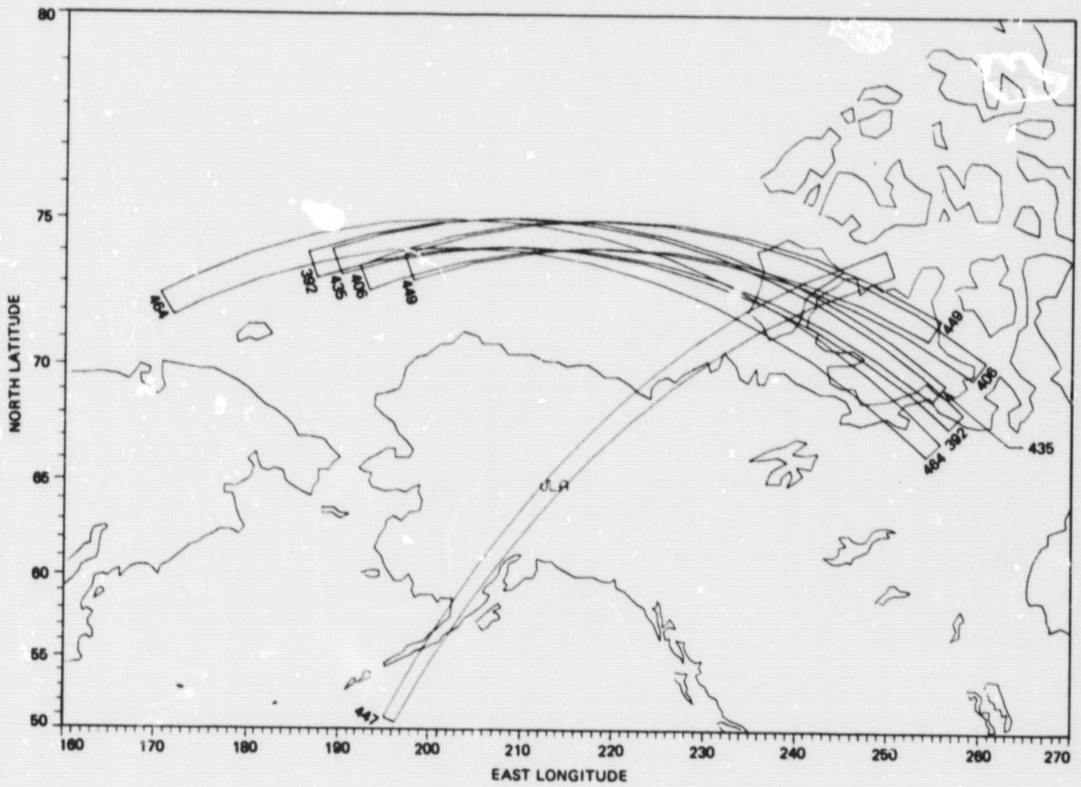

Figure A-18. Fairbanks, Alaska: July 24 through July 29

ORIGINAL PAGE IS
OF POOR QUALITY

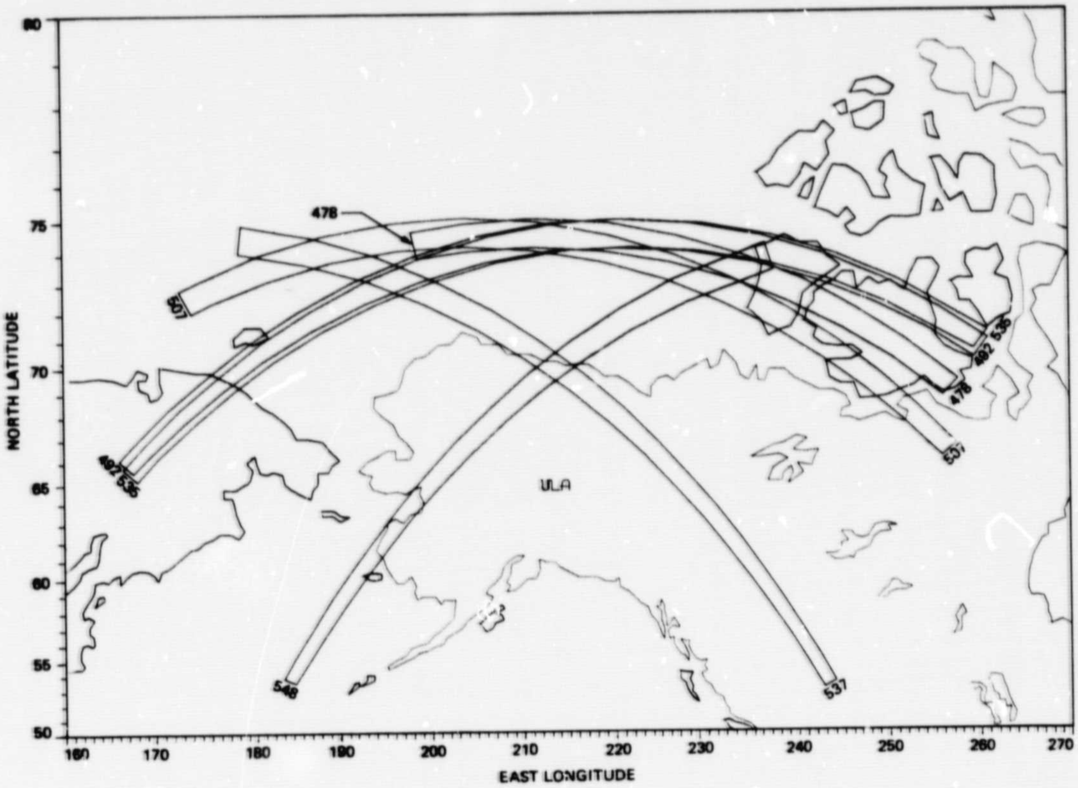

Figure A-19. Fairbanks, Alaska: July 30 through August 4

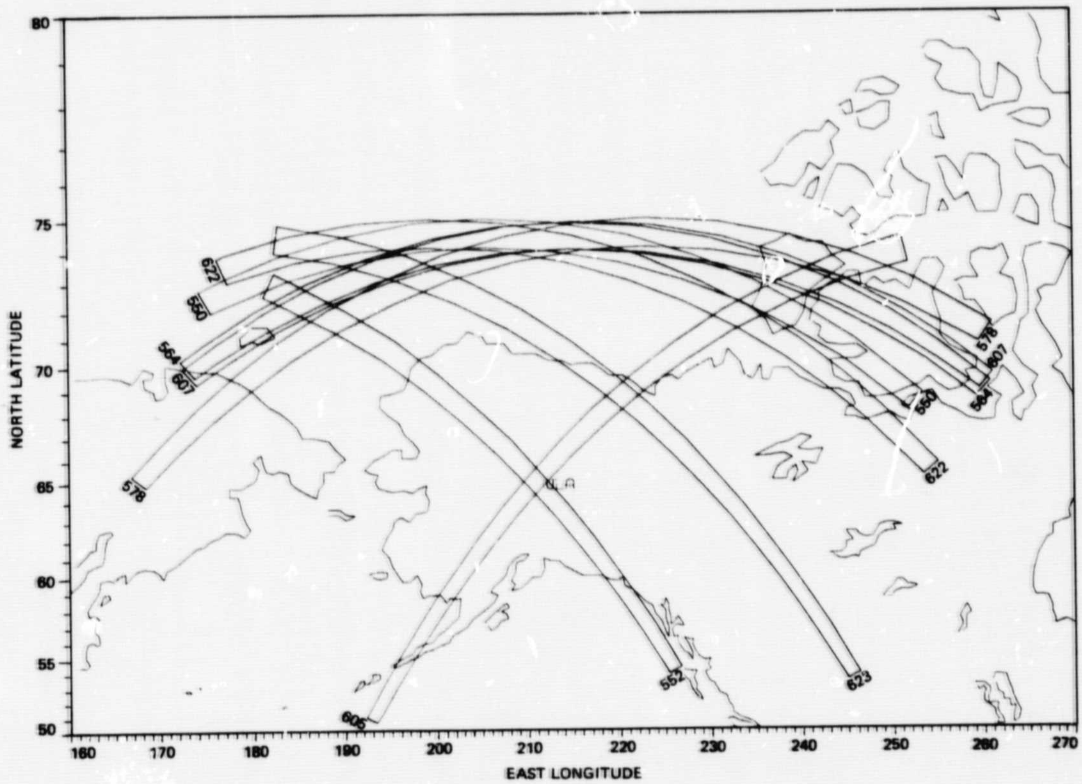

Figure A-20. Fairbanks, Alaska: August 4 through August 9

ORIGINAL PAGE IS
OF POOR QUALITY

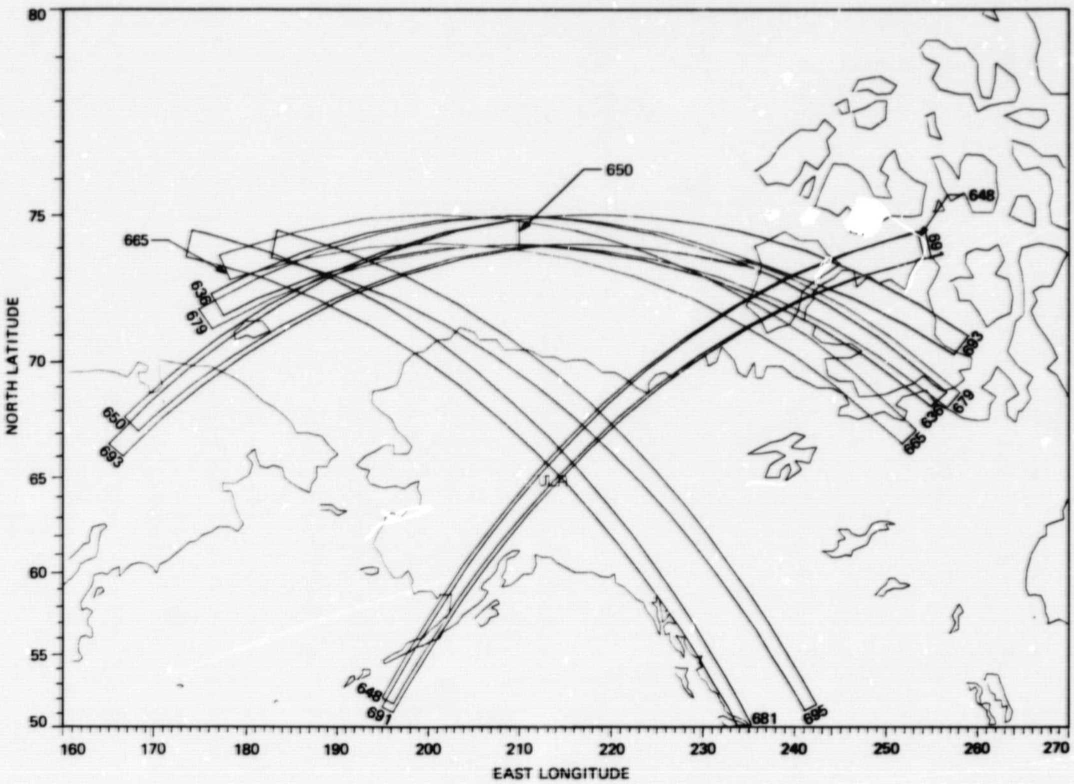

Figure A-21. Fairbanks, Alaska: August 10 through August 14

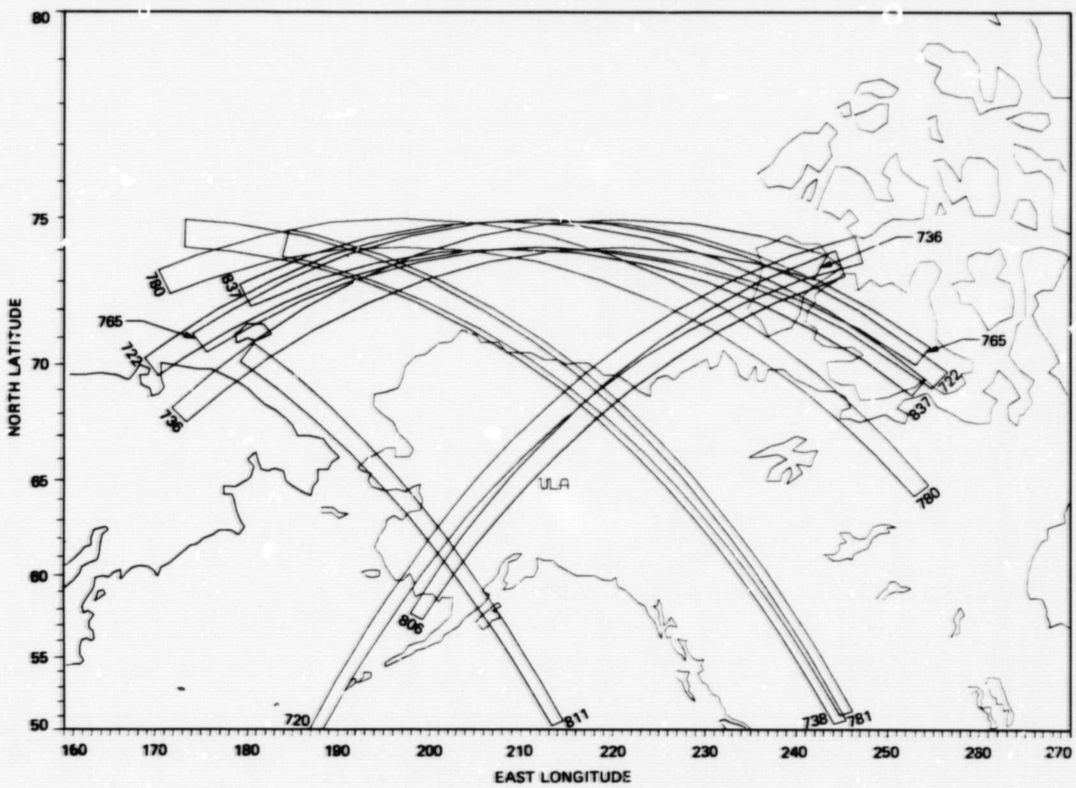

Figure A-22. Fairbanks, Alaska: August 15 through August 24

ORIGINAL PAGE IS
OF POOR QUALITY

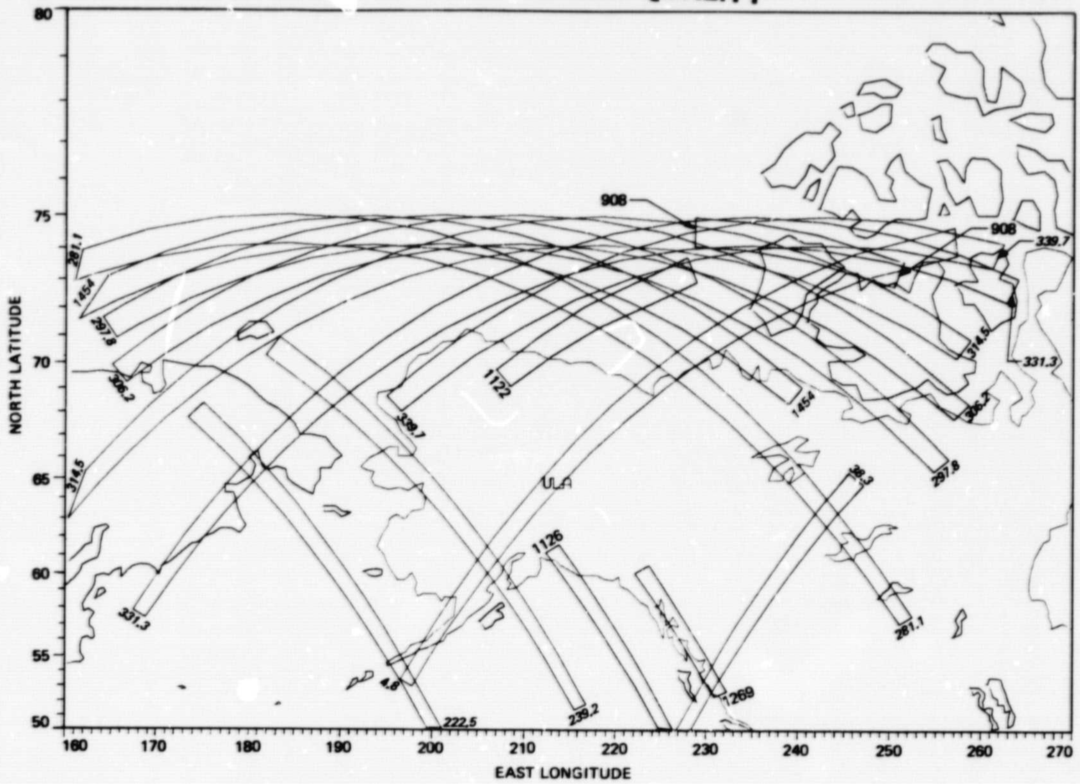

Figure A-23. Fairbanks, Alaska: August 25 through October 9

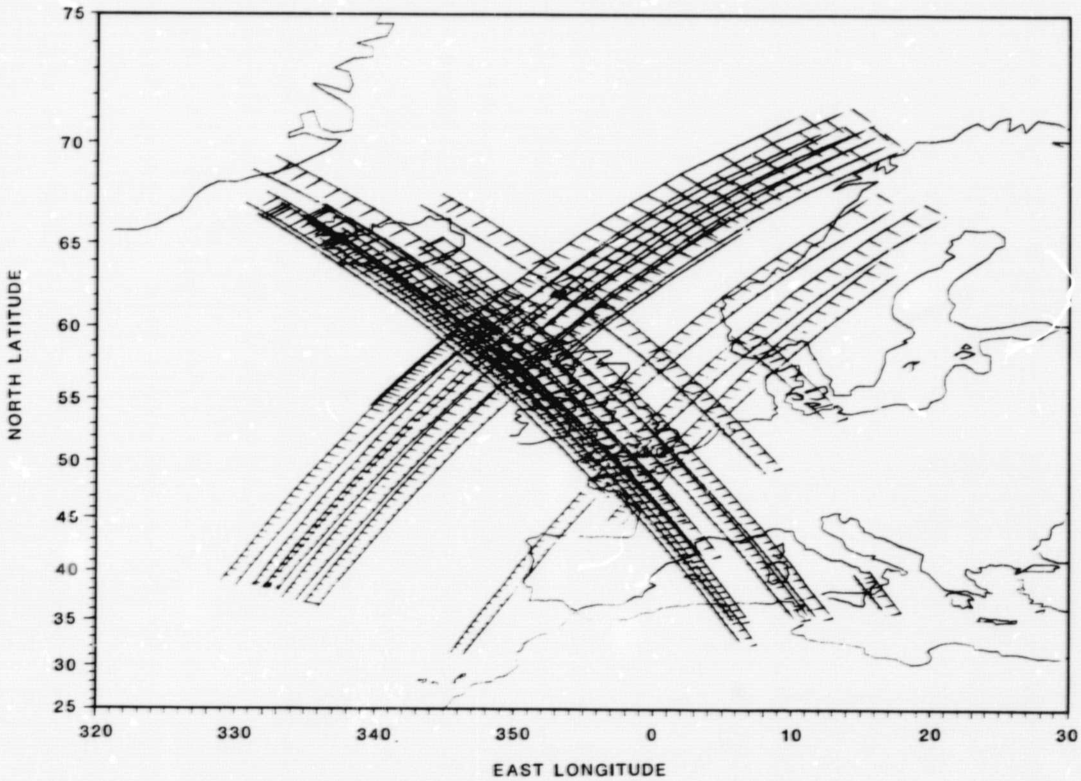

Figure A-24. Oakhanger, England: August 4 through October 10, 1978

ORIGINAL PAGE IS
OF POOR QUALITY

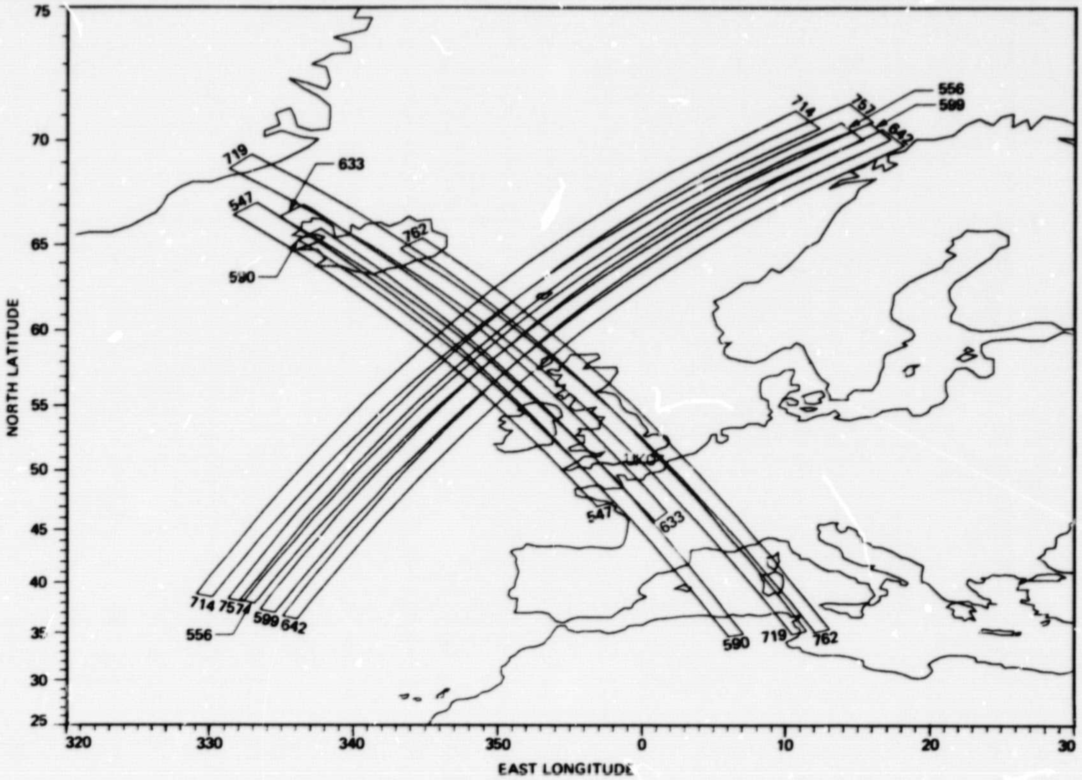

Figure A-25. Oakhanger, England: August 4 through August 19

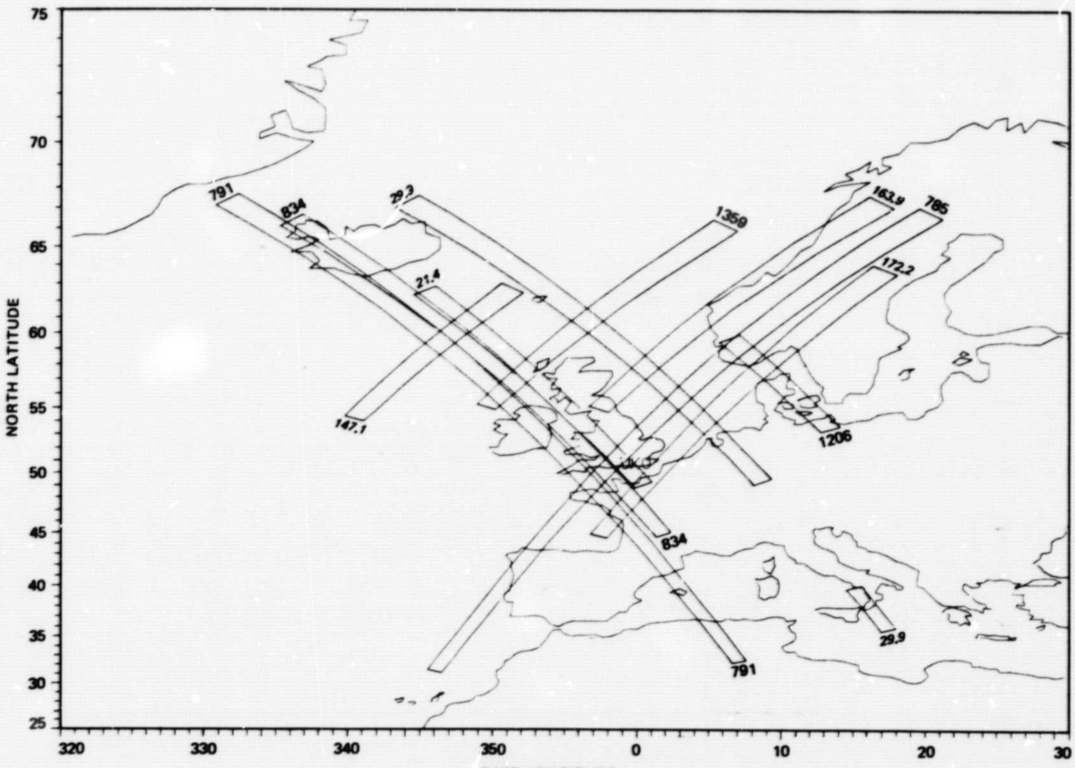

Figure A-26. Oakhanger, England: August 20 through October 10

II. Key Orbital Information

Tables A-1 and A-2 present key orbital information pertaining to the SAR swaths plotted on Figures A-1 through A-26. Table A-1 lists the revolution numbers consecutively while Table A-2 contains the same information resorted by node. All the data in the two tables have been optically processed except as noted under "COMMENTS." Nodes and node times are taken from Klose (1979), and all times are standardized to Greenwich Mean Time (GMT). Items listed include:

REV	revolution number
STA	receiving station acronym (Subsection A-I)
NODE	east longitude in degrees where the spacecraft nadir track crosses the equator in an ascending mode (passing from south to north)
DAT	month and day of 1978
JLN	Julian day of 1978
NODETIM	time (hour:minute:second) of spacecraft node crossing
LTON	north latitude in degrees where imagery starts in the center of the swath
LOFF	north latitude in degrees where imagery ends in the center of the swath
TIMEON	time (hour:minute:second) when imagery starts
OFF	time (hour:minute:second) when imagery ends
COMMENTS	NP: entire revolution not optically processed unless followed by time (minute:second) and letter (S. start; M. middle; E. end), which indicates the duration and location of the segment of the revolution that is not optically processed
	NTC: no time code on original high-density digital tape
	ENG: engineering revolutions in which the configuration of the SAR was altered to test various features of the system.

Table A-3 provides the approximate amount of time taken by the spacecraft to travel from the equator to the place where the center of the SAR swath (not the nadir track) crosses a given latitude, either in an ascending mode (passing from southeast to northwest) or a descending mode (passing from northeast to southwest). Items listed in this table include:

LAT	north latitude in degrees
TA	time (minute:second) from equator to latitude crossing in an ascending mode
TD	time (minute:second) from equator to latitude crossing in a descending mode

Effective use of Tables A-1, -2, and -3 in conjunction with the coverage plots will enable the reader to determine the revolution numbers, dates, and times of the SAR images covering an area of interest, and will thus facilitate the process of ordering SAR images.

III. Digitally Processed SAR Images

Table A-4 lists, by revolution number, the SAR images that have been digitally processed by JPL up to October 1, 1981. Each image is 100 km by 100 km in area and has a nominal ground resolution of 25 m in both range and azimuth (Wu et al., 1981). All processed digital imagery is available through the Environmental Data and Information Service (EDIS) of NOAA (see Section II for address). Items listed include:

REV	revolution number
STA	receiving station acronym (Subsection A-I)
LOCATION	site name, and state or country
LAT	north latitude in degrees and minutes for nominal center of image
LON	west longitude in degrees and minutes for nominal center image†
TIME	Julian day of 1978 followed by time (hour:minute:second) of center of image

Table A-5 lists, by revolution number and latitude, the digital SAR images processed in Europe up to August 1981. All processed imagery, available through ESRIN in Italy (see Section II for address), have full 25-m resolution and are 40 km by 40 km in size. Items listed include:

REV	revolution number

†Subtract the degrees in west longitude from 360 to convert to degrees in east longitude.

STA	receiving station acronym (Subsection A-I)
DATE	month and day, 1978
LOCATION	site name and country
LAT	north latitude in degrees and hundreths of a degree for center of image
LON	east or west longitude in degrees and hundredths of a degree for center of image
ARCH	archive number
*	Image slightly defocussed
**	larger scene 40 km in azimuth and 50 km in range

Table A-1. Orbital information for the Seasat SAR images by consecutive revolution numbers

REV	STA	NODE	DAT	JLN NODE TIM	LTON	LOFF	TIME ON	OFF	COMMENTS
107	GDS	253.67	J 4	185-12: 1: 3	18.5	47.8	12: 6:15	15: 0	
107	ULA	253.67	J 4	185-12: 1: 3	47.8	73.4	12:15: 0	24:20	NP
150	GDS	255.10	J 7	188-12: 8: 6	18.2	54.6	12:13:22	24:10	
150	ULA	255.10	J 7	188-12: 8: 6	49.8	73.4	12:22:40	31:30	
163	MIL	289.03	J 8	189- 9:56:17	10.8	49.1	9:59:20	10:38	
179	GDS	247.70	J 9	190-12:46:21	22.6	50.1	12:52:45	[illegible]: 0	
193	GDS	256.54	J10	191-12:15: 9	21.1	53.6	12:21: 7	30:53	
205	ULA	315.55	J11	192- 8:22:48	65.8	68.0	8:44:32	53:25	
207	GDS	265.38	J11	192-11:43:58	23.6	56.0	11:50:40	0:30	
207	ULA	265.38	J11	192-11:43:58	54.8	74.4	12: 0: 5	8:15	
220	ULA	299.30	J12	193- 9:32: 8	66.8	72.6	9:52:21	59:41	
221	MIL	274.22	J12	193-11:12:46	13.4	37.4	11:16:28	23:35	
221	ULA	274.22	J12	193-11:12:46	53.3	74.7	11:28:25	37:50	
222	GDS	249.14	J12	193-12:53:24	19.5	50.4	12:57:25	8:10	
230	GDS	48.48	J13	194- 2:18:26	53.8	23.4	2:53: 0	2:10	
232	ULA	358.31	J13	194- 5:39:41	74.6	51.2	6: 5:32	15: 3	
234	ULA	308.15	J13	194- 9: 0:56	69.9	70.1	9:22:25	29:45	
236	GDS	257.98	J13	194-12:22:12	18.6	52.5	12:27:25	38: 5	NP1:40M
242	MIL	107.48	J13	194-22:25:58	35.9	14.4	23: 6: 0	12:20	
251	GDS	241.74	J14	195-13:31:38	15.6	45.9	13:35:58	45: 0	
263	MIL	300.74	J15	196- 9:39:11	16.6	51.1	9:43:48	54: 8	
263	ULA	300.74	J15	196- 9:39:11	66.4	72.4	9:59:25	6:50	
273	GDS	49.92	J16	197- 2:25:28	53.4	22.5	3: 0:10	9:28	
277	ULA	309.59	J16	197- 9: 7:59	69.2	69.7	9:29:10	37: 0	
279	GDS	259.42	J16	197-12:29:14	33.2	54.2	12:38:46	45:10	
279	ULA	259.42	J16	197-12:29:14	51.3	73.9	12:44:15	53: 0	
289	ULA	8.59	J17	198- 5:15:32	72.5	51.8	5:43:10	50:43	
292	ULA	293.34	J17	198-10:17:25	63.5	73.3	10:36:25	44:30	
308	GDS	252.02	J18	199-13: 7:29	20.6	53.4	13:13:18	23:10	
320	ULA	311.03	J19	200- 9:15: 1	71.3	69.4	9:37:18	44:10	
322	GDS	260.86	J19	200-12:36:17	23.3	50.6	12:43: 4	51: 5	
322	ULA	260.86	J19	200-12:36:17	50.8	74.0	12:51:10	0: 9	
323	ULA	235.78	J19	200-14:16:54	51.4	70.6	14:31:57	38:40	
335	MIL	294.78	J20	201-10:24:27	13.0	41.4	10:28: 2	36:14	
337	ULA	244.62	J20	201-13:45:42	50.8	72.2	14: 0:35	8:17	
349	ULA	303.63	J21	202- 9:53:15	67.8	72.2	10:13:50	21:15	
350	ULA	278.54	J21	202-11:33:53	57.4	74.7	11:50:50	59:20	
351	GDS	253.46	J21	202-13:14:39	14.4	51.8	13:19:58	29:40	
351	ULA	253.46	J21	202-13:14:39	50.5	73.2	13:29:17	37:45	
363	ULA	312.47	J22	203- 9:22: 3	69.9	68.8	9:43:30	51:39	
365	ULA	262.30	J22	203-12:43:18	58.9	74.1	13: 0: 4	7:15	
371	MIL	111.81	J22	203-22:47: 5	20.9	10.9	23:31:30	34:30	
378	MIL	296.23	J23	204-10:31:29	13.6	46.3	10:35:15	45: 0	
378	ULA	296.23	J23	204-10:31:29	69.4	73.1	10:52:45	58:43	
380	ULA	246.06	J23	204-13:52:44	49.9	72.4	14: 7:20	15:25	
387	GDS	70.48	J24	205- 1:37: 8	34.7	16.7	2:17:30	22:40	
388	GDS	45.40	J24	205- 3:17:4[illegible]	51.1	27.2	3:53:12	0:22	
392	ULA	305.07	J24	205-10: 0:17	68.4	73.5	10:21: 8	27:12	
393	MIL	279.99	J24	205-11:40:54	10.8	42.1	11:43:50	53:22	

ORIGINAL PAGE IS
OF POOR QUALITY

Table A-1 (contd)

REV	STA	NODE	DAT	JLN NODE TIM	LTON	LOFF	TIME ON	OFF	COMMENTS
394	GDS	254.91	J24	205-13:21:32	18.2	53.2	13:26:38	37:10	
400	MIL	104.41	J24	205-23:25:18	43.4	9.8	0: 2:40	13: 2	
406	ULA	313.91	J25	206- 9:29: 5	70.5	72.6	9:50:50	56:39	
407	MIL	288.83	J25	206-11: 9:42	11.8	47.1	11:12:55	23:25	
416	GDS	63.08	J26	207- 2:15:22	49.6	26.0	2:51:15	58:20	ENG
422	MIL	272.59	J26	207-12:19: 8	14.2	34.1	12:23: 3	29:56	
430	GDS	71.93	J27	208- 1:44:10	25.8	16.3	2:27:10	30: 0	
435	ULA	306.51	J27	208-10: 7:18	69.3	73.5	10:28:30	34:16	
443	MIL	105.85	J27	208-23:32:20	27.0	9.6	0:14: 0	20: 7	
447	ULA	5.52	J28	209- 6:14:51	74.4	50.9	6:41: 0	50:20	
449	ULA	315.36	J28	209- 9:36: 6	71.6	72.2	9:57:50	3:50	
450	MIL	290.27	J28	209-11:16:44	12.5	47.0	11:20:10	30:26	NP4:30E
464	ULA	299.12	J29	210-10:45:32	66.8	72.5	11: 5:45	13:10	
465	MIL	274.03	J29	210-12:26: 9	13.1	38.7	12:29:45	37:21	
466	GDS	248.95	J29	210-14: 6:47	26.8	52.7	14:14:26	21:14	
472	MIL	98.45	J30	211- 0:10:33	47.4	12.0	0:47:16	57:48	
473	GDS	73.37	J30	211- 1:51:11	47.1	16.3	2:27:50	36:59	
474	GDS	46.29	J30	211- 3:31:49	53.6	23.6	4: 6:27	15:30	
478	ULA	307.96	J30	211-10:14:20	69.3	73.4	10:35:33	41:23	
480	GDS	257.79	J30	211-13:35:35	18.9	54.1	13:40:47	51:30	
488	GDS	57.13	J31	212- 3: 0:37	54.0	19.1	3:35: 7	45:38	
492	ULA	316.80	J31	212- 9:43: 7	71.0	65.4	10: 5: 5	13:49	PD4:30E
493	MIL	291.72	J31	212-11:23:45	12.8	45.8	11:27:16	37: 0	
495	GDS	241.55	J31	212-14:45: 1	20.5	46.4	14:50:48	58:32	
502	GDS	65.97	A 1	213- 2:29:25	51.1	25.2	3: 4:50	12:38	
507	ULA	300.56	A 1	213-10:52:33	66.7	72.5	11:12:43	20:10	
508	MIL	275.48	A 1	213-12:33:11	12.1	37.9	12:36:30	44: 8	
509	GDS	250.40	A 1	213-14:13:48	17.5	51.4	14:18:38	28:51	
517	GDS	49.73	A 2	214- 3:38:50	49.6	26.0	4:12:55	22:25	
522	MIL	284.32	A 2	214-12: 1:59	10.4	45.0	12: 4:48	15: 5	
523	GDS	259.24	A 2	214-13:42:36	20.9	54.6	13:47:55	58:40	
529	MIL	108.74	A 2	214-23:46:22	41.3	13.0	0:24:45	33: 6	
531	GDS	58.58	A 3	215- 3: 7:38	53.6	18.5	3:42:15	52:48	
535	ULA	318.24	A 3	215- 9:50: 9	71.3	64.7	10:12:17	21: 6	
536	MIL	293.16	A 3	215-11:30:46	21.3	43.9	11:37: 5	43:33	
537	ULA	268.08	A 3	215-13:11:24	53.5	74.6	13:27: 2	35:55	NP4:00S
538	GDS	243.00	A 3	215-14:52: 2	18.4	47.4	14:57:12	5:52	
545	GDS	67.42	A 4	216- 2:36:26	50.5	24.6	3:12: 2	19:48	NP3:28S/:48E
547	UKO	17.25	A 4	216- 5:57:41	47.4	69.6	6:11:31	18:12	NTC
548	ULA	352.17	A 4	216- 7:38:19	74.6	53.4	8: 3:10	13: 0	
550	ULA	302.00	A 4	216-10:59:34	68.6	72.3	11:20:27	27:16	
552	GDS	251.84	A 4	216-14:20:50	17.3	45.8	14:25:40	34:10	
552	ULA	251.84	A 4	216-14:20:50	54.1	73.1	14:36:45	44: 0	
556	UKO	151.51	A 4	216-21: 3:20	70.3	38.4	21:32: 3	42:38	NTC
558	MIL	101.34	A 5	217- 0:24:36	46.1	10.8	1: 1:33	12: 3	
559	GDS	76.26	A 5	217- 2: 5:14	45.0	17.0	2:42:35	50:50	
564	ULA	310.85	A 5	217-10:28:22	69.3	69.4	10:49:35	57:29	
565	MIL	285.76	A 5	217-12: 9: 0	10.5	45.5	12:11:51	22:18	
574	GDS	60.02	A 6	218- 3:14:39	50.0	19.4	3:50:25	59:54	
578	ULA	319.69	A 6	218- 9:57:10	71.6	64.2	10:19:25	28:17	

ORIGINAL PAGE IS
OF POOR QUALITY

Table A-1 (contd)

REV	STA	NODE	DAT	JLN NODE TIM	LTON	LOFF	TIME ON	OFF	COMMENTS
580	GDS	269.53	A 6	218-13:18:25	24.0	56.7	13:25:15	35: 0	
581	GDS	244.44	A 6	218-14:59: 3	19.3	48.2	15: 4:30	13: 8	
590	UKO	18.70	A 7	219- 6: 4:42	35.4	65.7	6:14:55	24:30	NTC
595	GDS	253.29	A 7	219-14:27:51	17.3	52.3	14:32:42	43:13	
599	UKO	152.95	A 7	219-21:10:22	70.3	37.7	21:39: 7	49:50	NTC
605	ULA	2.46	A 8	220- 7:14: 8	74.7	51.2	7:39:34	49:30	
607	ULA	312.29	A 8	220-10:35:23	69.7	69.0	10:56:45	4:40	
608	MIL	287.21	A 8	220-12:16: 1	11.1	44.4	12:19: 2	28:38	ENG
617	GDS	61.47	A 9	221- 3:21:40	52.8	18.0	3:56:37	7: 0	ENG
622	ULA	296.05	A 9	221-11:44:.9	65.8	73.2	12: 4:38	12: 0	
623	MIL	270.97	A 9	221-13:25:26	15.7	37.1	13:29:49	36: 9	
623	GDS	270.97	A 9	221-13:25:26	23.1	54.6	13:32: 0	41:30	NP4:30E
623	ULA	270.97	A 9	221-13:25:26	53.7	74.6	13:41:12	50: 0	
631	GDS	70.31	A10	222- 2:50:28	49.1	17.8	3:26:29	35:50	ENG
633	UKO	20.14	A10	222- 6:11:44	45.3	68.1	6:24:54	32:27	NTC
636	ULA	304.89	A10	222-11:13:37	68.5	71.6	11:34:30	41:45	
637	MIL	279.81	A10	222-12:54:14	11.0	42.5	12:57:30	7: 0	
638	GDS	254.73	A10	222-14:34:52	17.5	52.7	14:39:46	50:20	ENG
642	UKO	154.40	A10	222-21:17:23	70.1	36.9	21:46:13	57: 2	NTC
648	ULA	3.90	A11	223- 7:21: 9	74.6	51.8	7:46:52	56:40	
650	ULA	313.74	A11	223-10:42:24	74.6	68.0	11: 8: 8	12: 5	
651	MIL	288.66	A11	223-12:23: 2	10.8	41.2	12:25:58	34:59	
659	MIL	88.00	A12	224- 1:48: 4	48.7	17.6	2:24:12	33:31	
660	GDS	62.91	A12	224- 3:28:41	52.5	26.6	4: 3:39	10:30	NP3:00S
665	ULA	297.50	A12	224-11:51:50	67.1	73.1	12:12:10	19: 5	
674	GDS	71.75	A13	225- 2:57:29	37.0	16.7	3:37:10	43:11	
679	ULA	306.34	A13	225-11:20:38	68.5	71.1	11:41:35	49: 0	
681	GDS	256.18	A13	225-14:41:53	17.7	54.8	14:47: 0	56:30	NP1:30E
681	ULA	256.18	A13	225-14:41:53	49.2	73.4	14:56:15	5:17	
687	MIL	105.63	A14	226- 0:45:39	44.2	9.7	1:23:11	33:25	
691	ULA	5.35	A14	226- 7:28:10	74.5	50.6	7:54:10	3:43	
693	ULA	315.18	A14	226-10:49:25	70.9	66.8	11:11:20	29:35	
694	MIL	290.10	A14	226-12:30: 3	12.6	46.8	12:33:30	43:42	
695	GDS	265.02	A14	226-14:10:41	26.4	50.1	14:18:14	25:21	
695	ULA	265.02	A14	226-14:10:41	51.2	74.3	14:25:40	34:50	
710	GDS	248.78	A15	227-15:20: 6	27.6	50.4	15:28: 0	34:52	
714	UKO	148.45	A15	227-22: 2:37	70.4	39.2	22:31:17	41:41	NTC
716	MIL	98.34	A16	228- 1:23:38	46.1	10.9	2: 0:34	11: 2	NP5:00S
719	UKO	23.11	A16	228- 6:25:27	35.1	70.0	6:35:33	46:56	NTC
720	ULA	358.04	A16	228- 8: 6: 3	74.6	50.4	8:31:48	41:40	
722	ULA	307.88	A16	228-11:27:15	69.8	69.7	11:48:40	56:15	
723	MIL	282.81	A16	228-13: 7:52	11.6	45.4	13:11: 1	21: 5	
724	GDS	257.73	A16	228-14:48:28	19.7	51.9	14:54: 1	4:40	
731	GDS	82.19	A17	229- 2:32:42	31.6	14.2	3:12:43	18:12	NP
731	MIL	82.19	A17	229- 2:32:42	31.6	29.9	3:12:43	14:30	
736	ULA	316.81	A17	229-10:55:44	74.4	66.6	11:20: 0	26:58	
737	MIL	291.73	A17	229-12:36:20	14.6	47.7	12:40:23	50:15	NP5:00S
738	GDS	266.66	A17	229-14:16:56	24.6	51.4	14:24:38	32: 0	NP2:00E
738	ULA	266.66	A17	229-14:16:56	50.4	74.4	14:31:42	42: 0	
739	GDS	241.58	A17	229-15:57:33	21.4	48.6	16: 3:37	11:44	

ORIGINAL PAGE IS
OF POOR QUALITY

Table A-1 (contd)

REV	STA	NODE	DAT	JLN NODE TIM	LTON	LOFF	TIME ON	OFF	COMMENTS
757	UKO	150.27	A18	230-22: 8: 9	70.7	38.9	22:36:43	47:17	
759	MIL	100.13	A19	231- 1:29:18	47.2	11.9	2: 5:55	16:25	
761	GDS	50.00	A19	231- 4:50:27	55.9	23.6	5:24:21	34: 9	
762	UKO	24.92	A19	231- 6:31: 2	35.7	65.7	6:41:20	52: 7	NP1:20E
765	ULA	309.72	A19	231-11:32:45	70.1	70.5	11:54:18	1:24	
766	MIL	284.65	A19	231-13:13:19	9.6	44.2	13:15:54	26:10	
774	MIL	84.10	A20	232- 2:37:54	44.1	21.1	3:13:58	22:18	
780	ULA	293.68	A20	232-12:41:20	64.9	73.6	13: 0:50	8:10	
781	GDS	268.62	A20	232-14:21:55	22.6	51.5	14:28:20	38:30	
781	ULA	268.62	A20	232-14:21:55	51.0	74.7	14:36:50	46: 5	
782	GDS	243.55	A20	232-16: 2:29	16.7	46.8	16: 7:19	16: 8	
785	UKO	168.34	A20	232-21: 4:12	67.2	31.8	21:34:12	45:26	
788	MIL	93.14	A21	233- 2: 5:55	42.1	18.8	2:44: 0	50: 0	NP1:00E
789	GDS	68.07	A21	233- 3:46:30	46.2	30.4	4:23:24	28:10	
791	UKO	17.73	A21	233- 7: 7:39	33.4	67.4	7:17:15	28: 5	NP2:00E
795	MIL	277.66	A21	233-13:49:56	18.1	38.3	13:55: 0	1: 0	
802	MIL	102.17	A22	234- 1:33:57	39.9	14.4	2:12:47	19:20	
806	ULA	1.90	A22	234- 8:16:14	74.0	57.3	8:42:48	49:30	
809	MIL	286.69	A22	234-13:17:57	13.8	43.3	13:21:45	30:32	
810	GDS	261.62	A22	234-14:58:32	22.6	47.5	15: 4:56	12:23	
811	ULA	236.56	A22	234-16:39: 6	50.8	70.3	16:53:59	0:43	
825	GDS	245.57	A23	235-16: 7:13	19.2	47.7	16:12:37	21: 7	
834	UKO	19.90	A24	236- 7:12:35	44.9	67.2	7:25:40	32:56	
837	ULA	304.68	A24	236-12:14:22	68.7	72.7	12:35:20	41:53	
838	MIL	279.60	A24	236-13:54:58	22.0	40.4	14: 1:12	6:40	
845	MIL	104.08	A25	237- 1:39: 7	40.9	26.3	2:17:39	22: 0	
849	ULA	3.78	A25	237- 8:21:31	74.6	67.9	8:47:20	55:10	
852	MIL	288.56	A25	237-13:23:18	21.1	34.9	13:29:16	35:56	
853	GDS	263.49	A25	237-15: 3:54	26.4	39.1	15:12:20	16: 7	
874	MIL	96.53	A27	239- 2:17:58	46.9	11.4	2:54:39	5:13	
880	MIL	305.84	A27	239-12:22:29	32.9	46.7	12:31:56	36: 0	
880	ULA	305.84	A27	239-12:22:29	71.8	74.0	12:44:50	49: 0	
882	GDS	255.62	A27	239-15:43:59	28.0	41.4	15:52: 0	56: 0	
888	MIL	104.93	A28	240- 1:48:31	51.9	32.2	2:23:39	29:39	
891	UKO	29.59	A28	240- 6:50:47	49.4	64.9	7: 5:24	10:24	NP BY JPL
894	ULA	314.24	A28	240-11:53: 2	70.9	73.5	12:14:57	19:59	
908	ULA	322.65	A29	241-11:23:34	73.1	73.9	11:46:41	50:11	ENG
909	MIL	297.53	A29	241-13: 4:20	31.7	38.4	13:13:26	15:26	
931	MIL	105.02	A31	243- 2: 0:53	41.5	28.6	2:38:13	42: 5	
947	GDS	63.19	S 1	244- 4:52:56	39.7	33.0	5:31:50	33:50	NP
957	UKO	172.05	S 1	244-21:40:28	55.4	49.0	22:14:31	16:31	NP
958	UKO	146.94	S 1	244-23:21:13	62.5	56.5	23:52:56	54:56	
963	UKO	21.37	S 2	245- 7:44:59	49.2	55.5	7:59:22	1:20	
966	ULA	306.02	S 2	245-12:47:14	73.4	74.7	13:10:36	12:36	
968	GDS	255.80	S 2	245-16: 8:45	43.7	50.2	16:21:27	23:27	NP
968	GDS	255.80	S 2	245-16: 8:45	32.6	39.3	16:18: 7	20: 7	NP
974	MIL	105.11	S 3	246- 2:13:16	50.0	32.7	2:49: 1	53:57	
980	ULA	314.43	S 3	246-12:17:47	74.0	74.6	12:41:38	43:38	
990	GDS	63.29	S 4	247- 5: 5:19	39.3	32.6	5:44:19	46:19	NP
991	GDS	38.17	S 4	247- 6:46: 4	51.2	44.8	7:21:24	23:24	

ORIGINAL PAGE IS
OF POOR QUALITY

Table A-1 (contd)

REV	STA	NODE	DAT	JLN NODE TIM	LTON	LOFF	TIME ON	OFF	COMMENTS
1001	UKO	147.03	S 4	247-23:33:36	61.5	68.7	0: 5:40	6:55	
1005	GDS	46.57	S 5	248- 6:16:36	51.4	44.9	6:51:55	53:55	
1006	UKO	21.46	S 5	248- 7:57:22	55.7	61.8	8:13:47	15:47	
1009	ULA	306.12	S 5	248-12:59:37	74.1	74.5	13:23:35	25:35	
1011	GDS	255.89	S 5	248-16:21: 7	43.2	49.8	16:33:40	35:40	NP
1011	GDS	255.89	S 5	248-16:21: 7	33.0	37.9	16:30:37	32: 4	
1017	MIL	105.20	S 6	349- 2:25:38	45.9	39.6	3: 2:37	4:36	
1020	GDS	29.86	S 6	249- 7:27:54	51.5	45.0	8: 3:11	5:11	
1023	ULA	314.52	S 6	249-12:30: 9	71.6	74.4	12:52:26	54:26	
1024	MIL	289.40	S 6	249-14:10:54	21.0	27.8	14:16:51	13:51	
1033	GDS	63.38	S 7	250- 5:17:41	41.2	34.5	5:56: 7	58: 7	NP
1034	GDS	38.26	S 7	250- 6:58:26	50.8	46.7	7:33:55	35:12	
1038	ULA	297.81	S 7	250-13:41:27	69.0	74.4	14: 2:52	5:42	
1038	MIL	297.81	S 7	250-13:41:27	32.7	36.1	13:50:52	51:52	
1040	GDS	247.58	S 7	250-17: 2:57	44.7	48.0	17:15:58	16:58	NP
1044	UKO	147.12	S 7	250-23:45:58	62.9	56.8	0:17:33	19:33	
1048	GDS	46.67	S 8	251- 6:28:59	51.3	44.3	7: 4:20	6:20	
1049	UKO	21.55	S 8	251- 8: 9:44	55.8	61.9	8:26:10	28:10	
1052	ULA	306.21	S 8	251-13:11:59	71.0	74.1	13:33:57	35:57	
1054	GDS	255.98	S 8	251-16:33:30	31.3	38.0	16:42:42	44:29	
1080	ULA	323.00	S10	253-12:13: 8	73.2	74.2	12:36:22	38:17	
1081	ULA	297.68	S10	253-13:53:53	73.7	74.6	14:16:30	18:30	
1081	MIL	297.88	S10	253-13:53:53	33.4	36.8	14: 3:30	4:30	
1083	GDS	247.65	S10	253-17:15:25	42.7	49.5	17:27:59	29:59	
1087	UKO	147.18	S10	253-23:58:28	62.3	59.3	0:30:16	32:16	
1095	ULA	306.25	S11	254-13:24:33	74.3	74.4	13:38:42	50:42	
1096	MIL	281.14	S11	254-15: 5:19	22.7	29.4	15:11:45	13:45	
1097	GDS	256.02	S11	254-16:46: 5	47.3	53.8	16:59:53	1:53	NP
1097	GDS	256.02	S11	254-16:46: 5	31.8	38.5	16:55:13	57:13	NP
1109	ULA	314.62	S12	255-12:55:13	73.1	74.7	13:17:21	21:21	
1110	MIL	289.50	S12	255-14:35:59	18.3	38.5	14:41: 7	47: 7	
1112	GDS	239.27	S12	255-17:57:31	40.6	46.8	18: 9:17	11:10	
1122	ULA	348.11	S13	256-10:45: 8	73.3	69.4	11:12:15	14:15	
1126	ULA	247.64	S13	256-17:28:11	50.0	61.5	17:42:48	46:30	
1126	GDS	247.64	S13	256-17:28:11	42.7	55.7	17:40:35	44:36	
1138	ULA	306.24	S14	257-13:37:19	72.5	74.7	14: 0: 5	2:25	
1139	MIL	281.13	S14	257-15:18: 5	22.0	31.6	15:24:20	27:10	
1140	GDS	256.01	S14	257-16:56:51	23.6	53.7	17: 5:33	14:48	
1149	UKO	29.96	S15	258- 8: 5:42	53.8	67.3	8:21:30	26: 5	
1149	UKO	29.96	S15	258- 8: 5:42	36.0	40.3	8:16: 5	17:23	
1153	MIL	289.50	S15	258-14:48:45	20.8	34.3	14:54:38	58:38	
1155	GDS	239.27	S15	258-18:10:16	26.9	46.3	18:17:57	23:46	
1163	GDS	38.33	S16	259- 7:36:22	51.8	45.0	8:11:34	14:40	
1167	ULA	297.87	S16	259-14:19:25	65.4	73.0	14:39: 5	46:45	
1167	MIL	297.87	S16	259-14:19:25	15.1	30.8	14:23:17	28:16	
1169	GDS	247.64	S16	259-17: 4:56	36.6	49.5	17:51:30	55:24	
1177	GDS	46.70	S17	260- 7: 7: 2	51.2	44.7	7:42:24	44:24	
1181	SNF	306.24	S17	260-13:50: 5	41.7	48.3	14: 2:11	4:11	
1182	MIL	281.12	S17	260-15:30:51	30.3	35.5	15:39:33	41: 5	
1183	GDS	256.01	S17	260-17:11:36	20.7	52.5	17:17:26	26:55	

Table A-1 (contd)

ORIGINAL PAGE IS
OF POOR QUALITY

REV	STA	NODE	DAT	JLN NODE TIM	LTON	LOFF	TIME ON	OFF	COMMENTS
1193	ULA	4.84	S18	261- 9:59:14	73.4	63.6	10:26: 4	30:34	
1195	ULA	314.61	S18	261-13:20:45	72.6	74.7	13:43:35	46: 5	
1196	MIL	289.49	S18	261-15: 1:31	18.9	30.0	15: 6:51	10:21	
1197	GDS	264.38	S18	261-16:42:16	24.1	53.9	16:49: 7	58: 7	
1198	GDS	239.26	S18	261-18:23: 2	40.0	46.6	18:34:36	36:36	NF
1201	UKO	163.91	S18	261-23:25:19	67.8	[illegible]	23:55: 6	57: 6	
1204	MIL	88.56	S19	262- 4:27:36	49.7	[illegible]	5: 3:26	13:26	
1205	GDS	63.44	S19	262- 6: 8:22	39.9	31.4	6:47:12	49:42	
1206	GDS	38.33	S19	262- 7:49: 8	56.2	49.6	8:22:57	24:57	
1206	UKO	38.33	S19	262- 7:49: 8	53.7	59.9	8: 4:55	6:55	
1209	SNF	322.98	S19	262-12:51:25	44.1	56.0	13: 4:14	8:14	
1210	ULA	297.86	S19	262-14:32:11	72.6	74.7	14:55: 0	57: 0	
1210	MIL	297.86	S19	262-14:32:11	27.6	37.5	14:40: 2	42:58	
1211	MIL	272.74	S19	262-16:12:56	10.4	17.2	16:15:46	18:46	
1212	GDS	247.63	S19	262-17:53:42	44.0	50.6	18: 6:31	8:31	
1215	UKO	172.28	S19	262-22:55:59	58.6	52.6	23:29: 0	30:48	
1224	ULA	306.23	S20	263-14: 2:51	72.2	74.7	14:25:25	27:49	
1225	MIL	281.11	S20	263-15:43:36	20.6	27.3	15:49:24	52:24	
1226	GDS	256.00	S20	263-17:24:22	24.5	37.4	17:31:20	35:10	
1231	SNF	130.42	S21	264- 1:48:11	45.0	38.4	2:25:28	27:28	
1232	MIL	105.30	S21	264- 3:28:56	44.3	30.0	4: 6:25	12:34	NP2:09E
1232	SNF	105.30	S21	264- 3:28:56	56.8	42.4	4: 2:34	4: 7	
1235	GDS	29.95	S21	264- 8:31:14	57.6	53.1	9: 4:35	6: 1	
1236	ULA	4.83	S21	264-10:11:59	73.1	64.3	10:39:15	43: 0	
1238	SNF	314.60	S21	264-13:33:31	42.3	55.3	13:45:48	49:48	
1239	MIL	289.48	S21	264-15:14:16	18.8	30.6	15:19:33	23: 3	
1241	ULA	239.25	S21	264-18:35:48	52.7	58.9	18:51:15	53:15	
1248	GDS	63.44	S22	265- 6:21: 8	40.0	33.6	6:59:54	1:54	NP
1249	GDS	38.32	S22	265- 8: 1:53	56.3	49.9	8:35:40	37:40	
1249	UKO	38.22	S22	265- 8: 1:53	53.7	59.9	8:17:40	19:40	NF BY JPL
1252	SNF	322.97	S22	265-13: 4:10	43.9	55.3	13:16:56	21:56	
1253	MIL	297.85	S22	265-14:44:56	15.3	39.9	14:49:12	57:12	
1254	MIL	272.74	S22	265-16:25:42	13.6	39.9	16:29:28	34: 5	
1254	GDS	272.74	S22	265-16:25:42	27.8	44.6	16:33:40	38:40	
1255	GDS	247.62	S22	265-18: 6:28	40.6	50.4	18:18:13	21:13	
1258	UKO	172.27	S22	265-23: 8:45	59.9	53.2	23:41:30	43:30	
1259	UKO	147.16	S23	266- 0:49:30	62.3	56.5	1:21:16	23:10	
1261	SNF	96.92	S23	266- 4:11: 2	50.0	40.1	4:46:47	49:48	
1263	GDS	46.69	S23	266- 7:32:33	50.8	45.3	8: 8: 2	9:45	
1265	SNF	356.46	S23	266-10:54: 5	60.9	65.6	11:12:10	13:50	
1267	MIL	306.22	S23	266-14:15:36	27.1	40.6	14:23:21	27:21	
1267	ULA	306.22	S23	266-14:15:36	73.9	74.6	14:39:21	41:21	
1269	GDS	255.99	S23	266-17:37: 7	27.2	59.1	17:44:53	54:38	
1269	ULA	255.99	S23	266-17:37: 7	53.0	60.4	17:52:40	55: 0	
1275	SNF	105.29	S24	267- 3:41:42	46.6	36.6	4:18:30	21:30	
1279	ULA	4.83	S24	267-10:24:45	73.8	65.3	10:51:28	55:28	
1281	ULA	314.59	S24	267-13:46:16	73.9	74.6	14:10: 0	12: 0	
1282	MIL	289.48	S24	267-15:27: 2	18.6	41.7	15:32:15	39:18	
1283	GDS	264.36	S24	267-17: 7:47	27.0	47.1	17:15:31	22:31	NP
1284	ULA	239.25	S24	267-18:48:33	55.0	61.2	19: 4:46	6:46	

ORIGINAL PAGE IS
OF POOR QUALITY

Table A-1 (contd)

REV	STA	NODE	DAT	JLN NODE TIM	LTON	LOFF	TIME ON	OFF	COMMENTS
1287	UKO	163.90	S24	267-23:50:50	66.7	61.0	0:21: 3	23: 3	
1290	MIL	88.55	S25	268- 4:53: 7	48.9	42.3	5:29:12	31:12	NP
1291	GDS	63.43	S25	268- 6:33:53	52.6	26.0	7: 8:50	16:50	ENG
1292	ULA	38.31	S25	268- 8:14:39	65.0	49.8	8:45:29	50:28	
1296	MIL	297.85	S25	268-14:57:41	28.8	42.9	15: 5:55	9:51	
1296	ULA	297.85	S25	268-14:57:41	70.0	74.7	15:19:10	23:10	
1298	GDS	247.62	S25	268-18:19:13	38.0	51.2	18:30:13	34:13	
1299	ULA	222.50	S25	268-19:59:59	56.0	62.0	20:16:29	18:29	
1306	GDS	46.69	S26	269- 7:45:18	55.8	42.8	8:19:14	23:14	
1307	UKO	21.57	S26	269- 9:26: 4	51.2	63.6	9:41: 5	45: 5	
1310	ULA	306.22	S26	269-14:28:21	68.6	73.9	14:49:15	55: 0	
1311	ULA	281.10	S26	269-16: 9: 7	58.6	72.9	16:26:27	32: 6	
1312	GDS	255.99	S26	269-17:49:52	17.4	44.2	17:54:45	2:42	ENG-NP2:45S
1316	UKO	155.52	S26	270- 0:32:55	66.3	55.4	1: 3:17	7:17	NP BY JPL
1318	SNF	105.29	S27	270- 3:54:27	50.1	36.9	4:30:10	34:10	
1321	GDS	29.94	S27	270- 8:56:44	55.8	43.1	9:30:40	34:35	
1322	ULA	4.82	S27	270-10:37:30	74.3	66.6	11: 3:44	7:44	
1324	SNF	314.59	S27	270-13:59: 1	37.2	43.8	14: 9:45	11:45	
1325	MIL	289.47	S27	270-15:39:46	20.2	33.7	15:45:28	49:28	
1327	GDS	239.24	S27	270-19: 1:18	33.6	46.8	19:10:57	14:57	
1333	MIL	88.54	S28	271- 5: 5:52	50.2	43.8	5:41:33	43:30	
1334	GDS	63.43	S28	271- 6:46:38	53.0	26.2	7:21:26	29:22	ENG-NP3:00S
1335	ULA	38.31	S28	271- 8:27:24	65.2	48.5	8:58:10	3:37	
1339	ULA	297.85	S28	271-15:10:26	72.0	74.5	15:32:53	34:53	
1339	MIL	297.85	S28	271-15:10:26	28.4	41.8	15:18:34	22:34	
1340	GDS	272.73	S28	271-16:51:12	29.8	43.1	16:59:43	3:43	
1341	GDS	247.61	S28	271-18:31:57	38.6	51.7	18:43: 6	47: 6	
1344	UKO	172.26	S28	271-23:34:15	58.7	52.3	0: 7:16	9:16	NP BY JPL
1349	GDS	46.68	S29	272- 7:58: 3	55.9	42.6	8:31:58	35:58	
1352	SNF	331.33	S29	272-13: 0:20	45.9	61.8	13:13:42	18:42	
1353	ULA	306.22	S29	272-14:41: 6	73.8	72.4	15: 4:45	8:45	
1354	ULA	281.10	S29	272-16:21:51	58.5	72.9	16:39:10	44:49	NP
1355	GDS	255.99	S29	272-18: 2:37	26.5	43.3	18:10:11	15:11	
1359	UKO	155.52	S30	273- 0:45:40	67.0	55.6	1:15:45	19:45	
1360	SNF	130.40	S30	273- 2:26:25	48.7	35.4	3: 2:35	6:35	
1361	SNF	105.29	S30	273- 4: 7:11	52.4	36.2	4:42:30	47: 7	NP
1364	GDS	29.94	S30	273- 9: 9:28	56.0	43.4	9:43:20	47:13	
1365	ULA	4.82	S30	273-10:50:14	74.3	72.4	11:16:27	20:27	
1367	SNF	314.59	S30	273-14:11:45	37.1	43.8	14:22:28	24:28	
1368	MIL	289.47	S30	273-15:52:31	20.1	33.6	15:58:11	2:11	
1370	GDS	239.24	S30	273-19:14: 2	33.6	46.8	19:23:41	27:41	
1376	MIL	88.54	0 1	274- 5:18:36	49.1	42.6	5:54:37	56:37	NP
1377	GDS	63.43	0 1	274- 6:59:22	43.8	30.4	7:37: 1	41: 1	
1378	GDS	38.31	0 1	274- 8:40: 8	56.2	43.5	9:13:57	17:54	
1378	ULA	38.31	0 1	274- 8:40: 8	59.0	49.2	9:13: 0	16: 8	
1382	ULA	297.84	0 1	274-15:23:10	72.0	74.5	15:45:36	47:36	
1383	GDS	272.73	0 1	274-17: 3:56	31.8	43.0	17:13: 5	16:25	
1384	GDS	247.61	0 1	274-18:44:41	38.0	51.2	18:55:40	59:40	
1385	ULA	222.50	0 1	274-20:25:27	55.9	62.0	20:41:55	43:55	
1387	UKO	172.26	0 1	274-23:46:58	58.6	52.3	0:19:59	21:59	

ORIGINAL PAGE IS
OF POOR QUALITY

Table A-1 (contd)

REV	STA	NODE	DAT	JLN NODE TIM	LTON	LOFF	TIME ON	OFF	COMMENTS
1391	GDS	71.80	0 2	275- 6:30: 1	39.6	26.1	7: 8:57	12:37	
1395	ULA	331.33	0 2	275-13:13: 4	72.8	58.1	13:36: 2	46:15	
1395	SNF	331.33	0 2	275-13:13: 4	31.6	66.1	13:22: 4	33: 0	
1396	ULA	306.22	0 2	275-14:53:49	68.1	69.4	15:14:32	22:56	
1397	ULA	281.10	0 2	275-16:34:35	57.8	74.3	16:51:40	1: 0	NP3:20S
1397	MIL	281.10	0 2	275-16:34:35	10.2	23.7	16:37:20	41:20	
1398	GDS	255.99	0 2	275-18:15:21	17.6	44.4	18:20:17	28:16	ENG-NP:51E
1403	SNF	130.40	0 3	276- 2:39: 9	51.2	31.6	3:14:32	20:32	
1404	SNF	105.29	0 3	276- 4:19:55	57.0	44.0	4:53:27	57: 3	NP
1404	MIL	105.29	0 3	276- 4:19:55	44.8	22.4	4:57:15	3:57	
1404	MIL	105.29	0 3	276- 4:19:55	27.3	7.2	5: 2:30	8:26	NP
1406	GDS	55.06	0 3	276- 7:41:26	48.4	35.2	8:17:40	21:40	
1408	ULA	4.82	0 3	276-11: 2:57	74.6	63.5	11:28:36	34:20	
1409	ULA	339.71	0 3	276-12:43:43	73.6	68.5	13: 7:15	13:13	
1411	MIL	289.47	0 3	276-16: 5:14	17.9	37.7	16:10: 8	16: 8	
1412	GDS	264.36	0 3	276-17:46: 0	27.7	47.8	17:53:56	59:56	NP
1419	MIL	88.54	0 4	277- 5:31:20	48.8	29.1	6: 7:28	13:22	
1420	GDS	63.43	0 4	277- 7:12: 5	52.3	29.2	7:47: 7	54: 5	ENG-NP3:00S
1421	ULA	38.31	0 4	277- 8:52:51	65.2	49.7	9:23:36	28:41	NP
1425	ULA	297.85	0 4	277-15:35:53	65.8	71.7	15:55:43	3:57	
1425	MIL	297.85	0 4	277-15:35:53	18.8	39.3	15:41:10	47:10	ENG
1426	GDS	272.73	0 4	277-17:16:39	27.0	47.1	17:24:23	30:23	NP2:00SE
1428	ULA	222.50	0 4	277-20:38:11	50.2	68.0	20:52:52	58:52	
1430	UKO	172.27	0 4	277-23:59:42	63.9	45.2	0:30:56	36:56	
1434	GDS	71.80	0 5	278- 6:42:44	38.0	26.4	7:22: 7	25:35	
1438	ULA	331.34	0 5	278-13:25:47	73.0	58.0	13:48:50	59: 0	
1438	SNF	331.34	0 5	278-13:25:47	31.6	67.1	13:34:47	46: 6	
1439	ULA	306.22	0 5	278-15: 6:33	68.0	69.5	15:27:13	35:38	
1440	ULA	281.10	0 5	278-16:47:18	57.7	74.3	17: 4:22	13:34	
1440	MIL	281.10	0 5	278-16:47:18	10.8	23.7	16:50:15	54: 1	
1441	GDS	255.99	0 5	278-18:28: 4	17.6	45.0	18:33: 0	41: 9	ENG
1446	SNF	130.41	0 6	279- 2:51:52	51.3	31.4	3:27:13	33:13	
1447	SNF	105.29	0 6	279- 4:32:38	57.2	41.4	5: 6: 8	11: 0	NP
1447	MIL	105.29	0 6	279- 4:32:57	44.3	15.3	5:10: 0	18:45	
1447	MIL	105.29	0 6	279- 4:32:57	17.0	7.2	5:18:30	21: 8	NP
1449	GDS	55.06	0 6	279- 7:54: 9	48.6	35.3	8:30:21	34:21	
1451	ULA	4.83	0 6	279-11:15:41	74.5	60.5	11:41:40	47: 5	NP3:00E
1452	ULA	339.71	0 6	279-12:56:26	73.8	71.0	13:20: 6	25:50	
1454	ULA	289.48	0 6	279-16:17:57	68.9	71.0	16:39: 1	45: 1	
1455	GDS	264.36	0 6	279-17:58:43	27.6	47.5	18: 6:37	12:37	NP
1462	MIL	88.55	0 7	280- 5:44: 3	48.8	29.2	6:20:10	26: 3	NP3:47S
1463	GDS	63.43	0 7	280- 7:24:48	52.3	22.4	7:59:50	8:53	
1464	ULA	38.32	0 7	280- 9: 5:34	65.3	49.8	9:36:18	41:23	NP
1468	ULA	297.85	0 7	280-15:48:36	65.6	71.7	16: 8:25	16:39	
1468	MIL	297.85	0 7	280-15:48:36	22.1	42.2	15:54:51	0:51	ENG
1469	GDS	272.74	0 7	280-17:29:22	27.0	47.0	17:37: 4	43: 4	NP2:00SE
1471	ULA	222.50	0 7	280-20:50:53	50.1	68.1	21: 5:33	11:33	
1473	UKO	172.27	0 8	281- 0:12:25	64.1	48.4	0:43:37	48:40	
1481	ULA	331.34	0 8	281-13:38:30	72.9	58.2	14: 1:30	11:40	
1482	ULA	306.23	0 8	281-15:19:15	68.6	64.3	15:40:10	48:20	

Table A-1 (contd)

REV	STA	NODE	DAT	JLN NODE TIM	LTON	LOFF	TIME ON	OFF	COMMENTS
1483	ULA	281.11	0 8	281-17: 0: 1	59.8	74.3	17:17: 4	26:16	NP6:26E
1483	MIL	281.11	0 8	281-17: 0: 1	10.7	23.5	17: 2:55	6:42	
1484	GDS	256.00	0 8	281-18:40:47	12.6	55.0	18:45:42	57: 2	
1489	SNF	130.41	0 9	282- 3: 4:35	44.3	38.2	3:42: 4	43:56	
1490	SNF	105.30	0 9	282- 4:45:20	65.3	43.7	5:16: 5	23: 0	NP2:00E
1490	MIL	105.30	0 9	282- 4:45:20	45.4	14.4	5:22:48	31:42	
1490	MIL	105.30	0 9	282- 4:45:20	17.0	7.0	5:30:58	33:54	
1492	GDS	55.06	0 9	282- 8: 6:52	54.6	38.2	8:41:12	46:12	
1493	UKO	29.95	0 9	282- 9:47:38	49.2	55.6	10: 2: 1	4: 1	
1494	ULA	4.83	0 9	282-11:26:23	74.0	53.9	11:54:55	2:55	
1496	ULA	314.60	0 9	282-14:49:54	70.8	65.2	15:11:46	20:39	
1497	MIL	289.48	0 9	282-16:30:40	25.1	31.3	16:37:48	39:39	
1498	GDS	264.37	0 9	282-18:11:26	34.8	41.8	18:21:27	23:27	NP
1499	ULA	239.25	0 9	282-19:52:11	52.0	70.6	20: 7:27	13:57	
1502	UKO	163.90	010	283- 0:54:28	67.6	55.0	1:24:14	29:40	

ORIGINAL PAGE IS
OF POOR QUALITY

Table A-2. Orbital information for the Seasat SAR images by consecutive node numbers

REV	STA	NODE	DAT	JLN NODE TIM	LTON	LOFF	TIME ON	OFF	COMMENTS
806	ULA	1.90	A22	234- 8:16:14	74.0	57.3	8:42:48	49:30	
605	ULA	2.46	A 8	220- 7:14: 8	74.7	51.2	7:39:34	49:30	
849	ULA	3.78	A25	237- 8:21:31	74.6	67.9	8:47:20	55:10	
648	ULA	3.90	A11	223- 7:21: 9	74.6	51.8	7:46:52	56:40	
1322	ULA	4.82	S27	270-10:37:30	74.3	66.6	11: 3:44	7:44	
1365	ULA	4.82	S30	273-10:50:14	74.3	72.4	11:16:27	20:27	
1408	ULA	4.82	O 3	276-11: 2:57	74.6	63.5	11:28:36	34:20	
1279	ULA	4.83	S24	267-10:24:45	73.8	65.3	10:51:28	55:28	
1236	ULA	4.83	S21	264-10:11:59	73.1	64.3	10:39:15	43: 0	
1451	ULA	4.83	O 6	279-11:15:41	74.5	60.5	11:41:40	47: 5	NP3:00E
1494	ULA	4.83	O 9	282-11:28:23	74.0	53.9	11:54:55	2:55	
1193	ULA	4.84	S18	261- 9:59:14	73.4	63.6	10:26: 4	30:34	
691	ULA	5.35	A14	226- 7:28:10	74.5	50.6	7:54:10	3:43	
447	ULA	5.52	J28	209- 6:14:51	74.4	50.9	6:41: 0	50:20	
289	ULA	8.59	J17	198- 5:15:32	72.5	51.8	5:43:10	50:43	
547	UKO	17.25	A 4	216- 5:57:41	47.4	69.6	6:11:31	18:12	NTC
791	UKO	17.73	A21	233- 7: 7:39	33.4	67.4	7:17:15	28: 5	NP2:00E
590	UKO	18.70	A 7	219- 6: 4:42	35.4	65.7	6:14:55	24:30	NTC
834	UKO	19.90	A24	236- 7:12:35	44.9	67.2	7:25:40	32:56	
633	UKO	20.14	A10	222- 6:11:44	45.3	68.1	6:24:54	32:27	NTC
963	UKO	21.37	S 2	245- 7:44:59	49.2	55.5	7:59:22	1:20	
1006	UKO	21.46	S 5	248- 7:57:22	55.7	61.8	8:13:47	15:47	
1049	UKO	21.55	S 8	251- 8: 9:44	55.8	61.9	8:26:10	28:10	
1307	UKO	21.57	S26	269- 9:25: 4	51.2	63.6	9:41: 5	45: 5	
719	UKO	23.11	A16	228- 6:25:27	35.1	70.0	6:35:33	46:56	NTC
762	UKO	24.92	A19	231- 6:31: 2	35.7	65.7	6:41:20	52: 7	NP1:20E
891	UKO	29.59	A28	240- 6:50:47	49.4	64.9	7: 5:24	10:24	NP BY JPL
1020	GDS	29.86	S 6	249- 7:27:54	51.5	45.0	8: 3:11	5:11	
1364	GDS	29.94	S30	273- 9: 9:28	56.0	43.4	9:43:20	47:13	
1321	GDS	29.94	S27	270- 8:56:44	55.8	43.1	9:30:40	34:35	
1235	GDS	29.95	S21	264- 8:31:14	57.6	53.1	9: 4:35	6: 1	
1493	UKO	29.95	O 9	282- 9:47:38	49.2	55.6	10: 2: 1	4: 1	
1149	UKO	29.96	S15	258- 8: 5:42	36.0	40.3	8:16: 5	17:23	
1149	UKO	29.96	S15	258- 8: 5:42	53.8	67.[illegible]	8:21:30	26: 5	
991	GDS	38.17	S 4	247- 6:46: 4	51.2	44.8	7:21:24	23:24	
1249	UKO	38.22	S22	265- 8: 1:53	53.7	59.9	8:17:40	19:40	NP BY JPL
1034	GDS	38.26	S 7	250- 6:58:26	50.6	46.7	7:33:55	35:12	
1335	ULA	38.31	S20	271- 8:27:24	65.2	48.5	8:58:10	3:37	
1378	ULA	38.31	O 1	274- 8:40: 8	59.0	49.2	9:13: 0	16: 8	
1378	GDS	38.31	O 1	274- 8:40: 8	56.2	43.5	9:13:57	17:54	
1292	ULA	38.31	S25	268- 8:14:39	65.0	49.8	8:45:29	50:28	
1421	ULA	38.31	O 4	277- 8:52:51	65.2	49.7	9:23:3[illegible]	28:41	NP
1249	GDS	38.32	S22	265- 8: 1:53	56.3	49.9	8:35:40	37:40	
1464	ULA	38.32	O 7	280- 9: 5:34	65.3	49.8	9:36:18	41:23	NP
1163	GDS	38.33	S16	259- 7:36:22	51.8	45.0	8:11:34	14:40	
1206	UKO	38.33	S19	262- 7:49: 8	53.7	59.9	8: 4:55	6:55	
1206	GDS	38.33	S19	262- 7:49: 8	56.2	49.6	8:22:57	24:57	
388	GDS	45.40	J24	205- 3:17:46	5[illegible].1	27.2	3:53:12	0:22	
474	GDS	46.29	J30	211- 3:31:49	53.6	23.6	4: 6:27	15:30	

Table A-2 (contd)

REV	STA	NODE	DAT	JLN NODE TIM	LTON	LOFF	TIME ON	OFF	COMMENTS
1005	GDS	46.57	S 5	248- 6:16:36	51.4	44.9	6:51:55	53:55	
1048	GDS	46.67	S 8	251- 6:28:59	51.3	44.3	7: 4:20	6:20	
1349	GDS	46.68	S29	272- 7:58: 3	55.9	42.6	8:31:58	35:58	
1306	GDS	46.69	S26	269- 7:45:18	55.8	42.8	8:19:14	23:14	
1263	GDS	46.69	S23	266- 7:32:33	50.8	45.3	8: 8: 2	9:45	
1177	GDS	46.70	S17	260- 7: 7: 2	51.2	44.7	7:42:24	44:24	
230	GDS	48.48	J13	194- 2:18:26	53.8	23.4	2:53: 0	2:10	
517	GDS	49.73	A 2	214- 3:38:50	49.6	26.0	4:12:55	22:25	
273	GDS	49.92	J16	197- 2:25:28	53.4	22.5	3: 0:10	9:28	
761	GDS	50.00	A19	231- 4:50:27	55.9	23.6	5:24:21	34: 9	
1449	GDS	55.06	O 6	279- 7:54: 9	48.6	35.3	8:30:21	34:21	
1492	GDS	55.06	O 9	282- 8: 6:52	54.6	38.2	8:41:12	46:12	
1406	GDS	55.06	O 3	276- 7:41:26	48.4	35.2	8:17:40	21:40	
488	GDS	57.13	J31	212- 3: 0:37	54.0	19.1	3:35: 7	45:38	
531	GDS	58.58	A 3	215- 3: 7:38	53.6	18.5	3:42:15	52:48	
574	GDS	60.02	A 6	218- 3:14:39	50.0	19.4	3:50:25	59:54	
617	GDS	61.47	A 9	221- 3:21:40	52.8	18.0	3:56:37	7: 0	ENG
660	GDS	62.91	A12	224- 3:28:41	52.5	26.6	4: 3:39	10:30	NP3:00S
416	GDS	63.08	J26	207- 2:15:22	49.6	26.0	2:51:15	58:20	ENG
947	GDS	63.19	S 1	244- 4:52:56	39.7	33.0	5:31:50	33:50	NP
990	GDS	63.29	S 4	247- 5: 5:19	39.3	32.6	5:44:19	46:19	NP
1033	GDS	63.38	S 7	250- 5:17:41	41.2	34.5	5:56: 7	58: 7	NP
1334	GDS	63.43	S28	271- 6:46:38	53.0	26.2	7:21:26	29:22	ENG-NP3:00S
1377	GDS	63.43	O 1	274- 6:59:22	43.8	30.4	7:37: 1	41: 1	
1291	GDS	63.43	S25	268- 6:33:53	52.6	26.0	7: 8:50	16:50	ENG
1463	GDS	63.43	O 7	280- 7:24:48	52.3	22.4	7:59:50	8:53	
1420	GDS	63.43	O 4	277- 7:12: 5	52.3	29.2	7:47: 7	54: 5	ENG-NP3:00S
1205	GDS	63.44	S19	262- 6: 8:22	39.9	31.4	6:47:12	49:42	
1248	GDS	63.44	S22	265- 6:21: 8	40.0	33.6	6:59:54	1:54	NP
502	GDS	65.97	A 1	213- 2:29:25	51.1	25.2	3: 4:50	12:38	
545	GDS	67.42	A 4	216- 2:36:26	50.5	24.6	3:12: 2	19:48	NP3:28S/:48E
789	GDS	68.07	A21	233- 3:46:30	46.2	30.4	4:23:24	28:10	
631	GDS	70.31	A10	222- 2:50:28	49.1	17.8	3:26:29	35:50	ENG
387	GDS	70.48	J24	205- 1:37: 8	34.7	16.7	2:17:30	22:40	
674	GDS	71.75	A13	225- 2:57:29	37.0	16.7	3:37:10	43:11	
1434	GDS	71.80	O 5	278- 6:42:44	38.0	26.4	7:22: 7	25:35	
1391	GDS	71.80	O 2	275- 6:30: 1	39.6	26.1	7: 8:57	12:57	
430	GDS	71.93	J27	208- 1:44:10	25.8	16.3	2:27:10	30: 0	
473	GDS	73.37	J30	211- 1:51:11	47.1	16.3	2:27:50	36:59	
559	GDS	76.26	A 5	217- 2: 5:14	45.0	17.0	2:42:35	50:50	
731	MIL	82.19	A17	229- 2:32:42	31.6	29.9	3:12:43	14:30	
731	GDS	82.19	A17	229- 2:32:42	31.6	14.2	3:12:43	18:12	NP
774	MIL	84.10	A20	232- 2:37:54	44.1	21.1	3:13:58	22:18	
659	MIL	88.00	A12	224- 1:48: 4	48.7	17.6	2:24:12	33:31	
1333	MIL	88.54	S28	271- 5: 5:52	50.2	43.8	5:41:33	43:30	
1376	MIL	88.54	O 1	274- 5:18:36	49.1	42.6	5:54:37	56:37	NP
1419	MIL	88.54	O 4	277- 5:31:20	48.8	29.1	6: 7:28	13:22	
1462	MIL	88.55	O 7	280- 5:44: 3	48.8	29.2	6:20:10	26: 3	NP3:47S
1290	MIL	88.55	S25	268- 4:53: 7	48.9	42.3	5:29:12	31:12	NP
1204	MIL	88.56	S19	262- 4:27:36	49.7	16.5	5: 3:26	13:26	

ORIGINAL PAGE IS
OF POOR QUALITY

Table A-2 (contd)

REV	STA	NODE	DAT	JLN NODE TIM	LTON	LOFF	TIME ON	OFF	COMMENTS
788	MIL	93.14	A21	233- 2: 5:55	42.1	18.8	2:44: 0	50: 0	NP1:00E
874	MIL	96.53	A27	239- 2:17:58	46.9	11.4	2:54:39	5:13	
1261	SNF	96.92	S23	266- 4:11: 2	50.0	40.1	4:46:47	49:48	
716	MIL	98.34	A16	228- 1:23:38	46.1	10.9	2: 0:34	11: 2	NP5:00S
472	MIL	98.45	J30	211- 0:10:33	47.4	12.0	0:47:16	57:43	
759	MIL	100.13	A19	231- 1:29:18	47.2	11.9	2: 5:55	16:25	
558	MIL	101.34	A 5	217- 0:24:36	46.1	10.8	1: 1:33	12: 3	
802	MIL	102.17	A22	234- 1:33:57	39.9	14.4	2:12:47	19:20	
845	MIL	104.08	A25	237- 1:39: 7	40.9	26.3	2:17:39	22: 0	
400	MIL	104.41	J24	205-23:25:18	43.4	9.8	0: 2:40	13: 2	
888	MIL	104.93	A28	240- 1:48:31	51.9	32.2	2:23:39	29:39	
931	MIL	105.02	A31	243- 2: 0:53	41.5	28.6	2:38:13	42: 5	
974	MIL	105.11	S 3	246- 2:13:16	50.0	32.7	2:49: 1	53:57	
1017	MIL	105.20	S 6	249- 2:25:38	45.9	39.6	3: 2:37	4:36	
1361	SNF	105.29	S30	273- 4: 7:11	52.4	36.2	4:42:30	47: 7	NP
1275	SNF	105.29	S24	267- 3:41:42	46.6	36.6	4:18:30	21:30	
1404	SNF	105.29	O 3	276- 4:19:55	57.0	44.0	4:53:27	57: 3	NP
1404	MIL	105.29	O 3	276- 4:19:55	44.8	22.4	4:57:15	3:57	
1404	MIL	105.29	O 3	276- 4:19:55	27.3	7.2	5: 2:30	8:26	NP
1447	SNF	105.29	O 6	279- 4:32:38	57.2	41.4	5: 6: 8	11: 0	NP
1447	MIL	105.29	O 6	279- 4:32:57	44.3	15.3	5:10: 0	18:45	
1447	MIL	105.29	O 6	279- 4:32:57	17.0	7.2	5:18:30	21: 8	NP
1318	SNF	105.29	S27	270- 3:54:27	50.1	36.9	4:30:10	34:10	
1232	MIL	105.30	S21	264- 3:28:56	44.3	30.0	4: 6:25	12:34	NP2:09E
1232	SNF	105.30	S21	264- 3:28:56	56.8	42.4	4: 2:34	4: 7	
1490	SNF	105.30	O 9	282- 4:45:20	65.3	43.7	5:16: 5	23: 0	NP2:00E
1490	MIL	105.30	O 9	282- 4:45:20	45.4	14.4	5:22:48	31:42	
1490	MIL	105.30	O 9	282- 4:45:20	17.0	7.0	5:30:58	33:54	
687	MIL	105.63	A14	226- 0:45:39	44.2	9.7	1:23:11	33:25	
443	MIL	105.85	J27	208-23:32:20	27.0	9.6	0:14: 0	20: 7	
242	MIL	107.48	J13	194-22:25:58	35.9	14.4	23: 6: 0	12:20	
529	MIL	108.74	A 2	214-23:46:22	41.3	13.0	0:24:45	33: 6	
371	MIL	111.81	J22	203-22:47: 5	20.9	10.9	23:31:30	34:30	
1403	SNF	130.40	O 3	276- 2:39: 9	51.2	31.6	3:14:32	20:32	
1360	SNF	130.40	S30	273- 2:26:25	48.7	35.4	3: 2:35	6:35	
1446	SNF	130.41	O 6	279- 2:51:52	51.3	31.4	3:27:13	33:13	
1489	SNF	130.41	O 9	282- 3: 4:35	44.3	38.2	3:42: 4	43:56	
1231	SNF	130.42	S21	264- 1:48:11	45.0	38.4	2:25:28	27:28	
958	UKO	146.94	S 1	244-23:21:13	62.5	56.5	23:52:56	54:56	
1001	UKO	147.03	S 4	247-23:33:36	61.5	68.7	0: 5:40	6:55	
1044	UKO	147.12	S 7	250-23:45:58	62.9	56.8	0:17:33	19:33	
1259	UKO	147.16	S23	266- 0:49:30	62.3	56.5	1:21:16	23:10	
1087	UKO	147.18	S10	253-23:58:28	62.3	59.3	0:30:16	32:16	
714	UKO	148.45	A15	227-22: 2:37	70.4	39.2	22:31:17	41:41	NTC
757	UKO	150.27	A18	230-22: 8: 9	70.7	38.9	22:36:43	47:17	
556	UKO	151.51	A 4	216-21: 3:20	70.3	38.4	21:32: 3	42:38	NTC
599	UKO	152.95	A 7	219-21:10:22	70.3	37.7	21:39: 7	49:50	NTC
642	UKO	154.40	A10	222-21:17:23	70.1	36.9	21:46:13	57: 2	NTC
1359	UKO	155.52	S30	273- 0:45:40	67.0	55.6	1:15:45	19:45	
1316	UKO	155.52	S26	270- 0:32:55	66.3	55.4	1: 3:17	7:17	NP BY JPL

ORIGINAL PAGE IS
OF POOR QUALITY

Table A-2 (contd)

REV	STA	NODE	DAT	JLN NODE TIM	LTON	LOFF	TIME ON	OFF	COMMENTS
1502	UKO	163.90	O10	283- 0:54:28	67.8	55.0	1:24:14	29:40	
1287	UKO	163.90	S24	267-23:50:50	66.7	61.0	0:21: 3	23: 3	
1201	UKO	163.91	S18	261-23:25:19	67.8	63.3	23:55: 6	57: 6	
785	UKO	168.34	A20	232-21: 4:12	67.2	31.8	21:34:12	45:26	
957	UKO	172.05	S 1	244-21:40:28	55.4	49.0	22:14:31	16:31	NP
1387	UKO	172.26	O 1	274-23:46:58	58.6	52.3	0:19:59	21:59	
1344	UKO	172.26	S28	271-23:[illegible]:15	58.7	52.3	0: 7:16	9:16	NP BY JPL
1473	UKO	172.27	O 8	281- 0:[illegible]2:25	64.1	48.4	0:43:37	48:40	
1258	UKO	172.27	S22	265-23: 8:45	59.9	53.2	23:41:30	43:30	
1430	UKO	172.27	O 4	277-23:59:42	63.9	45.2	0:30:56	36:56	
1215	UKO	172.28	S19	262-22:55:59	58.6	52.6	23:29: 0	30:48	
1428	ULA	222.50	O 4	277-20:38:11	50.2	68.0	20:52:52	58:52	
1385	ULA	222.50	O 1	274-20:25:27	55.9	62.0	20:41:55	43:55	
1299	ULA	2[illegible].50	S25	268-19:59:59	56.0	62.0	20:16:29	18:29	
1471	ULA	222.50	O 7	280-20:50:53	50.1	68.1	21: 5:33	11:33	
323	ULA	235.78	J19	200-14:16:54	51.4	70.6	14:31:57	38:40	
811	ULA	236.56	A22	234-16:39: 6	50.8	70.3	16:53:59	0:43	
13[illegible]	GDS	239.24	S30	273-19:14: 2	33.6	46.8	19:23:41	27:41	
1327	GDS	239.24	S27	270-19: 1:18	33.6	46.8	19:10:57	14:57	
1241	ULA	239.25	S21	264-18:35:48	52.7	58.9	18:51:15	53:15	
1499	ULA	239.25	O 9	282-19:52:11	52.0	70.6	20: 7:27	13:57	
1284	ULA	239.25	S24	267-18:48:33	55.0	61.2	19: 4:46	6:46	
1198	GDS	239.26	S18	261-18:23: 2	40.0	46.6	18:34:36	36:36	NP
1155	GDS	239.27	S15	258-18:10:16	26.9	46.3	18:17:57	23:46	
1112	GDS	239.27	S12	255-17:57:31	40.6	46.8	18: 9:17	11:10	
495	GDS	241.55	J31	212-14:45: 1	20.5	46.4	14:50:48	58:32	
739	GDS	241.58	A17	229-15:57:33	21.4	48.6	16: 3:37	11:44	
251	GDS	241.74	J14	195-13:31:38	15.6	45.9	13:35:58	45: 0	
538	GDS	243.00	A 3	215-14:52: 2	18.4	47.4	14:57:12	5:52	
782	GDS	243.55	A20	232-16: 2:29	16.7	46.8	16: 7:19	16: 8	
581	GDS	244.44	A 6	218-14:59: 3	19.3	48.2	15: 4:30	13: 8	
337	ULA	244.62	J20	201-13:45:42	50.8	72.2	14: 0:35	8:17	
825	GDS	245.57	A23	235-16: 7:13	19.2	47.7	16:12:37	21: 7	
380	ULA	246.06	J23	204-13:52:44	49.9	72.4	14: 7:20	15:25	
1040	GDS	247.58	S 7	250-17: 2:57	44.7	48.0	[illegible]:25:58	16:58	NP
1341	GDS	247.61	S28	271-18:31:57	38.6	51.7	18:[illegible]: 6	47: 6	
1384	GDS	247.61	O 1	274-18:44:41	38.0	51.2	[illegible]:40	59:40	
1255	GDS	247.62	S22	265-18: 6:28	40.6	50.4	18:18:13	21:13	
1298	GDS	247.62	S25	268-18:19:13	38.0	51.2	18:30:13	34:13	
1212	GDS	247.63	S19	262-17:53:42	44.0	50.6	18: 6:31	8:31	
1126	GDS	247.64	S13	256-17:28:11	42.7	55.7	17:40:35	44:36	
1126	ULA	247.64	S13	256-17:28:11	50.0	61.5	17:42:48	46:30	
1169	GDS	247.64	S16	259-17: 4:56	36.6	49.5	17:51:30	55:24	
1083	GDS	247.65	S10	253-17:15:25	42.7	49.5	17:27:59	29:59	
179	GDS	247.70	J 9	190-12:46:21	22.6	50.1	12:52:45	1[illegible] 0	
710	GDS	248.78	A15	227-15:20: 6	27.6	50.4	15:28: 0	34:52	
466	GDS	248.95	J29	210-14: 6:47	26.8	52.7	14:14:26	21:14	
222	GDS	249.14	J12	193-12:53:24	19.5	50.4	12:57:25	8:10	
509	GDS	250.40	A 1	213-14:13:48	17.5	51.4	14:18:38	28:51	
552	GDS	251.84	A 4	216-14:20:50	17.3	45.8	14:25:40	34:10	

ORIGINAL PAGE IS
OF POOR QUALITY

Table A-2 (contd)

REV	STA	NODE	DAT	JLN NODE TIM	LTON	LOFF	TIME ON	OFF	COMMENTS
552	ULA	251.84	A 4	216-14:20:50	54.1	73.1	14:36:45	44: 0	
308	GDS	252.02	J18	199-13: 7:29	20.6	53.4	13:13:18	23:10	
595	GDS	253.29	A 7	219-14:27:51	17.3	52.3	14:32:42	43:13	
351	GDS	253.46	J21	202-13:14:39	14.4	51.8	13:19:58	29:40	
351	ULA	253.46	J21	202-13:14:39	50.5	73.2	13:29:17	37:45	
107	GDS	253.67	J 4	185-12: 1: 3	18.5	47.8	12: 6:15	15: 0	
107	ULA	253.67	J 4	185-12: 1: 3	47.8	73.4	12:15: 0	24:20	NP
638	GDS	254.73	A10	222-14:34:52	17.5	52.7	14:39:46	50:20	ENG
394	GDS	254.91	J24	205-13:21:32	18.2	53.2	13:26:38	37:10	
150	GDS	255.10	J 7	188-12: 8: 6	18.2	54.6	12:13:22	24:10	
150	ULA	255.10	J 7	188-12: 8: 6	49.8	73.4	12:22:40	31:30	
882	GDS	255.62	A27	239-15:43:59	28.0	41.4	15:52: 0	56: 0	
968	GDS	255.80	S 2	245-16: 8:45	43.7	50.2	16:21:27	23:27	NP
968	GDS	255.80	S 2	245-16: 8:45	32.6	39.3	16:18: 7	20: 7	NP
1011	GDS	255.89	S 5	248-16:21: 7	43.2	49.8	16:33:40	35:40	NP
1011	GDS	255.89	S 5	248-16:21: 7	33.0	37.9	16:30:37	32: 4	
1054	GDS	255.98	S 8	251-16:33:30	31.3	38.0	16:42:42	44:29	
1441	GDS	255.99	O 5	278-18:28: 4	17.6	45.0	18:33: 0	41: 9	ENG
1269	GDS	255.99	S23	266-17:37: 7	27.2	59.1	17:44:53	54:38	
1312	GDS	255.99	S26	269-17:49:52	17.4	44.2	17:54:45	2:42	ENG-NP2:45S
1398	GDS	255.99	O 2	275-18:15:21	17.6	44.4	18:20:17	28:16	ENG-NP:51E
1269	ULA	255.99	S23	266-17:37: 7	53.0	60.4	17:52:40	55: 0	
1355	GDS	255.99	S29	272-18: 2:37	26.5	43.3	18:10:11	15:11	
1226	GDS	256.00	S20	263-17:24:22	24.5	37.4	17:31:20	35:10	
1484	GDS	256.00	O 8	281-18:40:47	12.6	55.0	18:45:42	57: 2	
1140	GDS	256.01	S14	257-16:58:51	23.6	53.7	17: 5:33	14:48	
1183	GDS	256.01	S17	260-17:11:36	20.7	52.5	17:17:26	26:55	
1097	GDS	256.02	S11	254-16:46: 5	47.3	53.8	16:59:53	1:53	NP
1097	GDS	256.02	S11	254-16:46: 5	31.8	38.5	16:55:13	57:13	NP
681	GDS	256.18	A13	225-14:41:53	17.7	54.8	14:47: 0	56:30	NP1:30E
681	ULA	256.18	A13	225-14:41:53	49.2	73.4	14:56:15	5:17	
193	GDS	256.54	J10	191-12:15: 9	21.1	53.6	12:21: 7	30:53	
724	GDS	257.73	A16	228-14:48:28	19.7	51.9	14:54: 1	4:40	
480	GDS	257.79	J30	211-13:35:35	18.9	54.1	13:40:47	51:30	
236	GDS	257.98	J13	194-12:22:12	18.6	52.5	12:27:25	38: 5	NP1:40M
523	GDS	259.24	A 2	214-13:42:36	20.9	54.6	13:47:55	58:40	
279	ULA	259.42	J16	197-12:29:14	51.3	73.9	12:44:15	53: 0	
279	GDS	259.42	J16	197-12:29:14	33.2	54.2	12:38:46	45:10	
322	ULA	260.86	J19	200-12:36:17	50.8	74.0	12:51:10	0: 9	
322	GDS	260.86	J19	200-12:36:17	23.3	50.6	12:43: 4	51: 5	
810	GDS	261.62	A22	234-14:58:32	22.6	47.5	15: 4:56	12:23	
365	ULA	262.30	J22	203-12:43:18	58.9	74.1	13: 0: 4	7:15	
853	GDS	263.49	A25	237-15: 3:54	26.4	39.1	15:12:20	16: 7	
1412	GDS	264.36	O 3	276-17:46: 0	27.7	47.8	17:53:56	59:56	NP
1283	GDS	264.36	S24	267-17: 7:47	27.0	47.1	17:15:31	22:31	NP
1455	GDS	264.36	O 6	279-17:58:43	27.6	47.5	18: 6:37	12:37	NP
1498	GDS	264.37	O 9	282-18:11:26	34.8	41.8	18:21:27	23:27	NP
1197	GDS	264.38	S18	261-16:42:16	24.1	53.9	16:49: 7	58: 7	
695	GDS	265.02	A14	226-14:10:41	26.4	50.1	14:18:14	25:21	
695	ULA	265.02	A14	226-14:10:41	51.2	74.3	14:25:40	34:50	

ORIGINAL PAGE IS
OF POOR QUALITY

Table A-2 (contd)

REV	STA	NODE	DAT	JLN NODE TIM	LTON	LOFF	TIME ON	OFF	COMMENTS
207	ULA	265.38	J11	192-11:43:58	54.8	74.4	12: 0: 5	8:15	
207	GDS	265.38	J11	192-11:43:58	23.6	56.0	11:50:40	0:30	
738	ULA	266.66	A17	229-14:16:56	50.4	74.4	14:31:42	42: 0	
738	GDS	266.66	A17	229-14:16:56	24.6	51.4	14:24:38	32: 0	NP2:00E
537	ULA	268.08	A 3	215-13:11:24	53.5	74.6	13:27: 2	35:55	NP4:00S
781	ULA	268.62	A20	232-14:21:55	51.0	74.7	14:36:50	46: 5	
781	GDS	268.62	A20	232-14:21:55	22.6	51.5	14:28:20	38:30	
580	GDS	269.53	A 6	218-13:18:25	24.0	56.7	13:25:15	35: 0	
623	MIL	270.97	A 9	221-13:25:26	15.7	37.1	13:29:49	36: 9	
623	GDS	270.97	A 9	221-13:25:26	23.1	54.6	13:32: 0	41:30	NP4:30E
623	ULA	270.97	A 9	221-13:25:26	53.7	74.6	13:41:12	50: 0	
422	MIL	272.59	J26	207-12:19: 8	14.2	34.1	12:23: 3	29:56	
1383	GDS	272.73	O 1	274-17: 3:56	31.8	43.0	17:13: 5	16:25	
1340	GDS	272.73	S28	271-16:51:12	29.8	43.1	16:59:43	3:43	
1426	GDS	272.73	O 4	277-17:16:39	27.0	47.1	17:24:23	30:23	NP2:00SE
1254	MIL	272.74	S22	265-16:25:42	13.6	39.9	16:29:28	34: 5	
1254	GDS	272.74	S22	265-16:25:42	27.8	44.6	16:33:40	38:40	
1211	MIL	272.74	S19	262-16:12:56	10.4	17.2	16:15:46	18:46	
1469	GDS	272.74	O 7	280-17:29:22	27.0	47.0	17:37: 4	43: 4	NP2:00SE
465	MIL	274.03	J29	210-12:26: 9	13.1	38.7	12:29:45	37:21	
221	ULA	274.22	J12	193-11:12:46	53.3	74.7	11:28:25	37:50	
221	MIL	274.22	J12	193-11:12:46	13.4	37.4	11:16:28	23:35	
508	MIL	275.48	A 1	213-12:33:11	12.1	37.9	12:36:30	44: 8	
795	MIL	277.66	A21	233-13:49:56	18.1	38.3	13:55: 0	1: 0	
350	ULA	278.54	J21	202-11:33:53	57.4	74.7	11:50:50	59:20	
838	MIL	279.60	A24	236-13:54:58	22.0	40.4	14: 1:12	6:40	
637	MIL	279.81	A10	222-12:54:14	11.0	42.5	12:57:30	7: 0	
393	MIL	279.99	J24	205-11:40:54	10.8	42.1	11:43:50	53:22	
1440	MIL	281.10	O 5	278-16:47:18	10.8	23.7	16:50:15	54: 1	
1440	ULA	281.10	O 5	278-16:47:18	57.7	74.3	17: 4:22	13:34	
1397	ULA	281.10	O 2	275-16:34:35	57.8	74.3	16:51:40	1: 0	NP3:20S
1311	ULA	281.10	S26	269-16: 9: 7	58.6	72.9	16:26:27	32: 6	
1354	ULA	281.10	S29	272-16:21:51	58.5	72.9	16:39:10	44:49	NP
1397	MIL	281.10	O 2	275-16:34:35	10.2	23.7	16:37:20	41:20	
1483	ULA	281.11	O 8	281-17: 0: 1	59.8	74.3	17:17: 4	26:16	NP6:26E
1225	MIL	281.11	S20	263-15:43:36	20.6	27.3	15:49:24	52:24	
1483	MIL	281.11	O 8	281-17: 0: 1	10.7	23.5	17: 2:55	6:42	
1182	MIL	281.12	S17	260-15:30:51	30.3	35.5	15:39:33	41: 5	
1139	MIL	281.13	S14	257-15:18: 5	22.0	31.6	15:24:20	27:10	
1096	MIL	281.14	S11	254-15: 5:19	22.7	29.4	15:11:45	13:45	
723	MIL	282.81	A16	228-13: 7:52	11.6	45.4	13:11: 1	21: 5	
522	MIL	284.32	A 2	214-12: 1:59	10.4	45.0	12: 4:48	15: 5	
766	MIL	284.65	A19	231-13:13:19	9.6	44.2	13:15:54	26:10	
565	MIL	285.76	A 5	217-12: 9: 0	10.5	45.5	12:11:51	22:18	
809	MIL	286.69	A22	234-13:17:57	13.8	43.3	13:21:45	30:32	
608	MIL	287.21	A 8	220-12:16: 1	11.1	44.4	12:19: 2	28:38	ENG
852	MIL	288.56	A25	237-13:23:18	21.1	34.9	13:29:16	35:56	
651	MIL	288.66	A11	223-12:23: 2	10.8	41.2	12:25:58	34:59	
407	MIL	288.83	J25	206-11: 9:42	11.8	47.1	11:12:55	23:25	
163	MIL	289.03	J 8	189- 9:56:17	10.8	49.1	9:59:20	10:38	

Table A-2 (contd)

REV	STA	NODE	DAT	JLN NODE TIM	LTON	LOFF	TIME ON	OFF	COMMENTS
1024	MIL	289.40	S 6	249-14:10:54	21.0	27.8	14:16:51	13:51	
1325	MIL	289.47	S27	270-15:39:46	20.2	33.7	15:45:28	49:28	
1411	MIL	289.47	O 3	276-16: 5:14	17.9	37.7	16:10: 8	16: 8	
1368	MIL	289.47	S30	273-15:52:31	20.1	33.6	15:58:11	2:11	
1239	MIL	289.48	S21	264-15:14:16	18.8	30.6	15:19:33	23: 3	
1497	MIL	289.48	O 9	282-16:30:40	25.1	31.3	16:37:48	39:39	
1454	ULA	289.48	O 6	279-16:17:57	68.9	71.0	16:39: 1	45: 1	
1282	MIL	289.48	S24	267-15:27: 2	18.6	41.7	15:32:15	39:18	
1196	MIL	289.49	S18	261-15: 1:31	18.9	30.0	15: 6:51	10:21	
1153	MIL	289.50	S15	258-14:48:45	20.8	34.3	14:54:38	58:38	
1110	MIL	289.50	S12	255-14:35:59	18.3	38.5	14:41: 7	47: 7	
694	MIL	290.10	A14	226-12:30: 3	12.6	46.8	12:33:30	43:42	
450	MIL	290.27	J28	209-11:16:44	12.5	47.0	11:20:10	30:26	NP4:30E
493	MIL	291.72	J31	212-11:23:45	12.8	45.8	11:27:16	37: 0	
737	MIL	291.73	A17	229-12:36:20	14.6	47.7	12:40:23	50:15	NP5:00S
536	MIL	293.16	A 3	215-11:30:46	21.3	43.9	11:37: 5	43:33	
292	ULA	293.34	J17	198-10:17:25	63.5	73.3	10:36:25	44:30	
780	ULA	293.68	A20	232-12:41:20	64.9	73.6	13: 0:50	8:10	
335	MIL	294.78	J20	201-10:24:27	13.0	41.4	10:28: 2	36:14	
622	ULA	296.05	A 9	221-11:44:49	65.8	73.2	12: 4:38	12: 0	
378	ULA	296.23	J23	204-10:31:29	69.4	73.1	10:52:45	58:43	
378	MIL	296.23	J23	204-10:31:29	13.6	46.3	10:35:15	45: 0	
665	ULA	297.50	A12	224-11:51:50	67.1	73.1	12:12:10	19: 5	
909	MIL	297.53	A29	241-13: 4:20	31.7	38.4	13:13:26	15:26	
1038	MIL	297.81	S 7	250-13:41:27	32.7	36.1	13:50:52	51:52	
1038	ULA	297.81	S 7	250-13:41:27	69.8	74.4	14: 2:52	5:42	
1382	ULA	297.84	O 1	274-15:23:10	72.0	74.5	15:45:36	47:36	
1425	ULA	297.85	O 4	277-15:35:53	65.6	71.7	15:55:43	3:57	
1296	MIL	297.85	S25	268-14:57:41	28.8	42.9	15: 5:55	9:51	
1339	MIL	297.85	S28	271-15:10:26	28.4	41.8	15:18:34	22:34	
1339	ULA	297.85	S28	271-15:10:26	72.0	74.5	15:32:53	34:53	
1296	ULA	297.85	S25	268-14:57:41	70.0	74.7	15:19:10	23:10	
1468	MIL	297.85	O 7	280-15:48:36	22.1	42.2	15:54:51	0:51	ENG
1468	ULA	297.85	O 7	280-15:48:36	65.6	71.7	16: 8:25	16:39	
1253	MIL	297.85	S22	265-14:44:56	15.3	39.9	14:49:12	57:12	
1425	MIL	297.85	O 4	277-15:35:53	18.8	39.3	15:41:10	47:10	ENG
1210	MIL	297.86	S19	262-14:32:11	27.6	37.5	14:40: 2	42:58	
1210	ULA	297.86	S19	262-14:32:11	72.6	74.7	14:55: 0	57: 0	
1167	ULA	297.87	S16	259-14:19:25	65.4	73.0	14:39: 5	46:45	
1167	MIL	297.87	S16	259-14:19:25	15.1	30.8	14:23:17	28:16	
1081	ULA	297.88	S10	253-13:53:53	73.7	74.6	14:16:30	18:30	
1081	MIL	297.88	S10	253-13:53:53	33.4	36.8	14: 3:30	4:30	
464	ULA	299.12	J29	210-10:45:32	66.8	72.5	11: 5:45	13:10	
220	ULA	299.30	J12	193- 9:32: 8	66.8	72.6	9:52:21	59:41	
507	ULA	300.56	A 1	213-10:52:33	66.7	72.5	11:12:43	20:10	
263	ULA	300.74	J15	196- 9:39:11	66.4	72.4	9:59:25	6:50	
263	MIL	300.74	J15	196- 9:39:11	16.6	51.1	9:43:48	54: 8	
550	ULA	302.00	A 4	216-10:59:34	68.6	72.3	11:20:27	27:16	
349	ULA	303.63	J21	202- 9:53:15	67.8	72.2	10:13:50	21:15	
837	ULA	304.68	A24	236-12:14:22	68.7	72.7	12:35:20	41:53	

ORIGINAL PAGE IS OF POOR QUALITY

Table A-2 (contd)

REV	STA	NODE	DAT	JLN NODE TIM	LTON	LOFF	TIME ON	OFF	COMMENTS
636	ULA	304.89	A10	222-11:13:37	68.5	71.6	11:34:30	41:45	
392	ULA	305.07	J24	205-10: 0:17	68.4	73.5	10:21: 8	27:12	
880	ULA	305.84	A27	239-12:22:29	71.8	74.0	12:44:50	49: 0	
880	MIL	305.84	A27	239-12:22:29	32.9	46.7	12:31:56	36: 0	
966	ULA	306.02	S 2	245-12:47:14	73.4	74.7	13:10:36	12:36	
1009	ULA	306.12	S 5	248-12:59:37	74.1	74.5	13:23:35	25:35	
1052	ULA	306.21	S 8	251-13:11:59	71.0	74.1	13:33:57	35:57	
1353	ULA	306.22	S29	272-14:41: 6	73.8	72.4	15: 4:45	6:45	
1267	MIL	306.22	S23	266-14:15:36	27.1	40.6	14:23:21	27:21	
1310	ULA	306.22	S26	269-14:28:21	68.6	73.9	14:49:15	55: 0	
1267	ULA	306.22	S23	266-14:15:36	73.9	74.6	14:39:21	41:21	
1396	ULA	306.22	O 2	275-14:53:49	68.1	69.4	15:14:31	22:56	
1439	ULA	306.22	O 5	278-15: 6:33	68.0	69.5	15:27:13	35:38	
1482	ULA	306.23	O 8	281-15:19:15	68.6	64.3	15:40:10	48:20	
1224	ULA	306.23	S20	263-14: 2:51	72.2	74.7	14:25:25	27:49	
1181	SNF	306.24	S17	260-13:50: 5	41.7	48.3	14: 2:11	4:11	
1138	ULA	306.24	S14	257-13:37:19	72.5	74.7	14: 0: 5	2:25	
1095	ULA	306.25	S11	254-13:24:33	74.3	74.4	13:38:42	50:42	
679	ULA	306.34	A13	225-11:20:38	68.5	71.1	11:41:35	49: 0	
435	ULA	306.51	J27	208-10: 7:18	69.3	73.5	10:28:30	34:16	
722	ULA	307.88	A16	228-11:27:15	69.8	69.7	11:48:40	56:15	
478	ULA	307.96	J30	211-10:14:20	69.3	73.4	10:35:33	41:23	
234	ULA	308.15	J13	194- 9: 0:56	69.9	70.1	9:22:25	29:45	
277	ULA	309.59	J16	197- 9: 7:59	69.2	69.7	9:29:10	37: 0	
765	ULA	309.72	A19	231-11:32:45	70.1	70.5	11:54:18	1:24	
564	ULA	310.85	A 5	217-10:28:22	69.3	69.4	10:49:35	57:29	
320	ULA	311.03	J19	200- 9:15: 1	71.3	69.4	9:37:18	44:10	
607	ULA	312.29	A 8	220-10:35:23	69.7	69.0	10:56:45	4:40	
363	ULA	312.47	J22	203- 9:22: 3	69.9	68.8	9:43:30	51:39	
650	ULA	313.74	A11	223-10:42:24	74.6	68.0	11: 8: 8	12: 5	
406	ULA	313.91	J25	206- 9:29: 5	70.5	72.6	9:50:50	56:39	
894	ULA	314.24	A28	240-11:53: 2	70.9	73.5	12:14:57	19:59	
980	ULA	314.43	S 3	246-12:17:47	74.0	74.6	12:41:38	43:38	
1023	ULA	314.52	S 6	249-12:30: 9	71.6	74.4	12:52:26	54:26	
1367	SNF	314.59	S30	273-14:11:45	37.1	43.8	14:22:28	24:28	
1324	SNF	314.59	S27	270-13:59: 1	37.2	43.8	14: 9:45	11:45	
1281	ULA	314.59	S24	267-13:46:16	73.9	74.6	14:10: 0	12: 0	
1496	ULA	314.60	O 9	282-14:49:54	70.8	65.2	15:11:46	20:39	
1238	SNF	314.60	S21	264-13:33:31	42.3	55.3	13:45:48	49:48	
1195	ULA	314.61	S18	261-13:20:45	72.6	74.7	13:43:35	46: 5	
1109	ULA	314.62	S12	255-12:55:13	73.1	74.7	13:17:21	21:21	
693	ULA	315.18	A14	226-10:49:25	70.9	66.8	11:11:20	29:35	
449	ULA	315.36	J28	209- 9:36: 6	71.6	72.2	9:57:50	3:50	
205	ULA	315.55	J11	192- 8:22:48	65.8	68.0	8:44:32	53:25	
492	ULA	316.80	J31	212- 9:43: 7	71.0	65.4	10: 5: 5	13:49	PD4:30E
736	ULA	316.81	A17	229-10:55:44	74.4	66.6	11:20: 0	26:58	
535	ULA	318.24	A 3	215- 9:50: 9	71.3	64.7	10:12:17	21: 6	
578	ULA	319.69	A 6	218- 9:57:10	71.6	64.2	10:19:25	28:17	
908	ULA	322.65	A29	241-11:23:34	73.1	73.9	11:46:41	50:11	ENG
1252	SNF	322.97	S22	265-13: 4:10	43.9	55.3	13:16:56	21:56	

ORIGINAL PAGE IS
OF POOR QUALITY

Table A-2 (contd)

REV	STA	NODE	DAT	JLN NODE TIM	LTON	LOFF	TIME ON	OFF	COMMENTS
1209	SNF	322.98	S19	262-12:51:25	44.1	56.0	13: 4:14	8:14	
1060	ULA	323.00	S10	253-12:13: 8	73.2	74.2	12:36:22	38:17	
1352	SNF	331.33	S29	272-13: 0:20	45.9	61.8	13:13:42	18:42	
1395	SNF	331.33	0 2	275-13:13: 4	31.6	66.1	13:22: 4	33: 0	
1395	ULA	331.33	0 2	275-13:13: 4	72.8	58.1	13:36: 2	46:15	
1438	ULA	331.34	0 5	278-13:25:47	73.0	58.0	13:48:50	59: 0	
1481	ULA	331.34	0 8	281-13:38:30	72.9	58.2	14: 1:30	11:40	
1438	SNF	331.34	0 5	278-13:25:47	31.6	67.1	13:34:47	46: 6	
1409	ULA	339.71	0 3	276-12:43:43	73.6	68.5	13: 7:15	13:13	
1452	ULA	339.71	0 6	279-12:56:26	73.8	71.0	13:20: 6	25:50	
1122	ULA	348.11	S13	256-10:45: 8	73.3	69.4	11:12:15	14:15	
548	ULA	352.17	A 4	216- 7:38:19	74.6	53.4	8: 3:10	13: 0	
1265	SNF	356.46	S23	266-10:54: 5	60.9	65.6	11:12:10	13:50	
720	ULA	358.04	A16	228- 8: 6: 3	74.6	50.4	8:31:48	41:40	
232	ULA	358.31	J13	194- 5:39:41	74.6	51.2	6: 5:32	15: 3	

Table A-3. Spacecraft travel time from the equator to image latitude

LAT	TA	TD	LAT	TA	TD
1	00:03	50:20	41	11:53	38:29
2	00:20	50:02	42	12:11	38:11
3	00:38	49:44	43	12:29	37:53
4	00:56	49:27	44	12:48	37:35
5	01:13	49:09	45	13:06	37:17
6	01:31	48:51	46	13:24	36:58
7	01:49	48:34	47	13:42	36:40
8	02:06	48:16	48	14:01	36:22
9	02:24	47:58	49	14:19	36:03
10	02:42	47:41	50	14:38	35:45
11	02:59	47:23	51	14:56	35:26
12	03:17	47:05	52	15:15	35:07
13	03:35	46:48	53	15:34	34:49
14	03:52	46:30	54	15:53	34:30
15	04:10	46:12	55	16:12	34:11
16	04:28	45:55	56	16:31	33:52
17	04:45	45:37	57	16:50	33:32
18	05:03	45:19	58	17:10	33:13
19	05:21	45:02	59	17:29	32:53
20	05:38	44:44	60	17:49	32:34
21	05:56	44:26	61	18:09	32:13
22	06:14	44:09	62	18:29	31:53
23	06:32	43:51	63	18:50	31:33
24	06:49	43:33	64	19:11	31:12
25	07:07	43:15	65	19:32	30:50
26	07:25	42:58	66	19:54	30:28
27	07:43	42:40	67	20:17	30:06
28	08:00	42:22	68	20:40	29:42
29	08:18	42:04	69	21:05	29:18
30	08:36	41:47	70	21:30	28:52
31	08:54	41:29	71	21:58	28:25
32	09:12	41:11	72	22:28	27:54
33	09:29	40:53	73	23:04	27:19
34	09:47	40:35	74	23:50	26:33
35	10:05	40:17	74.4	24:18	26:08
36	10:23	39:59	74.7	24:58	25:28
37	10:41	39:41			
38	10:59	39:24			
39	11:17	39:06			
40	11:35	38:47			

ORIGINAL PAGE IS
OF POOR QUALITY

Table A-4. Digital images processed by JPL up to October 1, 1981

REV	STA	LOCATION	LAT		LON		TIME
107	ULA	PRINCE OF WALES IS	55	35	132	45	185-12:17:25
107	CDS	CA KERN COUNTY 1	35	7	119	6	185-12:11:10
107	CDS	CA POINT LOMA	32	5	117	5	185-12:10:19
107	CDS	CA MEDICINE LAKE	41	20	121	30	185-12:12:59
205	ULA	CAN BEAU SEA VIC I	73	32	114	15	192- 8:45:50
207	CDS	NM C MESA PRIETA	35	31	107	1	192-11:54: 9
207	CDS	NM ALBUQUERQUE	34	50	106	30	192-15:53:56
207	CDS	SW COLORADO	38	30	108	20	192-11:55: 2
207	CDS	MONTANA DILLON	45	13	112	38	192-11:57: 5
207	CDS	MONTANA ANACONDA	45	56	113	14	192-11:57:18
221	ULA	CAN FT SIMPSON NWT	61	57	120	16	193-11:31: 9
221	MIL	OK CHICKASHA 2	35	0	98	0	193-11:22:46
221	MIL	KS COLBY 1	39	20	100	50	193-11:24:13
221	ULA	CAN MACKENZIE R.	68	59	135	25	193-11:33:45
230	CDS	CA STR. OF 2 B. C.	49	0	123	0	194- 2:54:29
232	ULA	AK KUSKOKWIM R.	60	0	162	30	194- 6:12:20
236	CDS	CA STR. OF 3 B. C.	49	0	123	0	194-12:36:27
242	MIL	BLAKE ESCARPMENT	32	30	73	0	194-23: 7: 4
251	CDS	HURRICANE FICO 3	18	50	122	52	195-13:36:51
251	CDS	HURRICANE FICO 1	16	46	122	2	195-13:36:15
251	CDS	HURRICANE FICO 2	17	48	122	27	195-13:36:33
263	MIL	NY NYC	40	30	74	15	196- 9:50:51
289	ULA	AK ANCHORAGE	61	13	150	25	198- 5:47:46
289	ULA	AK DELTA II	63	50	146	0	198- 5:46:48
289	ULA	AK KATMAI	58	25	154	15	198- 5:48:39
308	CDS	CA SAN NICHOLAS IS	33	45	119	20	199-13:17: 6
308	CDS	PAC OCEAN COASEX	30	18	117	40	199-13:16: 5
308	CDS	CA SUTTER'S BUTTE	39	13	121	50	199-13:18:45
308	CDS	CA SANTA BARBARA 1	34	10	119	36	199-13:17:17
322	CDS	AZ SAFFORD 1	32	50	109	40	200-12:45:35
322	ULA	AK DEASE INLET	70	48	156	25	200-12:58: 9
322	CDS	AZ GRAND CANYON 2	36	15	112	15	200-12:46:45
322	CDS	UT BLACK MTS. 1	38	10	112	50	200-12:47:14
322	CDS	UT SEVIER LAKE	38	55	113	10	200-12:47:27
335	MIL	DOM. REPUBLIC B	18	40	69	50	201-10:29:39
335	MIL	WV LOST RIVER	39	0	78	52	201-10:35:36
335	MIL	DOMIN REPUBLIC A	19	30	70	0	201-10:29:52
350	ULA	CAN LAC LA MARTE	63	17	118	15	202-11:52:48
351	CDS	CA GARLOCK FAULT	34	40	118	30	202-13:24:27
351	CDS	CA CINDER CONE	40	35	121	20	202-13:26:14
351	CDS	CA LOS ANGELES 1	34	0	118	20	202-13:24:18
351	CDS	CA LOS ANGELES 3	33	55	118	5	202-13:24:15
371	MIL	JAM PORT ANTONIO	18	2	76	32	203-23:32:25
371	MIL	CUBA MICARO MTS	20	20	75	30	203-23:31:43
378	MIL	VA PAMLICO/HALL SW	35	20	76	0	204-10:41:38
378	MIL	VA WINCHESTER 2	39	20	78	8	204-10:42:49
378	MIL	PA BEDFORD	40	5	78	30	204-10:43: 3

ORIGINAL PAGE IS OF POOR QUALITY

Table A-4 (contd)

REV	STA	LOCATION	LAT		LON		TIME
378	MIL	VA FREDERICKSBURG2	38	7	77	24	204-10:42:25
380	ULA	AK RANGE GLACIER	62	56	150	50	204-14:11:32
380	ULA	AK KUSKOKWIM MTS.	64	5	151	50	204-14:11:55
393	MIL	MO CLINTON	38	15	93	45	205-11:51:55
393	MIL	MO GUILDFORD	40	9	94	52	205-11:52:30
393	MIL	LA MISS. DELTA 2	29	13	89	29	205-11:49:17
393	MIL	AR LITTLE ROCK	35	0	92	5	205-11:50:55
393	MIL	LA NEW ORLEANS 2	30	4	89	51	205-11:49:31
394	GDS	CA PANAMINT MTNS.	36	40	117	35	205-13:32: 7
407	MIL	IN KOKOMO	40	11	86	21	206-11:21:19
407	MIL	IN INDIANAPOLIS	39	51	85	56	206-11:21:12
416	GDS	CA LOS ANGELES 4	34	4	118	0	207- 2:55:57
422	MIL	TX TEMPLE	31	11	97	25	207-12:28: 3
447	ULA	N. ALASKA RANGE II	64	12	148	40	206- 6:46: 0
450	MIL	HAITI PORT-A-PIMEN	18	18	74	7	209-11:21:50
465	MIL	MX CALAKMUL	18	17	90	19	210-12:31:13
465	MIL	GUATEMALA TIKAL	17	13	89	38	210-12:30:55
465	MIL	TX HOUSTON	29	44	95	22	210-12:34:38
465	MIL	OK CHICKASHA 1	35	0	98	0	210-12:36:13
465	MIL	TX HONEY	33	32	96	50	210-12:35:47
472	MIL	PA ALTOONA	40	43	79	0	211- 0:49: 9
472	MIL	WV ALTA	37	52	80	33	211- 0:50: 1
472	MIL	PA EMPORIUM	41	30	78	22	211- 0:48:55
473	GDS	CO DENVER	39	30	105	0	211- 2:30:10
474	GDS	BC STR OF GEORGIA	49	15	123	17	211- 4: 7:50
474	GDS	BC JUAN DE FUCA 3	48	20	124	0	211- 4: 8: 3
480	GDS	CA STR. OF 4 B. C.	48	54	122	54	211-13:49:50
480	GDS	WA SEATTLE 1	47	35	122	3	211-13:49:27
488	GDS	MT ELK RIVER	46	50	116	10	212- 3:37:18
493	MIL	SC KERSHAW COUNTY	34	20	80	35	212-11:33:36
493	MIL	WV BERNIE	38	11	82	1	212-11:34:45
502	GDS	UT SEVIER DESERT 2	39	0	112	28	213- 3: 8:30
502	GDS	UT BLACK MTS. II	38	13	112	50	213- 3: 8:43
502	GDS	WY EVANSTON 1	41	12	111	5	213- 3: 7:52
502	GDS	MT JORDAN	47	17	106	36	213- 3: 5:57
502	GDS	WY PINEDALE	45	55	110	0	213- 3: 7:19
502	GDS	CA ALGODONES DUNES	33	15	115	25	213- 3:10:14
508	MIL	OK TUSKAHOMA	34	25	95	45	213-12:43: 2
508	MIL	NICARAGUA	12	49	86	39	213-12:36:42
508	MIL	HONDURAS	13	39	86	58	213-12:36:52
522	MIL	MINN TWIN CITIES	44	50	93	20	214-12:14:59
523	GDS	AZ SIERRITA	31	52	111	12	214-13:51:44
523	GDS	AZ HELVETIA 1	31	47	111	10	214-13:51:43
523	GDS	AZ SILVER BELL 1	32	30	111	40	214-13:51:54
523	GDS	AZ FOUR CORNERS	34	20	112	21	214-13:52:26
523	GDS	AZ PHOENIX	33	30	112	30	214-13:52:12
552	ULA	AK FAIRBANKS 1	64	40	147	15	216-14:40:12

ORIGINAL PAGE IS
OF POOR QUALITY

Table A-4 (contd)

REV	STA	LOCATION	LAT	LON	TIME
552	GDS	CA SB CHANNEL 3	34 10	120 0	216-14:30:41
552	ULA	AK MALASPINA GLAC	60 15	140 0	216-14:38:41
552	ULA	AK UTUKOK RIVER	69 33	159 48	216-14:42: 6
552	ULA	AK DELTA	63 50	146 0	216-14:39:55
552	GDS	SACRAMENTO DELTA	38 12	121 51	216-14:31:48
552	ULA	AK YAKUTAT	59 24	139 7	216-14:38:21
552	GDS	CA SANTA BARB CH 1	34 10	120 0	216-14:30:36
558	MIL	VA FREDERICKSBURG	37 56	77 35	108- 1: 4: 1
558	MIL	VA FORT PICKETT	37 10	78 0	217- 1: 4:14
558	MIL	WASHINGTON, DC	38 55	76 55	217- 1: 3:39
559	GDS	NM CLAYTON 1	36 24	103 8	217- 2:45:15
565	MIL	IN PRINC.-EVANS.	38 20	87 40	217-12:19:58
565	MIL	KY POND R.	37 15	87 15	217-12:19:39
565	MIL	KY OWENSBORO	37 40	87 15	217-12:19:45
574	GDS	CA KETTLEMAN HILLS	36 0	120 0	218- 3:54:41
580	GDS	NM CLAYTON 2	36 24	103 8	218-13:28:52
580	GDS	CO DENVER	39 37	105 0	218-13:29:50
580	GDS	WY SHIRLEY MTS. 1	42 3	106 22	218-13:30:34
580	GDS	CO GRAND COUNTY	40 0	105 50	218-13:29:57
595	GDS	CA KERN COUNTY 2	35 7	119 6	219-14:37:54
595	GDS	CA KERN COUNTY 3	35 19	119 6	219-14:37:58
595	GDS	CA BUCK'S LAKE	39 53	121 11	219-14:39:20
595	GDS	OR HUMBOLDT	41 26	122 0	219-14:39:48
605	ULA	AK TAN./KANT. R.	64 44	150 35	220- 7:45: 4
605	ULA	AK KUSKOKWIM MTS.	64 11	151 57	220- 7:45:17
605	ULA	AK UNIMAK ISLAND	54 50	164 0	220- 7:48:23
608	MIL	FL OKEECHOBEE	27 23	80 50	220-12:23:46
608	MIL	W. IN. JAMAICA 1	18 2	77 5	220-12:21: 6
608	MIL	FL MIAMI	25 57	80 27	220-12:23:22
617	GDS	CA SANTA BARB 2	34 10	119 36	221- 4: 2:10
617	GDS	NV BEOWAWE	40 30	116 30	221- 4: 0:17
623	GDS	OK GUYMON	36 36	101 36	221-13:35:56
623	MIL	TX LLANO	30 45	98 45	221-13:34:11
623	GDS	MT MILK RIVER	49 0	110 20	221-13:39:41
631	GDS	TABLE MT SD	45 54	103 37	222- 3:27:30
631	GDS	AZ SILVER BELL 2	32 30	111 40	222- 3:31:25
631	GDS	WY SHIRLEY MTS. 1	42 3	106 22	222- 3:28:40
631	GDS	WY N POWDER R BAS	44 3	105 0	222- 3:28: 4
631	GDS	WY POWDER R. BAS S	43 18	105 26	222- 3:28:17
638	GDS	NV WALKER LAKE 2	39 0	119 0	222-14:46: 4
638	GDS	SAN BERNARDINO 1	34 5	117 15	222-14:44:40
651	MIL	GA THOMSON APPALAC	33 33	82 40	223-12:32:39
651	MIL	GA ALTAMAHA RIVER	31 30	81 45	223-12:32: 3
660	GDS	LOS ANGELES 2	33 50	118 10	224- 4: 9:15
681	GDS	WA MT ST HELEN	46 12	122 11	225-14:55:15
681	ULA	AK CRAZY MTS.	65 45	145 10	225-15: 1:40
681	GDS	CA KELBAKER	35 2	115 45	225-14:51:56

Table A-4 (cont'd)

REV	STA	LOCATION	LAT		LON		TIME
681	CDS	OR NEWBERRY	43	30	121	10	225-14:54:28
681	ULA	AK COLVILLE RIVER	69	15	154	20	225-15: 3: 0
691	ULA	AK FAIRBANKS 2	64	22	148	30	226- 7:59:17
694	MIL	KY SALYERSVILLE	37	45	83	5	226-12:40:53
694	MIL	LAKE MICHIGAN	44	0	87	0	226-12:42:47
695	CDS	NM MT. TAYLOR	35	20	107	20	226-14:20:50
719	UKO	ICELAND	65	0	16	45	228- 6:44:54
719	UKO	FRANCE ALPS 1	44	10	354	35	228- 6:38:14
719	UKO	SCOT GR GLEN FAULT	57	0	4	40	228- 6:42:12
719	UKO	FRANCE ALPS 2	45	5	355	10	228- 6:38:28
719	UKO	ENGLAND LONDON	51	34	359	44	228- 6:40:31
719	UKO	FRANCE PARIS	48	50	357	40	228- 6:39:39
723	MIL	IA AMES	42	20	93	18	228-13:20: 5
723	MIL	MO ST FRANCOIS MTS	37	30	90	30	228-13:18:38
724	CDS	BC STR OF GA 5	49	0	123	0	228-15: 2:42
737	MIL	HAITI PORT-A-PRINC	18	15	72	30	229-12:41:25
737	MIL	HAITI ISLE CONAVE	18	55	72	48	229-12:41:37
737	MIL	HAITI ST NICOLAS	19	40	73	8	229-12:41:50
738	CDS	TX COYANOSA 1	31	20	103	15	229-14:25:33
738	CDS	CO DEL NORTE	37	25	106	25	229-14:27:41
738	GDS	TX COYANOSA 2	31	20	103	15	229-14:25:31
738	CDS	MX OBALLOS	27	30	101	30	229-14:24:42
738	CDS	NM A	36	35	105	49	229-14:27:28
738	CDS	NM B	35	40	105	57	229-14:27:11
738	CDS	WY PARTICK'S DRAW	41	30	108	40	229-14:28:52
738	GDS	AZ NEW MEXICO 2	36	35	105	49	229-14:27:24
759	MIL	GUAT-SALVADOR II	13	45	90	0	231- 2:15:48
759	MIL	GUAT MONJAS	14	30	89	43	231- 2:15:35
759	MIL	SC KERSHAW 2	34	27	80	48	231- 2: 9:43
759	MIL	VA WINCHESTER	39	10	78	10	231- 2: 8:22
759	MIL	PA HARRISBURG 2	40	26	77	18	231- 2: 7:57
759	MIL	PA APPALACHIAN	41	10	77	0	231- 2: 7:44
759	MIL	GUAT AMATIGUE BAY	15	58	89	4	231- 2:15: 9
759	MIL	GUAT LAKE IZABEL	15	16	89	19	231- 2:15:22
761	CDS	WA SEATTLE 2	47	47	122	42	231- 5:26:51
761	GDS	OR/WA COLUMBIA R.	46	17	123	44	231- 5:27:20
762	UKO	N AT OC FAEROE BK	61	33	9	13	231- 6:49:17
762	UKO	SWITZERLAND GENEVA	46	27	353	50	231- 6:44:27
762	UKO	ENG CHANNEL	51	32	2	5	231- 6:46: 0
774	MIL	OK TULSA	36	20	95	56	232- 3:17:48
774	MIL	OK OOLAGAH LAKE 1	36	40	95	33	232- 3:17:39
781	ULA	AK NORTH SLOPE 1	70	30	148	0	232-14:43:36
781	CDS	WY COPPER MT. 1	43	20	107	55	232-14:34:21
781	ULA	AK N SLOPE 2	70	0	145	0	232-14:43:23
785	UKO	AT OC OROMONDE	36	46	11	24	232-21:44: 0
788	MIL	LA NEW ORLEANS 1	30	6	89	41	233- 2:47:39
788	MIL	KY LOUISVILLE	38	25	85	40	233- 2:45:13
788	MIL	KY BIG CLIFTY	37	30	86	10	233- 2:45:27

C-2

Table A-4 (contd)

REV	STA	LOCATION	LAT		LON		TIME
789	CDS	AZ MOHAWK 2	32	3	113	30	233- 4:27:19
789	GDS	WY BITTER CREEK	41	30	108	40	233- 4:24:48
789	CDS	AZ MOHAWK 3	32	10	114	0	233- 4:27:32
789	GDS	UT SAN RAFAEL	38	50	110	45	233- 3:57:28
791	UKO	ALGERIA CHOTT MELR	34	15	353	47	233- 7:17:31
791	UKO	ALGERIA BISKRA	34	58	354	9	233- 7:17:44
791	UKO	ALGERIA SETIF	35	41	354	30	233- 7:17:57
791	UKO	ALGERIA BEJAIA	36	25	354	54	233- 7:18:10
791	UKO	JASIN 1	59	0	12	30	233- 7:25: 2
791	UKO	NW IREL DRUMLIN FD	54	12	7	17	233- 7:23:29
795	MIL	LA ALEXANDRIA	31	25	92	30	233-13:58:50
795	MIL	OK OOLOGAH LAKE II	36	36	95	15	233-14: 0:26
795	MIL	OK MOODYS	36	3	94	56	233-14: 0:18
795	MIL	AR FORT SMITH	35	20	94	35	233-14: 0: 1
795	MIL	LA ACADIA 1	30	8	92	10	223-13:58:29
795	MIL	AR MENA	34	40	94	16	233-13:59:48
795	MIL	AR NASHVILLE	33	58	93	55	233-13:59:35
802	MIL	MD UPPER CHESAPEAK	39	15	76	20	234- 2:12:56
806	ULA	AK YUKON-TANANA R.	64	54	151	54	234- 8:47: 8
809	MIL	FL CYPRESS SWAMP	26	0	81	0	234-13:25:19
809	MIL	WI WISCONSIN RIVER	43	18	90	2	234-13:30:29
809	MIL	W. IN. JAMAICA 2	18	8	77	50	234-13:23: 0
809	MIL	JAM. MONTEGO BAY	18	21	77	50	234-13:23: 7
809	MIL	FL EVERGLADES	25	26	80	43	234-13:25: 8
810	CDS	UT TUSHA MTS.	38	25	112	10	234-15: 9:35
810	GDS	UT SEVIER DESERT 1	39	9	112	30	234-15: 9:48
810	GDS	NM SPRINGERVILLE	33	50	109	40	234-15: 8:11
838	MIL	MS VICKSBURG	32	20	91	14	236-14: 4:13
838	MIL	LA MISS DELTA 1	29	0	89	15	236-14: 3: 8
838	MIL	KANSAS CITY	39	8	94	37	236-14: 6:13
845	MIL	NC DUCK	36	11	75	56	237- 2:19: 2
853	CDS	UT SAN RAFAEL	39	15	110	40	237-15:15: 8
853	CDS	NM ST AUGUSTINE PL	33	50	108	0	237-15:13:35
853	GDS	NM BANDERA LAVA FL	34	30	108	0	237-15:13:45
853	GDS	UT COMB RIDGE	37	15	109	38	237-15:14:35
853	CDS	UT ORANGE CLIFFS 1	37	56	110	5	237-15:14:48
874	MIL	ONTARIO BOBCAYGEON	44	32	78	30	239- 2:55:24
874	MIL	KY HUNTINGTON	38	22	82	34	239- 2:57:22
874	MIL	IN ZEBULON	37	34	82	28	239- 2:57:30
874	MIL	NY HAM., ONT/BUF.	43	8	79	18	239- 2:55:50
880	MIL	MA NANTUCKET IS.	41	10	69	40	239-12:34:23
880	MIL	ATL OC COLD RING 3	37	6	67	30	239-12:33: 7
882	CDS	CA IMPERIAL VAL 1	33	0	115	30	239-15:53:27
882	GDS	CA PISGAH	34	50	116	40	239-15:54: 8
882	GDS	CA GOLDSTONE	35	10	116	52	239-15:54: 2
888	MIL	MA MOOSEHEAD LAKE	45	35	69	25	240- 2:25:37
931	MIL	DE BAY I/WAVES A	38	49	73	28	243- 2:40: 3

Table A-4 (contd)

ORIGINAL PAGE IS OF POOR QUALITY

REV	STA	LOCATION	LAT		LON		TIME
931	MIL	DE BAY I/WAVES B	38	4	73	55	243- 2:40:17
931	MIL	DE BAY I/WAVES C	37	19	74	22	243- 2:40:31
974	MIL	NC CAPE HATTERAS	35	52	74	54	246- 2:53:20
974	MIL	NC CAPE HATTERAS 1	35	0	75	20	246- 2:53:33
1006	UKO	ATL OC N-JASIN 2	59	30	10	30	248- 8:15: 1
1049	UKO	ATL OC JASIN 3	59	30	10	30	251- 8:27:21
1126	ULA	AK CONTROLLER BAY	60	13	144	25	256-17:46: 5
1140	GDS	CA DEATH VALLEY	36	20	116	50	257-17: 9:20
1140	GDS	NV WALKER LAKE 1	38	20	118	10	257-17: 9:56
1140	GDS	MEX. SONORA DUNES	31	55	114	15	257-17: 7:57
1140	GDS	NV GOLDFIELD	37	40	117	15	257-17: 9:44
1140	GDS	CA ALCODONES	32	56	115	0	257-17: 8:17
1149	UKO	SHETLAND ISLAND	59	55	2	36	258- 8:23:25
1169	GDS	PAC OCEAN OCNOGPHR	48	40	132	53	259-17:55: 4
1183	GDS	ANGEL DE LA GUARDA	29	45	113	40	260-17:20: 9
1197	GDS	WY EVANSTON 2	41	20	111	5	261-16:54:11
1197	GDS	UT CANYONLANDS	38	13	109	32	261-16:53:17
1197	GDS	NM FARMINGTON	36	44	108	12	261-16:52:51
1197	GDS	UT UTE PEAK	37	30	108	52	261-16:53: 4
1204	MIL	MO ST FRANCOIS MTS	37	30	90	30	262- 5: 7: 9
1204	MIL	MO ST LOUIS	38	45	90	30	262- 5: 6:48
1211	MIL	GUAT LAKE AYARZA	14	20	89	55	262-16:16:53
1211	MIL	GUAT RIO SALINAS	0	0	0	0	262-16:17:18
1211	MIL	MEX RIO LAGANTUM	16	23	90	49	262-16:17:30
1211	MIL	GUAT SALAMA	15	5	90	15	262-16:17: 6
1211	MIL	GUAT-SALVADOR 1	13	31	89	40	262-16:16:40
1231	SNF	GRAND BANKS EDDY	38	18	48	15	264- 2:27:22
1232	MIL	ATL OC WARM RING	38	7	73	16	264- 4: 8:19
1253	MIL	PUERTO RICO	18	15	66	30	265-14:50: 2
1253	MIL	PA LOCK HAVEN	41	4	77	56	265-14:56:51
1254	GDS	KS SUBLETTE 5	37	44	100	50	265-16:36:36
1267	MIL	ATL OC CLD RING 1	34	22	65	48	266-14:25:22
1267	MIL	ATL OC COLD RING 2	34	22	65	48	266-14:25:29
1267	MIL	BERMUDA	32	23	64	39	266-14:24:51
1269	GDS	BC JUAN DE FUCA 2	48	0	124	0	266-17:51:15
1269	GDS	BC JUAN DE FUCA 1	48	55	124	32	266-17:49: 1
1291	GDS	SAN BERNARDINO II	34	5	117	15	268- 7:14:26
1292	ULA	WILLOW LAKE	62	14	119	17	268- 8:46:31
1296	MIL	PA HARRISBURG 2	40	20	77	0	268-15: 9:20
1296	MIL	PA HARRISBURG 1	40	9	77	3	268-15: 9:20
1296	MIL	CHESAPEAKE BAY 2	37	50	75	52	268-15: 8:33
1296	MIL	CHESAPEAKE BAY 1	30	9	75	52	268-15: 6:21
1296	ULA	BEAUFORT SEA 4	72	30	127	0	268-15:20:20
1306	GDS	PAC OC OCEO 1306	48	43	125	19	269- 8:21:26
1318	SNF	HUDSON CANYON	39	46	72	30	270- 4:33:23
1339	MIL	ATL OCEAN DUCK-X	36	20	74	56	271-15:20:55
1339	ULA	BEAUFORT SEA 5	72	30	127	0	271-15:33: 5
1340	GDS	KS SUBLETTE 2	37	44	100	50	271-17: 2: 6

Table A-4 (contd)

ORIGINAL PAGE IS
OF POOR QUALITY

REV	STA	LOCATION	LAT		LON		TIME
1382	ULA	BEAUFORT SEA 3	72	30	127	0	274-15:45:50
1382	ULA	BEAUFORT SEA 6	73	38	135	2	274-15:46:35
1383	GDS	KS SUBLETTE 1	37	44	100	50	274-17:14:52
1391	GDS	AZ HELVETIA 2	31	35	110	28	275- 7:11:20
1391	GDS	NM MAAR VOLCANOS	34	20	108	45	275- 7:10:29
1395	SNF	LABRADOR SEA	60	20	61	0	275-13:31: 0
1404	MIL	AT OC WARM RING 2B	37	2	74	6	276- 4:59:38
1404	MIL	WARM RING 2 A	37	50	73	43	276- 4:59:24
1406	GDS	CA MT. SHASTA LAKE	41	35	121	30	276- 8:19:45
1406	GDS	WA SPOKANF 1	47	36	117	38	276- 8:17:55
1409	ULA	BANKS ISLAND 1 CAN	0	0	0	0	276-13: 9:34
1425	ULA	BEAUFORT SEA 2	72	30	127	0	277-15:58:34
1426	GDS	KS SUBLETTE 3	37	44	100	50	277-17:27:34
1434	GDS	AZ SAFFORD 2	32	45	109	50	278- 7:23:42
1441	GDS	OR NEWBERRY 2	43	40	121	0	278-18:40:44
1441	GDS	CA IMPERIAL VAL 2	33	0	115	30	278-18:37:29
1446	SNF	AT OC ROCKAWAY B	34	26	50	23	279- 3:32:22
1446	SNF	AT OC ROCKAWAY A	35	13	49	58	279- 3:32: 8
1447	MIL	MA BOSTON	42	42	71	5	279- 5:10:41
1449	GDS	WA SPOKANE 2	47	36	117	38	279- 8:30:38
1452	ULA	BANKS ISLAND 2 CAN	74	40	125	35	279-13:22:16
1463	GDS	CA LOS ANGELES 4	33	56	117	33	280- 8: 5:27
1468	MIL	WASHINGTON DC 2	39	5	77	0	280-15:59:54
1468	ULA	ZERO BEAUFORT SEA	73	20	135	48	280-16:12: 1
1468	MIL	VA CHESAPEAKE BAY3	37	0	76	0	280-15:59:20
1469	GDS	KS SUBLETTE 4	37	44	100	50	280-17:40:17
1490	SNF	GREENLAND GLACIERS	64	0	49	0	282- 5:16:33
1492	GDS	OR NEWBERRY 3	43	40	121	0	282- 8:44:38
1494	ULA	AK NENANA-TANANA R	64	18	149	6	282-11:59:28
1498	GDS	CO PARADOX BASIN	38	10	109	20	282-18:22:24

Table A-5. Digital images processed in Europe up to August 1981

REV	STA	DATE	LOCATION	LAT	LON	ARCH
757	UKO	Aug 18	Faroer	62.28	7.15W	907**
			Faroer	62.22	6.57W	902
			Faroer	62.14	6.51W	901
			Faroer	62.12	7.42W	906**
			Faroer	62.04	7.19W	905
			Faroer	61.58	6.52W	903
762	UKO	Aug 19	Sardegna/G. di Orosei	40.04	9.34E	2101**
			Sardegna/Tortoli	40.06	9.50E	2801**
			Sardenga/G. di Orosei	40.18	10.20E	2103**
			Sardegna/Orosei	40.28	9.37E	2114**
			Sardegna/Capo Comino	40.37	10.09E	2106**
			Olbia	40.48	09.24E	6701
			Olbia	40.56	09.19E	6704
			Corsica/Str. of Bonifacio	41.13	9.09E	2401**
			Corsica/G. de Porto	42.14	8.14E	1901**
			Sardegna, Corsica/Isola Caprera	41.22	9.42E	2403**
			Sardegna, Corsica/Porto Vecchio	41.31	8.58E	2404**
			Corsica/G. de Porto Vecchio	41.40	9.31E	2406**
			Corsica/G. de Porto	42.19	8.28E	1911**
			Corsica/Calvi	42.29	9.01E	1913**
			Mont Blanc/Annecy	45.44	5.54E	2001**
			Annecy	45.49	05.09E	2011
			Mont Blanc	45.59	6.44E	2003**
			Mont Blanc/Thonon	46.07	5.56E	2004**
			Geneva	46.09	6.16E	204
			Mont Blanc/Geneva	46.13	6.18E	2006**
			Mont Blanc/Thonon	46.17	6.31E	2016**
			Jura	46.18	5.54E	003*
			Geneve/Oyonnax	46.23	5.45E	0214**
			Jura	46.26	6.10E	002*
			Lake of Geneva	46.32	6.30E	001*
			Geneve/Lac de Joux	46.34	6.20E	0216**
			W. Flanders/Hazebrouck	50.39	2.26E	4501**
			W. Flanders/Kortrijk	50.50	3.04E	4503**
			W. Flanders/Dunkerque	50.57	2.11E	4504**
			W. Flanders/Oostende	51.08	2.49E	4506**
			Channel/E. Margate	51.19	1.53E	2501**
			Channel/N. Dunkerque	51.30	2.31E	2503**
			Channel/N. Margate	51.37	1.37E	2504**
			Channel/N. E. Margate	51.48	2.16E	2506**
			E. Anglia/R. Ouse	52.41	0.39E	4001**
			E. Anglia/Cromer	52.53	1 19E	4003**
			E. Anglia/The Wash	52.59	0.23E	4004**
			E. Anglia/The Wash	53.11	1.02E	4006**
			Dundee/Firth of Forth	56.07	2.45W	3901**
			Dundee/Firth of Forth	56.20	2.03W	3903**
			Dundee/Tay	56.25	3.05W	3904
			Dundee/Dundee	56.31	2.42W	3905
			Dundee/Arbroath	56.37	2.22W	3906
			JASIN	59.58	7.10W	501
			JASIN	59.50	7.30W	503

Table A-5 (contd)

REV	STA	DATE	LOCATION	LAT	LON	ARCH
762 (contd)			JASIN	59.57	7.26W	0513
			JASIN	60.05	7.03W	0512
			JASIN	60.06	6.45W	502**
			JASIN	60.12	6.41W	0523**
785	UKO	Aug 20	Sweden/Stora Lulevatten	67.03	19.30E	7503
			Sweden/Björkholmen	66.49	18.54E	7506
			Sweden/Muddus Park	66.46	20.19E	7501
			Sweden/Lovos	66.36	18.37E	7203
			Sweden/Jokkmokk	66.31	19.44E	7504
			Sweden/Rappen	66.21	18.03E	7206
			Sweden/Pärl ävl	66.21	19.19E	7201
			Sweden/Forsnäs	66.06	18.45E	7204
			Sweden/Hornavan	66.05	17.28E	7303
			Sweden/Storyindeln	65.49	16.54E	7306
			Sweden/Storavan	65.47	18.17E	7301
			Sweden/Forgberg	65.36	16.25E	7403
			Sweden/Sorsele	65.32	17.44E	7304
			Sweden/Gardikfors	65.20	15.53E	7406
			Sweden/Blattnicksele	65.19	17.15E	7401
			Sweden/Storuman	65.04	16.43E	7404
			UK/Cape Spurn	53.58	00.28E	6903
			UK/Cape Spurn	53.45	01.07E	6901
			UK/Cape Spurn	53.39	00.10E	6906
			UK/Cape Spurn	53.27	00.50E	6904
			UK/Grimsby	53.24	00.03W	7003
			UK/Mablethorpe	53.13	00.37E	7001
			UK/Horncastle	53.07	00.15W	7006
			UK/The Wash	52.56	00.20E	7004
			England/Oxford	51.49	01.25W	7103
			England/Slough	51.37	00.46W	7101
			England/Swindon	51.31	01.41W	7106
			England/Reading	51.21	01.00W	7104
			UK/Salisbury	51.12	01.57W	8303
			UK/Southampton	51.01	01.18W	8301
			UK/The Stour	50.54	02.12W	8306
			UK/The Solent	50.43	01.33W	8304
			UK/Weymouth	50.39	02.25W	8203
			UK/Durlston Head	50.28	01.46W	8201
			Channel	50.21	02.40W	8206
			Channel	50.10	02.01W	8204
			Bretagne/Sept Isles	49.01	03.43W	6403
			Bretagne/Paimpol	48.51	03.06W	6401
			Bretagne/Roscoff	48.47	03.54W	6406
			Bretagne/Guingamp	48.36	03.17W	6404
			France/Brest	48.20	04.15W	7803
			France/Mont. noires	48.09	03.38W	7801
			France/Pte du Raz	48.02	04.28W	7806
			France/Audierne	47.56	04.33W	7703
			France/Quimper	47.51	03.52W	7804
			France/Concarneau	47.46	03.56W	7701

Table A-5 (contd)

REV	STA	DATE	LOCATION	LAT	LON	ARCH
785 (contd)			France/Atlantic	47.37	04.44W	7706
			France/Atlantic	47.27	04.10W	7704
			Atlantic	46.36	05.28W	7603
			Atlantic	46.26	04.52W	7601
			Atlantic	46.18	05.41W	7606
			Atlantic	46.07	05.05W	7604
			Portugal/Barcelos	41.35	08.44W	8403
			Portugal/Guimaraes	41.26	08.14W	8401
			Portugal/Povoa	41.16	08.55W	8406
			Portugal/Porto	41.06	08.22W	8404
			Portugal/Atlantic	41.00	09.05W	8103
			Portugal/Ovar	40.50	08.32W	8101
			Portugal/Atlantic	40.41	09.17W	8106
			Portugal/Aveiro	40.32	08.44W	8104
			Portugal/Atlantic	40.24	09.27W	8003
			Portugal/Figueira	40.15	08.54W	8001
			Portugal/Atlantic	40.07	09.37W	8006
			Portugal/Vieira	39.58	09.04W	8004
791	UKO	Aug 21	Algeria	35.28	5.20E	018
			Algeria	35.38	5.45E	027
			Algeria	35.47	5.10E	026
			Algeria	35.54	5.36E	023
			Barcelona West	41.23	1.58E	1601
			Barcelona	41.27	2.16E	1602
			Barcelona/Mataro	41.31	2.32E	1603**
			Barcelona/Manresa	41.41	1.47E	1604
			Barcelona/Manresa	41.46	2.04E	1605
			Barcelona/Vich	41.51	2.20E	1606**
			France/Blaye	45.11	00.26W	6601
			France/Emb. Gironde	45.30	00.39W	6604
			Royan	45.46	0.51W	1401
			Saintes	45.52	0.32W	1402
			St. Jean d'Angély	45.56	0.15W	1403**
			St. Jean d'Angély	45.56	0.15W	1413
			La Rochelle	46.05	1.04W	1404
			Surgères	46.10	0.45W	1405
			Niort	46.15	0.28W	1406**
			France/Pertuis Breton	46.19	1.14W	2701**
			France/Fontenay	46.29	0.38W	2703**
			France/La Roche	46.36	1.26W	2704**
			Nantes	47.03	1.42W	3401**
			Nantes/Loire	47.13	1.09W	3403**
			Nantes/St. Nazaire	47.21	1.56W	3404**
			France/St. Nazaire	47.27	1.59W	3301**
			Nantes/Erdre	47.32	1.20W	3406
			France/Redon	47.44	2.13W	3304**
			Bretagne/St. Brieuc	48.31	2.48W	1701
			Bretagne/Baie de St. Brieuc	48.36	2.29W	1702
			Bretagne/St. Malo	48.41	2.12W	1703**
			Bretagne/Tréguier	48.49	3.02W	1704

ORIGINAL PAGE IS
OF POOR QUALITY

Table A-5 (contd)

REV	STA	DATE	LOCATION	LAT	LON	ARCH
791 (contd)			Bretagne/Pte de Plouézec	48.55	2.44W	1715
			Bretagne/G. de St. Malo	48.59	2.25W	1706**
			Ireland/Cahore Pt	52.32	6.10W	4101**
			Ireland/Irish Sea	52.44	5.31W	4103**
			Ireland/Wicklow	53.02	5.47W	4106**
			Dublin/Kildare	53.08	6.42W	3601**
			Dublin	53.20	6.03W	3603**
			Dublin/Edenderry	53.26	6.59W	3604**
			Dublin/Drogheda	53.37	6.19W	3606**
			Dundalk/Cavan	53.40	7.13W	3501**
			Dundalk	53.52	6.33W	3503**
			Dundalk/Longford	53.57	7.30W	3504
			Dundalk/Monaghan	54.09	6.50W	3506**
			Donegal/Fermanagh	54.19	7.46W	3801**
			Donegal/Tyrone	54.30	7.09W	3803**
			Donegal/Donegal	54.36	8.04W	3804**
			Donegal/Strabane	54.48	7.24W	3806**
			Irish N. Coast/Gweebarra	54.52	8.19W	2601**
			Irish N. Coast/L. Swilly	55.03	7.39W	2603**
			Irish N. Coast/Bloody Foreland	55.09	8.37W	2604**
			Irish N. Coast/Sheep Haven	55.21	7.56W	2606**
			JASIN	59.08	11.50W	701
834	UKO	Aug 24	Cherbourg/Carantan	49.22	1.30W	4201**
			Cherbourg/B. de la Seine	49.33	0.53W	4203**
			Cherbourg/Cherbourg	49.40	1.44W	4204**
			Cherbourg/B. de la Seine	49.51	1.07W	4206**
			Channel/N. Cherbourg	49.54	1.56W	3001**
			Channel/N. E. Cherbourg	50.06	1.19W	3003**
			Channel/S. W. Wight	50.13	2.11W	3004**
			Channel/S. Wight	50.24	1.33W	3006**
			Bournemouth/Weymouth	50.29	2.25W	4601**
			Bournemouth/Bournemouth	50.41	1.47W	4603**
			JASIN	59.08	11.00W	1101
			Iceland/Medallandsbugur	63.31	17.40W	6101
			Iceland/Skeidarasandur	63.46	16.54W	6103
			Iceland/Landbrot	63.47	18.10W	6104
			Iceland/Skeidararjökull	64.03	17.23W	6106
			Iceland/Langjökull	64.50	20.09W	6201
			Iceland/Audkuluheidi	65.05	20.40W	6204
			Iceland/Audkuluheidi	65.07	19.23W	6203
			Iceland/Hrutafjördhur	65.19	21.08W	6301
			Iceland/Audkuluheidi	65.22	19.53W	6206
			Iceland/Fjardharhorn	65.33	21.38W	6304
			Iceland/Thingeyrar	65.49	20.49W	6306
			Iceland/Hunafloi	65.35	20.21W	6303
891	UKO	Aug 28	Bonn	50.40	7.07E	1011**
			Bonn	50.41	7.10E	051
			Bonn/Koeln	50.51	7.07E	108
			East of Bonn	50.51	7.45E	1012**

Table A-5 (contd)

REV	STA	DATE	LOCATION	LAT	LON	ARCH
891 (contd)			East of Bonn	50.51	7.41E	004
			Koeln	50.57	6.56E	003
			Koeln	50.58	6.51E	1013**
			Gummersbach	51.07	7.28E	006
			Gummersbach	51.10	7.29E	1014**
			Duesseldorf	51.14	6.38E	1015**
			Duesseldorf	51.15	6.41E	109
			Wuppertal	51.26	7.16E	112
			Wuppertal	51.26	7.16E	1016**
957	UKO	Sep 1	North Sea	51.37	02.00E	5403
			N. Sea/N. W. Ostend	51.25	02.39E	5401
			N. Sea/Goodwin Sands	51.19	01.45E	5406
			N. Sea/Dunkerque	51.08	02.24E	5404
			Strait of Dover	51.03	01.32E	5503
			France/St. Omer	50.52	02.10E	5501
			France/Boulogne	50.45	01.17E	5506
			France/La Canche	50.34	01.55E	5504
963	UKO	Sep 2	Channel	50.25	00.53W	5201
			Channel	50.36	00.15W	5203
			Isle of Wight	50.42	01.07W	5204
			England/Worthing	50.53	00.29W	5206
			England/Denbigh	53.11	03.21W	5301
			England/Liverpool	53.24	02.42W	5303
			UK/Colwyn Bay	53.30	03.39W	5304
			UK/Southport	53.41	02.57W	5306
			Irish Sea	53.45	03.54W	6801
			UK/Morecambe Bay	53.57	03.13W	6803
			Irish Sea	54.03	04.11W	6804
			UK/Barrow	54.15	03.30W	6806
1044	UKO	Sep 8	Atlantic	62.03	09.57W	8901
			JASIN	59.48	13.51W	1502
			JASIN	59.40	13.27W	1501
			JASIN	59.31	14.13W	1505
1149	UKO	Sep 15	Mediterranean	36.54	16.38E	8501
			Mediterranean	37.02	17.07E	8503
			Mediterranean	37.12	16.28E	8514
			Mediterranean	37.22	16.59E	8506
			Mediterranean	37.25	16.21E	8601
			Mediterranean	37.34	16.52E	8603
			Mediterranean	37.44	16.10E	8604
			Mediterranean	37.53	16.42E	8606
			Calabria/C. Spartivento	38.02	16.00E	2201**
			Calabria/Siderno	38.12	16.32E	2203**
			Calabria/C. di Gioia	38.20	15.50E	2204**
			Calabria/Monasterace	38.30	16.21E	2206**
			Italy/Scalea	39.22	15.14E	8701
			Italy/Belv. Mar.	39.31	15.46E	8703
			Italy/Scalea	39.41	15.03E	8704

Table A-5 (contd)

ORIGINAL PAGE IS
OF POOR QUALITY

REV	STA	DATE	LOCATION	LAT	LON	ARCH
1149 (contd)			Italy/Scalea	39.50	15.35E	8706
			G. di Salerno/S. Licosa pt	40.00	14.52E	2901**
			C. di Salerno/Mt. Cervati	40.12	15.22E	2903**
			G. di Salerno/Licosa pt.	40.15	14.43E	2904**
			G. di Salerno/F. Sele	40.28	15.13E	2906**
			Fair Isle	59.37	1.45W	404
			Shetland	59.50	1.25W	401
			South of Foula	59.58	2.00W	403
			S. W. Foula	60.03	2.32W	2304**
			Shetland	60.04	1.30W	402
			Shetland	60.18	1.46W	2306**
			Atlantic	62.12	05.44W	9301
			Atlantic	62.27	04.57W	9303
			Faroer	62.28	06.11W	9304
			Norwegian Sea	62.44	05.23W	9306
			Bakkafloi	66.15	13.28W	9601
			Bakkafloi	66.29	14.03W	9604
			Bakkafloi	66.33	12.38W	9603
			Bakkafloi	66.47	13.12W	9606
1249	UKO	Sep 22	Denmark/Vordingborg	54.57	11.54E	4801
			Denmark/Fakse Bay	55.10	12.35E	4803
			Denmark/Naestved	55.15	11.36E	4804
			Denmark/Köge	55.28	12.17E	4806
			N-Sjaelland/Slagelse	55.30	11.19E	4701**
			N-Sjaelland/Roskilde	55.43	12.01E	4703**
			Denmark/Samsö Belt	55.48	11.00E	4704
			Denmark/Isefjord	56.01	11.42E	4706
			Arhus bugt	56 03	10.44E	1301
			Kattegatt	56.10	11.06E	1302
			Kalø Vig	56.21	10.25E	1303
			Grena	56.28	10.47E	1305
			Kattegat	56.34	11.07E	1306
1307	UKO	Sep 26	UK/Isle of Man	54.16	04.13W	9401
			UK/Whitehaven	54.28	03.32W	9403
			UK/Burrow Head	54.35	04.27W	9404
			UK/Solway Firth	54.46	03.49W	9406
			UK/Arran	55.22	05.15W	9001
			UK/Prestwick	55.34	04.34W	9003
			UK/Kintyre	55.39	05.34W	9004
			UK/Firth of Clyde	55.52	04.52W	9006
1316	UKO	Sep 27	N. Atlantic	61.46	01.59W	8801
			N. Atlantic	61.45	03.12W	8806
			N. Atlantic	61.30	02.24W	8804
1344	UKO	Sep 29	NL/Vlieland	53.28	04.43E	7901
			NL/Texel	53.10	04.27E	7904
1473	UKO	Oct 8	Norway/Oslo	59.53	10.53E	5603
			Norway/Ostervallskog	59.39	11.39E	5601

ORIGINAL PAGE IS
OF POOR QUALITY

Table A-5 (contd)

REV	STA	DATE	LOCATION	LAT	LON	ARCH
1473 (contd)			Norway/Oslo Fjord	59.36	10.31E	5606
			Norway/Sarpsborg	59.22	11.16E	5604
			Norway/Horten	59.21	10.12E	6503
			Norway/Fredrikstad	59.07	10.56E	6501
			Norway/Porsgrun	59.04	09.50E	6506
			Norway/Oslo Fjord	58.50	10.35E	6504
			Norway/Kragerø	58.48	09.31E	5703
			N. Skagerrak	58.34	10.15E	5701
			Norway/Arendal	58.31	09.09E	5706
			N. Skagerrak	58.18	09.54E	5704
			S. Skagerrak	57.43	08.12E	5803
			S. Skagerrak	57.30	08.56E	5801
			S. Skagerrak	57.25	07.52E	5806
			Denmark/Lild Strand	57.13	08.36E	5804
			North Sea	51.28	2.05E	4903**
			Oostende	51.17	2.44E	4901**
			Calais	51.10	1.50E	4906**
			Dunkerque	50.59	2.28E	4904**
			France/Dieppe	49.52	00.46E	9203
			France/St. Saëns	49.41	01.23E	9201
			France/Seine	49.33	00.31E	9206
			France/Rouen	49.23	01.09E	9204
			France/Le Havre	49.19	00.20E	9103
			France/Elboeuf	49.08	00.57E	9101
			France/Lisieux	49.00	00.05E	9106
			France/Eure	48.50	00.43E	9104
1493	UKO	Oct 9	Frankfurt/Worms	49.38	8.19E	4401**
			Frankfurt/Darmstadt	49.49	8.56E	4403**
			Frankfurt/Wiesbaden	49.56	8.04E	4404**
			Frankfurt/Mainz	50.02	8.24E	4405
			Frankfurt/Frankfurt	50.07	8.42E	4406
			Frankfurt/Frankfurt	50.07	8.42E	4416**
			Koenigswinter	50.39	7.30E	803
			Siegen	50.50	8.05E	801
			Olpe	51.06	7.54E	802
			Holland/O. Flevoland	52.33	5.47E	1202
			Holland/Zwolle	52.41	6.08E	1203
			Holland/Meppel	52.46	6.28E	1201
			Holland/Ijsselmeer	52.52	5.30E	1204
			Holland/Heerenveen	52.56	5.54E	1205
			Holland/Drachten	53.04	6.11E	1206
			Holland/Alsluitdijk	53.06	5.18E	1801
			Holland/W. Leeuwarden	53.12	5.39E	1802
			Holland/E. Leeuwarden	53.18	5.58E	1803**
			Holland/Terschelling	53.23	5.01E	1804**
			Holland/Ameland	53.35	5.41E	1806**
1502	UKO	Oct 10	Norway/Frohavet	64.09	09.04E	5103
			Norway/Frohavet	63.53	09.53E	5101
			Norway/Frøya	63.52	08.39E	5106
			Norway/Orland	63.38	09.24E	5104

Table A-5 (contd)

REV	STA	DATE	LOCATION	LAT	LON	ARCH
1502 (contd)			England/Carlisle	54.59	03.05W	5003
			England/Alston	54.46	02.25W	5001
			England/Workington	54.40	03.20W	5006
			England/Ullswater	54.29	02.42W	5004
			UK/River Fsk	54.22	03.38W	5903
			UK/Morecambe Bay	54.10	02.57W	5901
			Irish Sea	54.04	03.55W	5906
			UK/Blackpool	53.52	03.15W	5904
			Irish Sea	53.48	04.10W	6003
			UK/Liverpool Bay	53.36	03.30W	6001
			UK/N. Anglesey	53.31	04.26W	6006
			UK/Conway Bay	53.19	03.46W	6004

Appendix B
Auxiliary Data Listing

I. General

The beginning of the listing includes the orbit and station identification, starting time (GMT), and pass duration. The time when each data listing was made is also given. Following the initial label are the data listings for the times evaluated (usually 30-s intervals). At the end of the data listing is the list of times when STC changes occurred. At these times, the digitization window changed, and there is a shear discontinuity in range within the image. Definitions of all the items listed are given below.

II. Radar Status Parameters

These values were transmitted in the engineering telemetry stream. They contain information about the operating mode of the radar and some data information. The parameters are defined below.

(1) RECEIVER AGC DC LEVEL: average power in the interpulse period (IPP) in dBm. It was zero when the automatic gain control (AGC) was off, which was the AGC's normal state.

(2) RECEIVER GAIN: gain of the receiver when the AGC is on. It will be identical to the gain for the manual mode listing when the AGC is off.

(3) GAIN MODE: indicates whether the AGC is on or off.

(4) ECHO SAMPLE GATE SCAN, EN: indicates whether the echo sample gate scans the IPP (ON), or is in a fixed position (OFF).

(5) ECHO SAMP. GATE PARK, POS: indicates the position of the echo sample gate (in the fixed mode). The integer listed (J) means it is J/64 of the way through the IPP.

(6) ECHO SAMPLE GATE CTR: value of a clock in the sample gate electronics (usually irrelevant).

(7) STC TRIGGER POSITION: fraction of the PRF (pulse-repetition frequency) interval (N/64) where the STC is initiated (precedes the digitization window by 4; i.e., the window is located (N + 4)/64 of the way through the IPP).

(8) STC TRIGGER: indicates whether the STC is on or off.

(9) RECEIVER GAIN MODE: indicates whether the receiver gain is manually selected (preprogrammed) or automatically selected.

(10) RECEIVER GAIN SEL: indicates the receiver gain value in the manual mode.

(11) CAL SIGN LEVEL: level of the calibration signal. The calibration signal is the retriggered chirp, so this level has meaning only when the retriggered chirp is on.

(12) XMTR CHIRP RETRIGGER EN: indicates whether the retriggered chirp is on or off.

(13) PRF CODE IN HERTZ: value of the PRF.

(14) TRANSMITTER POWER: supposed to be a measure of the transmitted power level, but usually reads 0.

(15), (16) RCVR ECHO AMPL MON: eight values of the received echo amplitude (located at the PARK position) spaced about 0.7 s apart. These values vary widely and may not be accurate.

III. Orbit Parameters

Several parameters give information about the spacecraft orbit and attitude as a function of time. These values were read from the SDR and interpolated to the times listed.

(17) NADIR LATITUDE, LONG: geodetic nadir of the spacecraft given in degrees, minutes, and seconds of latitude and longitude.

(18) S/C ALTITUDE, ALTIMETER: height of the spacecraft above the geodetic nadir point. It is first calculated by subtracting the oblate spheroid model from the orbit. This value can have up to a 100-m error due to model inaccuracies. The second value (ALTIMETER) is the height as measured by the spacecraft altimeter. This data is unrefined, but is supposed to be accurate to within a few meters.

(20) ATTITUDE PITCH, ROLL, YAW: spacecraft attitude errors in pitch, roll, and yaw given in degrees. Pitch is positive when the spacecraft "nose" is up. Roll is positive when the craft rotates clockwise (while looking forward). Yaw

is positive when the spacecraft rotates clockwise (looking down at nadir).

(21) POSITION X-, Y-, Z-AXIS: position of the spacecraft given in a Cartesian inertial coordinate system known as the GSFC (Goddard Space Flight Center) inertial corrdinate system. This system is Earth-centered, but does not rotate with the Earth.

(22) VELOCITY X-, Y-, Z-DOT: vector components of the spacecraft velocity in the same coordinate system as (21).

IV. Calculated Variables

The remainder of the parameters are those calculated from the preceding ones, with the oblate spheroid as the Earth model.

(19) RANGE STDN, EARTH RAD, CUR: range from the spacecraft to the Spaceflight Tracking and Data Network (STDN) station in kilometers. The Earth's radius (center of Earth to nadir point) and local radius of curvature are calculated from the Earth model. The radius of curvature is in the direction of the swath perpendicular, i.e., cross-track.

(23) SLANT RANGE SCALE FACTOR: the number of slant-range meters per mm of image film, expressed as slant-range scale factor $\times$ 10^{-3}. The values for each of the four subswaths are listed, the values being constant within each subswath since they are slant-range presentations.

(24) SWATH VELOCITY: the rate at which the image points cross the swath perpendicular. The rate changes slightly across the swath since the nadir track is not a straight line.

(25), (26) SLANT RANGES SWATHS 1-2, 3-4: slant ranges (from the spacecraft) to the near-range image point in each of the four subswaths. Ideally, they are the ranges to the crossmarks, but, as mentioned previously, their location is in error.

(27) INCIDENCE ANGLES: the angles between the local normal and the spacecraft-to-image point vectors for the image points in (25) and (26)

(28) GROUND RANGE COVERAGE: actual ground ranges covered between the range cross-marks in each of the subswaths. Again, accurate location of the crossmarks is assumed.

(29) TIME DELAYS: supposed to represent the time that elapsed from when the image points crossed the swath perpendicular to when the data was received at the STDN station. However, the value is incorrect.

(30) RADAR VELOCITIES: equivalent straight-line velocity of the spacecraft when determining the azimuth reference function. Since the spacecraft orbit curves towards the targets (deviating about 2 m during a synthetic aperture), the total phase angle is less than it would have been if the spacecraft had been traveling in a straight line. This effect can be accounted for by reducing the tangential velocity by a factor of approximately R_T/R_S where R_T is the target radius (from orbit center) and R_S is the orbit radius.

(31) CLOCK ANGLE PERPEN: angle (measuring clockwise from true north) of the swath perpendicular.

(32)–(36) DATA LAT. & LONG: locations of the near-range crossmarks (ideally). The far-range crossmarks of one swath are supposed to conform to the near-range crossmarks of the subsequent swath. The fifth value represents the far range of subswath 4.

(37)–(40) RECEIVED POWER-5 KM STEP: net gain function across the swath determined from the antenna pattern and the STC function. The relative locations are determined with respect to the swath, multiplied together, and the result is listed at every 5 km of ground range.

ORIGINAL PAGE IS
OF POOR QUALITY

Appendix C

Bibliography of Seasat SAR Scientific Publications

Alpers, W. R., and C. L. Rufenach, "The Effects of Orbital Motions on Synthetic Aperture Imagery of Ocean Waves," *IEEE Trans. Ant. Prop.*, Vol. AP-27, pp. 685-690, September 1979.

Alpers, W. R., D. B. Ross, and C. L. Rufenach, "On the Detectability of Ocean Surface Waves by Real and Synthetic Aperture Radar," *J. Geophys. Res.*, Vol. 86, p. 6481. 1981.

Apel, J. R., "Nonlinear Features of Internal Waves as Derived from the Seasat Imaging Radar," submitted to *J. Geophys. Res.*

Beal, R. C., "Spaceborne Imaging Radar Ocean Wave Monitoring," *Science*, Vol. 208, p. 4450, 1980.

Beal, R. C., F. Gonzales, W. Brown, P. DeLeonibus, J. Sherman, J. Gower, D. Ross, C. Rufenach, and R. Schuchman, "Seasat Synthetic Aperture Radar: Ocean Wave Detection Capabilities," *Science*, Vol. 204, No. 4400, 1979.

Beal, R. C., M. G. Mattie, and D. E. Lichy, "Seasat Detection of Waves, Currents, and Inlet Discharge," *Int. Remote Sensing*, Vol. 1, pp. 377-398, 1980.

Beal, R. C., and F. Monaldo, "Spatial Evolution of Ocean Wave Systems Monitored by the Seasat SAR," in preparation for submittal to *J. Geophys. Res.*

Blanchard, B. J., A. T. C. Chang, and A. J. Blanchard, "Seasat SAR Response from Water Resources Parameters," submitted to *J. Geophys. Res.*

Elachi, C. "Spaceborne Imaging Radar: Geologic and Oceanographic Applications," *Science*, Vol. 209, No. 4461, 1980.

Engheta, N., and C. Elachi, "Radar Scattering From a Diffuse Vegetation Layer Over a Smooth Surface," *IEEE Trans. Geosci. Rem. Sens.*, Vol. GE-20, p. 212, 1982.

Ford, J. P., "Resolution Versus Speckle Relative to Geologic Interpretability of Spaceborne Radar Images: A Survey of User Preference," *IEEE Trans. Geosci. Rem. Sens.* Vol. GE-20, p. 434, 1982.

Ford, J. P., R. G. Blom, M. L. Bryan, M. I. Daily, T. H. Dixon, C. Elachi, and E. C. Xenos, *Seasat Views North America, the Caribbean, and Western Europe With Imaging Radar*. Publication 80-67, Jet Propulsion Laboratory, Pasadena, Calif., 1980.

Fu, L.-L., and B. Holt, *Seasat Views Ocean and Sea Ice with Synthetic-Aperture Radar*. Publication 81-120, Jet Propulsion Laboratory, Pasadena, Calif., 1982.

Fu, L.-L., and B. Holt, "Some Examples of Detection of Mesoscale Eddies by the Seasat Synthetic-Aperture Radar," *J. Geophys. Res.* 2nd Seasat Special Issue, 1982 (in press).

Gonzalez, F. I., R. C. Beal, W. E. Brown, J. F. R. Gower, D. Lichy, D. B. Ross, C. L. Rufenach, and R. A. Shuchman, "Seasat Synthetic Aperture Radar: Ocean Wave Detection Capabilities," *Science*, Vol. 204, No. 4400, 1979.

Hall, R. T., and D. A. Rothrock, "Sea Ice Displacement from Seasat Synthetic Aperture Radar," *J. Geophys. Res.*, Vol. 86, p. 1078, 1981.

Jordan, R. L., "The Seasat-A Synthetic Aperture Radar System," *IEEE J. of Oceanic Eng.*, Vol. OE-5, No. 2, p. 154, 1980.

Kasischke, E. S., R. A. Schuchman, J. D. Lyden, R. F. Stewart, J. F. Vesecky, and H. A. Assal, "SAR Observations of Ocean Gravity Waves During the JASIN Experiment," submitted to *J. Geophys. Res.*

Kenyon, N. H., "Bedforms of Shelf Seas Viewed with Seasat Synthetic Aperture Radar," in *Advances in Hydrographic Surveying*, Society for Underwater Technology, London, 1981.

Meadows, G. A., R. A. Schuchman, E. E. Kasischke, and J. D. Lyden, "The Observation of Gravity Wave – Current Interactions Using Seasat Synthetic Aperture Radar," submitted to *J. Geophys. Res.*

Rufenach, C. L., and W. R. Alpers, "Imaging Ocean Waves by Synthetic Aperture Radar with Long Integration Times," *IEEE Trans. Ant. Prop.*, Vol. AP-29, pp. 422-428, May 1981.

Spaceborne Synthetic Aperture Radar for Oceanography. R. C. Beal, P. S. Deleonibus, and I. Katz, editors. Johns Hopkins University Press, Baltimore, Md., 1981.

Vesecky, J. F., and R. H. Stewart, "The Observation of Ocean Surface Phenomena Using Imagery from the Seasat Synthetic Aperture Radar," *J. Geophys. Res.*, Vol. 87, p. 3397, 1982.

Vesecky, J. F., R. H. Stewart, H. M. Assal, R. A. Schuchman, E. S. Kasischke, and J. D. Lyden, "Gravity Waves, Large-Scale Surface Features and Ships Observed by Seasat During the 1978 JASIN Experiment," submitted to *Science*.

Wu, C., B. Barkan, W. J. Karplus, and D. Caswell, "Seasat Synthetic-Aperture Radar Data Reduction Using Parallel Programmable Array Processors," *IEEE Trans. Geosci. Rem. Sens.*, Vol. GE-20, p. 352, 1982.

NASA—JPL—Coml., L.A., Calif.